# Structural Insights, Biochemical Characterization and Physiological Role of Pyruvate:Quinone Oxidoreductase in *Corynebacterium glutamicum*

Dissertation

For the fulfillment of the requirements for the doctoral degree Dr. rer. nat.
at the Faculty of Natural Sciences,
Ulm University

submitted by

**Cristiano Da Silva Lameira**

from Ulm, Germany

2024

The present work has been conducted under the supervision of Prof. Dr. Bernhard J. Eikmanns at the Institute of Molecular Biology and Biotechnology of Prokaryotes at the University of Ulm, Germany.

| | |
|---|---|
| Dean of Faculty: | Prof. Dr. Kay Gottschalk |
| First Reviewer: | Prof. Dr. Bernhard J. Eikmanns |
| Second Reviewer: | Prof. Dr. Peter Dürre |

Date of Examination: 20th march 2024

# Abstract

*Corynebacterium glutamicum*, an important model in industrial biotechnology for amino acid production, has been extensively studied for its central carbon metabolism. This thesis investigates the regulatory function and impact of the tetrameric flavoprotein pyruvate:quinone oxidoreductase (PQO) at the phosphoenolpyruvate-pyruvate-oxaloacetate node, with this node being a key metabolic link between glycolysis and the tricarboxylic acid (TCA) cycle.

PQO activities were analyzed in various strains across different growth phases and media conditions using shake flask experiments. Results indicated that PQO is non-essential in these conditions. In the wildtype strain, PQO activity varies with growth phase in complex media, being higher in the stationary than in the exponential phase. The highest specific activities were observed in cells grown in 2xTY complex medium, and the lowest in acetate minimal medium. Interestingly, PQO activity patterns in a PQO overproducer strain, where the native PQO gene (*pqo*) is deleted and the plasmid-encoded *pqo* expression is under control of an artificial promoter, suggest that post-translational modification (PTM) might play a more significant role than transcriptional regulation in PQO activity.

Native purification of PQO from a *C. glutamicum* PQO overproducer strain grown in either 2xTY complex- or in acetate minimal medium and subsequent analysis of their kinetic properties revealed significant differences in the catalytic turnover number (440 $s^{-1}$ vs. 78 $s^{-1}$), corroborating the idea that PTM modulate PQO activity. Mass spectrometry analysis identified lysine succinylation and acetylation as key PTMs, with specific lysine residues being more susceptible to these modifications. Particular attention was given to two lysine residues, K93 and K325, prone to acetylation and succinylation, respectively. This led to the creation and overproduction of PQO variants in the *C. glutamicum* Δ*pqo*-background, substituting the respective lysine residues with alanine or glutamate, respectively. For the K325 residue, the lysine-to-glutamate substitution generally led to decreased PQO activity. On the other hand, the lysine-to-alanine substitution at K325 led to similar activity compared to the lysine-to-glutamate variant. This finding suggests a more significant role of PQO's structural properties than previously understood. Both K93 variants generally showed PQO activity that was equal to or lower than the wildtype enzyme. These mutations affect the proximity at this residue to the FAD cofactor and potentially its binding stability.

The three-dimensional structure of PQO from *C. glutamicum* was successfully resolved. High-throughput crystallization, adapted from protocols for crystallizing the homologous PoxB from

*Escherichia coli*, produced protein crystals. X-ray crystallography, initially employing molecular replacement with *E. coli* PoxB as the model, refined the PQO structure to a 1.26 Å resolution. This surpassed the resolution of pyruvate oxidase from *Lactobacillus plantarum* and PoxB from *E. coli*, enabling detailed examination of intermolecular interactions and potential PTMs at lysine residues K121 and K325. Structural comparison highlighted the similarity between PQO and PoxB as tetrameric flavoproteins, with similar cofactor placements and active sites. However, the C-terminus of PQO distinctly features an amphipathic α-helix, leading to a different conformation and orientation with potential functional implications. Confirmation of this structure's accuracy came from X-ray analysis of a $His_6$-tagged *C. glutamicum* PQO variant purified from *E. coli*, which verified the unique α-helical structure at the C-terminus of PQO. Research on a truncated PQO variant (PQO-$\Delta_{C17}$), lacking the C-terminal α-helix, underscored its significance in lipid/detergent interaction and enzyme activation. The structural analysis of PQO-$\Delta_{C17}$ indicated enhanced flexibility in the remaining C-terminal domain, while largely preserving the structure of the full-length protein.

As the physiological role of PQO in *C. glutamicum* remained elusive, this study explored whether PQO, together with acetate kinase (ACK) and phosphotransacetylase (PTA), offers a bypass to the pyruvate dehydrogenase complex (PDHC) reaction. Specifically, it examines an *aceE*-deficient *C. glutamicum* strain, lacking the E1 subunit of PDHC and therefore requiring acetate supplementation for optimal growth. Interestingly, even with the overproduction of full-length PQO, this requirement persists. However, overproduction of PQO-$\Delta_{C17}$ in minimal medium containing glucose and acetate enabled partial utilization of glucose for biomass production, a capability absent with the overproduction of the full-length PQO variant.

Higher PQO activities were noted in *C. glutamicum* wildtype strain under acidic conditions in both shake flask experiments and bioreactor batch fermentations, indicating a significant role of PQO during intracellular pyruvate accumulation. Continuous fermentations at varying dilution rates also showed increased PQO activities in wildtype cells at slower growth rates, confirming the inverse correlation between growth rate and PQO activity.

PQO activity was analyzed in wildtype, PQO-deficient, and PQO overproducer strains under conditions inducing glutamate production via Penicillin G addition. Notably, PQO activity was higher under glutamate-producing conditions in both wildtype and PQO overproducing strains yet, no distinct growth phenotypes or significant variations in glutamate excretion were observed with the three strains studied. Co-culture experiments with fluorescently labeled *C. glutamicum* wildtype and PQO-deletion strains indicated no competitive advantage

conferred by the presence or absence of PQO, except under glutamate production conditions, where the PQO-deletion strain exhibited a growth advantage.

In conclusion, this research suggests that PQO, together with ACK and PTA, does not replace the PDHC reaction and is not essential for growth of *C. glutamicum* under all conditions tested. Instead, the primary role of PQO obviously is to direct the carbon flux away from the TCA cycle under specific conditions, such as pyruvate accumulation, with acetylation and succinylation of lysine residues playing a regulatory role in its activity.

# Zusammenfassung

*Corynebacterium glutamicum*, ein wichtiger Modellorganismus in der industriellen Biotechnologie für die Aminosäureproduktion, wird umfassend hinsichtlich seines zentralen Kohlenstoffstoffwechsels untersucht. Diese Arbeit untersucht die regulatorische Funktion und Wirkung des tetrameren Flavoproteins Pyruvat:Chinon-Oxidoreduktase (PQO) am Phosphoenolpyruvat-Pyruvat-Oxalacetat-Knotenpunkt, einem wichtigen metabolischen Verbindungsglied zwischen Glykolyse und dem Tricarbonsäure-Zyklus (TCA-Zyklus).

PQO-Aktivitäten wurden in verschiedenen Stämmen über verschiedene Wachstumsphasen und Medienbedingungen mittels Schüttelkolbenexperimenten analysiert. Die Ergebnisse zeigen, dass PQO unter diesen Bedingungen nicht essentiell ist. Im Wildtyp-Stamm variiert die PQO-Aktivität mit der Wachstumsphase in komplexen Medien, wobei sie in der stationären Phase höher als in der exponentiellen Phase ist. Die höchsten spezifischen Aktivitäten wurden in Zellen beobachtet, die in 2xTY-Komplexmedium gewachsen waren, und die niedrigsten im Acetat-Minimalmedium. Interessanterweise deuten die PQO-Aktivitätsmuster in einem PQO-Überproduzentenstamm, bei dem das native PQO-Gen (*pqo*) deletiert ist und die Plasmid-kodierte *pqo*-Expression unter der Kontrolle eines künstlichen Promotors steht, darauf hin, dass posttranslationale Modifikationen (PTM) eine bedeutendere Rolle spielen könnten als die transkriptionelle Regulation in der PQO-Aktivität.

Die native Reinigung von PQO aus einem *C. glutamicum* PQO-Überproduzentenstamm, der entweder in 2xTY-Komplexmedium oder Acetat-Minimalmedium gewachsen ist, und die anschließende Analyse seiner kinetischen Eigenschaften ergaben signifikante Unterschiede in der katalytischen Umsatzzahl (440 $s^{-1}$ vs. 78 $s^{-1}$), was die Idee stützt, dass PTM die PQO-Aktivität modulieren. Massenspektrometrie-Analysen identifizierten Lysin-Succinylierung und -Acetylierung als relevanteste PTMs, wobei bestimmte Lysinreste anfälliger für diese Modifikationen waren. Besondere Aufmerksamkeit wurde zwei Lysinresten gewidmet, K93 und K325, die anfällig für Acetylierung bzw. Succinylierung sind. Dies führte zur Erzeugung und anschließenden Überproduktion von PQO-Varianten im *C. glutamicum* Δ*pqo*-Hintergrund, indem die genannten Lysinreste durch Alanin oder Glutamat ersetzt wurden. Bei dem K325-Rest führte der Lysin-zu-Glutamat-Austausch, sowie der Lysin-zu-Alanin Austausch im Allgemeinen zu einer verringerten PQO-Aktivität. Dieser Befund deutet auf eine bedeutendere Rolle der strukturellen Eigenschaften von PQO hin, als bisher angenommen wurde. Beide K93-Varianten zeigten im Allgemeinen eine PQO-Aktivität, die gleich oder niedriger als die des

Wildtyp-Enzyms war. Diese Mutationen beeinflussen die Nähe dieses Rests zum FAD-Kofaktor und möglicherweise dessen Bindungsstabilität.

Die dreidimensionale Struktur von PQO aus *C. glutamicum* wurde erfolgreich aufgelöst. Hochdurchsatz-Kristallisation, angepasst von Protokollen zur Kristallisierung des homologen PoxB aus *Escherichia coli*, führte zu Proteinkristallen. Die Röntgenkristallstrukturanalyse, zunächst unter Verwendung von „*molecular replacement"* mit *E. coli* PoxB als Modell, verfeinerte die PQO-Struktur zu einer Auflösung von 1,26 Å. Dies übertraf die Auflösung der Pyruvatoxidase aus *Lactobacillus plantarum* und PoxB aus *E. coli* und ermöglichte eine detaillierte Untersuchung von intermolekularen Wechselwirkungen und potenziellen PTMs an den Lysinresten K121 und K325. Der strukturelle Vergleich hob die Ähnlichkeit zwischen PQO und PoxB als tetramere Flavoproteine hervor, mit ähnlichen Kofaktor-Platzierungen und aktiven Zentren. Jedoch weist der C-Terminus von PQO eine unterscheidbare amphipathische α-Helix auf, was zu einer anderen Konformation und Orientierung mit potenziellen funktionellen Implikationen führt. Die Bestätigung der Genauigkeit dieser Struktur kam von der Röntgenkristallstrukturanalyse einer $His_6$-getaggten *C. glutamicum* PQO-Variante, gereinigt aus *E. coli*, die die einzigartige α-helikale Struktur am C-Terminus von PQO bestätigte. Die Forschung an einer verkürzten PQO-Variante (PQO-$\Delta_{C17}$), dem die C-terminale α-Helix fehlt, unterstrich die Bedeutung dieser Helix in der Lipid/Detergenz-Interaktion und Enzymaktivierung. Die strukturelle Analyse von PQO-$\Delta_{C17}$ zeigte eine erhöhte Flexibilität im verbleibenden C-terminalen Bereich, während sie weitgehend die Struktur des Voll-Längen Proteins bewahrte.

Da die physiologische Rolle von PQO in *C. glutamicum* weiterhin unklar blieb, untersuchte diese Studie, ob PQO zusammen mit der Acetatkinase (ACK) und der Phosphotransacetylase (PTA) eine Alternative zur Reaktion des Pyruvat-Dehydrogenase-Komplexes (PDHC) bietet. Insbesondere wurde ein *aceE*-defizienter *C. glutamicum*-Stamm untersucht, dem die E1-Untereinheit von PDHC fehlt und daher Acetatzusatz für optimales Wachstum benötigt. Interessanterweise besteht diese Anforderung auch bei Überproduktion von Voll-Längen PQO weiterhin. Die Überproduktion von PQO-$\Delta_{C17}$ in Minimalmedium mit Glukose und Acetat ermöglichte jedoch die teilweise Nutzung von Glukose für die Biomasseproduktion, eine Fähigkeit, die bei der Überproduktion der Voll-Längen PQO-Variante fehlte.

Höhere PQO-Aktivitäten wurden im *C. glutamicum* Wildtyp-Stamm unter sauren Bedingungen sowohl in Schüttelkolbenexperimenten als auch in Batch-Fermentationen im Bioreaktor festgestellt, was auf eine bedeutende Rolle von PQO während intrazellulärer Pyruvat-

Akkumulation hinweist. Kontinuierliche Fermentationen bei verschiedenen Verdünnungsraten zeigten ebenfalls erhöhte PQO-Aktivitäten in Wildtypzellen bei langsameren Wachstumsraten, was die umgekehrte Korrelation zwischen Wachstumsrate und PQO-Aktivität bestätigt.

PQO-Aktivität wurde in Wildtyp-, PQO-Defizienz und PQO-Überproduzentenstämmen unter Bedingungen, unter denen Glutamat-Produktion durch Zugabe von Penicillin G induziert wurde, analysiert. Bemerkenswert ist, dass die PQO-Aktivität unter Glutamat-produzierenden Bedingungen in sowohl Wildtyp- als auch PQO-überproduzierenden Stämmen höher war, jedoch wurden keine ausgeprägten Wachstumsphänotypen oder signifikanten Variationen in der Glutamat-Ausscheidung bei den drei untersuchten Stämmen beobachtet. Kokultur-Experimente mit fluoreszenzmarkierten *C. glutamicum* Wildtyp- und *pqo*-Deletionsstämmen zeigten keinen kompetitiven Vorteil, der durch das Vorhandensein oder Fehlen von PQO verliehen wurde, außer unter Glutamat-Produktionsbedingungen, unter denen der PQO-Deletionsstamm einen Wachstumsvorteil zeigte.

Zusammenfassend lässt diese Forschung vermuten, dass PQO zusammen mit ACK und PTA die PDHC-Reaktion nicht ersetzen kann und für das Wachstum von *C. glutamicum* unter allen getesteten Bedingungen nicht essenziell ist. Stattdessen scheint die primäre Rolle von PQO offensichtlich darin zu bestehen, den Kohlenstoffffluss unter bestimmten Bedingungen, wie bei Pyruvat-Akkumulation, vom TCA-Zyklus wegzuleiten, wobei die Acetylierung und Succinylierung von Lysinresten eine regulierende Rolle in seiner Aktivität spielt.

# Table of Contents

**1 Introduction** ..... 1
**2 Material and methods** ..... 11
2.1 Chemicals ..... 11
2.2 Bacterial strains, plasmids, and oligonucleotides ..... 11
2.3 Media and cultivation conditions ..... 15
2.3.1 Cultivation in bioreactor (Münßinger, 2022) ..... 16
2.4 Molecular biology ..... 19
2.4.1 Polymerase chain reaction (PCR) (Mullis *et al*., 1986) ..... 19
2.4.2 Agarose gel electrophoresis ..... 19
2.4.3 DNA isolation ..... 19
2.4.4 Restriction digest of DNA ..... 19
2.4.5 Site directed *pqo* mutagenesis and ligation of DNA fragments with T4 ligase ..... 20
2.4.6 Gibson assembly (Gibson *et al*., 2009) ..... 20
2.5 Preparation of competent cells and transformation ..... 20
2.6 Biochemical methods ..... 22
2.6.1 Preparation of cell-free extracts (Schreiner, 2004) ..... 22
2.6.2 Determination of protein concentrations ..... 22
2.6.3 Purification of PQO and PQO variants ..... 22
2.6.4 PQO assay (Schreiner and Eikmanns, 2005) ..... 23
2.6.5 SDS-PAGE (Laemmli, 1970) and Western blot (adapted from Towbin *et al.*, 1979) ..... 24
2.7 Miscellaneous ..... 25
2.7.1 Fluorescence measurements ..... 25
2.7.2 Bioinformatics ..... 25
**3 Results** ..... 27
3.1 Carbon source and growth phase modulate PQO activity in *C. glutamicum* ..... 27
3.2 Investigating PQO activity in *C. glutamicum*: Purification of the enzyme and effects of cultivation conditions and post-translational modifications ..... 29
3.2.1 Purification and kinetic analysis of PQO enzyme activity ..... 29
3.2.2 Corynebacterial PQO is abundantly acylated ..... 32
3.2.3 Sequence analysis of corynebacterial PQO and mutant characterization ..... 34
3.2.4 Modifying lysine residues in PQO: Effects on enzyme activity in *C. glutamicum* ..... 37
3.3 Structural analysis of PQO from *C. glutamicum* ..... 39
3.3.1 The corynebacterial PQO contains a structurally unique C-terminus ..... 40

3.3.2 A C-terminal truncated PQO exhibits detergent-independent activity ..... 51
3.3.3 Lysine residues found to be post-translationally modified are located at the surface of PQO ..... 59
3.4 Physiological role of PQO in *C. glutamicum* ..... 63
3.4.1 Overproduction of PQO-$\Delta_{C17}$ enables pyruvate decarboxylase-deficient *C. glutamicum* strains to use glucose partially for biomass generation ..... 63
3.4.2 PQO presence in *C. glutamicum* is detrimental in Penicillin G induced glutamate producing conditions ..... 67
3.4.3 PQO is highly active when *C. glutamicum* is cultivated in acidic conditions ..... 78
3.4.4 Low growth rates during cultivations with *C. glutamicum* are associated with high PQO activity ..... 88
**4 Discussion** ..... 90
4.1 High *in vitro* PQO activity may be negatively correlated with *in vivo* TCA cycle activity ..... 90
4.2 PQO may be regulated via acetylation and succinylation through non-enzymatic means ..... 92
4.3 PQO is very similar to PoxB from *E. coli*, but differs significantly at its C-terminus important for membrane binding and activation mechanism ..... 97
4.4 PQO and its potential role in redirecting carbon flux away from the TCA cycle ..... 104
**References** ..... 113
**List of acronyms** ..... 129
**Poster presentations and publication** ..... 132
**Declaration** ..... 133
**DANKSAGUNG** ..... 134
**LEBENSLAUF** ..... 136

# 1 Introduction

*Corynebacterium glutamicum* is a facultative anaerobic, Gram-positive bacterium with a moderate to high GC content, classified under the actinobacteria phylum (Abe *et al*., 1967). Actinobacteria constitute one of the most diverse bacterial phyla, encompassing key pathogens like *Mycobacterium tuberculosis*, crucial antibiotic producers such as *Streptomycetes*, and important industrial microorganisms like *C. glutamicum* (Ventura *et al*., 2007).

*C. glutamicum*, whose genome was fully sequenced (Kalinowski *et al*., 2003), is predominantly employed in the production of amino acids such as L-glutamate, L-lysine, L-arginine, and L-tryptophan through fermentation processes (reviewed in Wendisch, 2020). The development of metabolic engineering has greatly benefited from the plethora of genetic tools available for *C. glutamicum*, resulting in an expansion of its product spectrum to include over 70 distinct compounds, which includes bulk chemicals like lactate, succinate, and glutarate (reviewed in Becker *et al*., 2018). Noteworthy traits of *C. glutamicum* include its ability to rapidly grow to high cell densities without autolysis, the scalability of cultivations to large volumes and its safety profile, as it does not produce endotoxins, is resistant to phage lysis, and has been designated as Generally Recognized as Safe (GRAS) by the United States Food and Drug Administration (reviewed in Wolf *et al*., 2021). Additionally, *C. glutamicum* can metabolize a diverse range of carbon substrates, including mixtures of carbohydrates, organic acids and alcohols (reviewed in Blombach and Seibold, 2010), making it suitable for the use of hydrolyzed lignocellulosic biomass and waste materials as environmentally friendly fermentation feedstocks (reviewed in Kogure and Inui, 2018).

Owing to its significance in industrial biotechnology and its position as a model for pathogens like *M. tuberculosis* and *C. diphtheriae*, there is a growing interest in elucidating the molecular physiology of *C. glutamicum* for both therapeutic and biotechnological applications. A promising avenue of exploration lies on the central carbon metabolism of *C. glutamicum*. Like in many aerobic and facultatively anaerobic bacteria, its central carbon metabolism encompasses glycolysis, the oxidative pentose phosphate pathway, and the tricarboxylic acid (TCA) cycle (Eikmanns, 2005 in Handbook of *Corynebacterium glutamicum*). Carbohydrate breakdown via glycolysis and the oxidative pentose phosphate pathway leads to the generation of phosphoenolpyruvate (PEP), pyruvate, and acetyl-CoA. In the energy metabolism, these compounds are then fully oxidized to $CO_2$ within the TCA-cycle (Eikmanns, 2005 in Handbook of *Corynebacterium glutamicum*). These fundamental metabolic pathways enable the organisms the processing of carbon substrates, converting them to intermediate compounds

useful for building biomass and generating ATP. The importance of both PEP and pyruvate in carbon metabolism is underscored by their role as precursors in numerous synthetic and catabolic pathways. Consequently, the PEP-pyruvate-oxaloacetate node, which comprises a multitude of significant enzymes, has been a focal point of rigorous research in earlier studies (reviewed in Sauer and Eikmanns, 2005; **Fig. 1**).

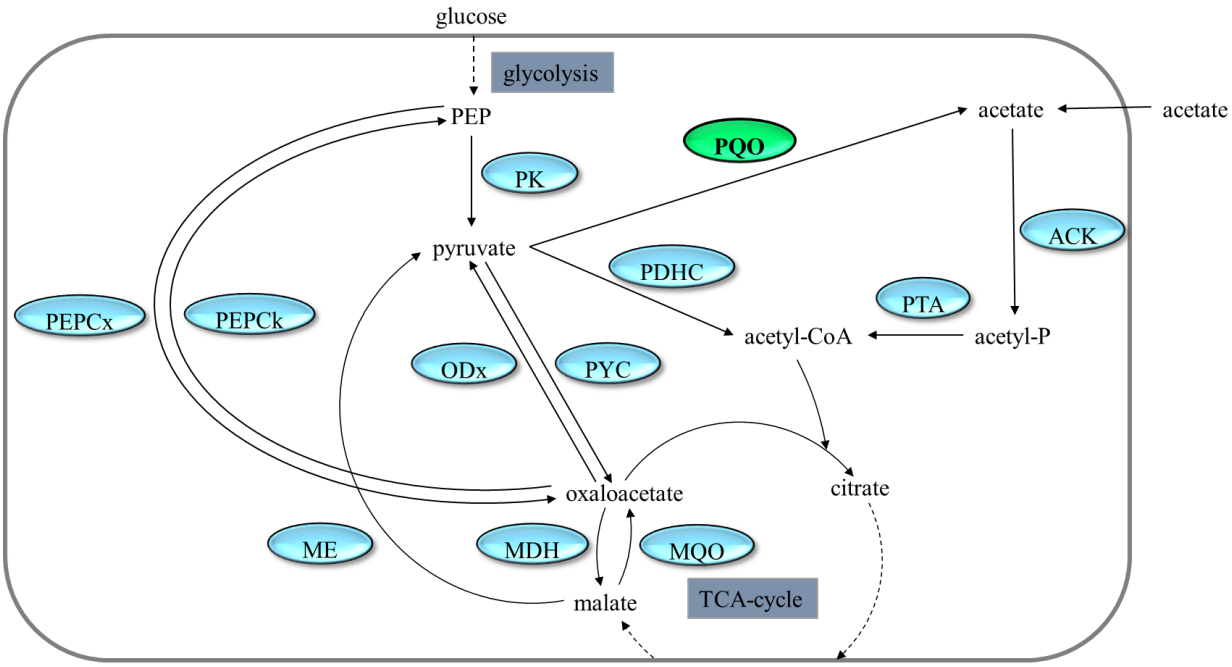


**Fig. 1: Simplified PEP-pyruvate-oxaloacetate node in *C. glutamicum*.**

Abbreviations: ACK = acetate kinase, CoA = coenzyme A, ME = malic enzyme, MDH = malate dehydrogenase, MQO = malate:quinone oxidoreductase, ODx = oxaloacetate decarboxylase, P = phosphate, PYC = pyruvate carboxylase, PDHC = pyruvate dehydrogenase complex, PEP = phosphoenolpyruvate, PEPCk = PEP carboxykinase, PK = pyruvate kinase, PEPCx = PEP carboxylase, PQO = pyruvate:quinone oxidoreductase, PTA = phosphotransacetylase.

Relative to other organisms, *C. glutamicum* is distinguished by a significant presence of carboxylating and decarboxylating enzymes at this node. Notably, *C. glutamicum* contains anaplerotic enzymes such as PEP carboxylase (PEPCx) (Eikmanns *et al.*, 1989) and pyruvate carboxylase (PYC) (Peters-Wendisch *et al.*, 1997). Moreover, *C. glutamicum* also possesses three C4-decarboxylating enzymes, catalyzing the conversion of oxaloacetate or malate to PEP or pyruvate. These include the PEP carboxykinase (PEPCk) (Riedel *et al.*, 2001), malic enzyme (ME) (Gourdon *et al.*, 2000), and oxaloacetate decarboxylase (ODx) (Klaffl and Eikmanns, 2010). Additionally, *C. glutamicum* possesses the enzymes malate:quinone oxidoreductase

(MQO) and malate dehydrogenase (MDH). While MQO plays a crucial role in maintaining a functional TCA cycle, MDH does not exhibit significant relevance under the tested conditions. Nevertheless, MDH is hypothesized to be involved in the reverse reaction converting oxaloacetate back to malate (Molenaar *et al*. 1998, Molenaar *et al*., 2000).

One of the most important intermediates within the PEP-pyruvate-oxaloacetate node is acetyl-CoA, one of the primary carriers of carbon units in biological systems. Beyond fueling the TCA cycle, acetyl-CoA in general also serves as an essential precursor for anabolic pathways, including the synthesis of fatty acids (Eikmanns, 2005 in Handbook of *Corynebacterium glutamicum*). In the context of *C. glutamicum*, the conversion of pyruvate, the end product of glycolysis, to acetyl-CoA is predominantly mediated by the oxidative decarboxylation process catalyzed by the pyruvate dehydrogenase complex (PDHC) (Schreiner *et al*., 2005).

The PDHC is a tripartite complex prevalent in most aerobic bacteria, consisting of the subunits E1p, E2p and E3 and structurally characterized by a central core composed by a varying number of E2p subunits (Bruch *et al*., 2021). E2p is a multi-domain protein equipped with acetyltransferase activity crucial for transferring the acetyl group from decarboxylated pyruvate to the CoA-SH recipient (Hoffelder *et al*., 2010). The E1p subunit of the PDHC, also known as AceE or pyruvate decarboxylase, catalyzes the oxidative thiamine diphosphate-dependent decarboxylation of pyruvate, while concurrently acetylating the E2 component with its lipoyl groups. When the chromosomal *aceE* gene was inactivated in *C. glutamicum*, the organism could no longer grow on glucose when it was the sole carbon source (Schreiner *et al*., 2005). Additionally, there was a complete absence of PDHC and E1 activity (Schreiner *et al*., 2005). This suggests that *C. glutamicum* has only one E1p enzyme and highlights the vital importance of the PDHC for the growth of this bacterium on carbohydrate-substrates (Schreiner *et al*., 2005). The E3 subunit of the PDHC, known as Lipoamide Dehydrogenase (LPD), catalyzes the FAD-dependent reoxidation of dihydrolipoyl groups by reducing $NAD^+$. The dihydrolipoyl groups are covalently bound to the E2 subunit as they receive the acetyl group from pyruvate (Schwinde *et al*., 2001).

At the PEP-pyruvate-oxaloacetate node in *C. glutamicum*, an additional enzyme decarboxylates pyruvate: the pyruvate:quinone oxidoreductase (PQO). This enzyme was thoroughly characterized by M. Schreiner in his doctoral thesis (Schreiner, 2004). Activity was identified *in vitro* using cell extracts with 2,6-dichloroindophenol as an artificial electron acceptor. The highest activity (0.055 ± 0.005 U/mg protein) was noted in cells grown in complex medium, with a roughly threefold decrease when cells were cultivated in minimal medium using glucose,

pyruvate, or acetate as carbon sources. To ascertain the cellular localization of PQO, *C. glutamicum* cells were mechanically lysed, and the resultant cell extract was divided into membrane and supernatant fractions via ultracentrifugation. Over 90 % of the PQO activity was found in the supernatant fraction, suggesting the enzyme might only have a weak association with the cytoplasmic membrane (Schreiner and Eikmanns, 2005). The ability of the enzyme to bind to the detergent Triton X-114 in the presence of its substrate and cofactors, unlike other cytosolic proteins in *C. glutamicum*, facilitated its purification to nearly 180-fold purity from wildtype *C. glutamicum* (Schreiner and Eikmanns, 2005). PQO is a flavoprotein, contains FAD, has a molecular mass of approximately 232 kDa and is composed of four identical subunits of a theoretical size of about 62 kDa each. Its activation was evident with Triton X-100, phosphatidylglycerol, and dipalmitoyl-phosphatidylglycerol. Recognized substrates were 2-oxoacids such as pyruvate ($k_{cat} = 37.8 \pm 3\ s^{-1}$; $K_m = 30 \pm 3$ mM) and 2-oxobutyrate ($k_{cat} = 33.2 \pm 3\ s^{-1}$; $K_m = 90 \pm 8$ mM). The cofactors of the enzyme included thiamine diphosphate ($K_m = 1$ µM) and $Mg^{2+}$ ($K_m = 29$ µM). The enzyme also efficiently reduced menaquinone ($K_m = 106$ µM), pointing to the possibility that a naphthoquinone could serve as the enzyme's physiological electron acceptor (Schreiner and Eikmanns, 2005).

For its purification process, Triton X-114 is preferred over Triton X-100, given the considerably lower cloud point of the former (25 °C compared to 67 °C). The cloud point refers to the temperature at which a detergent solution divides into two distinct phases, thus facilitating the enrichment of the activated PQO (Gu and Galera-Gómez, 1995; Schreiner and Eikmanns, 2005). The stability and thermostability of purified PQO were investigated under various conditions. PQO showed stability for at least one week when stored at −20 °C in a specific buffer and maintained full activity at 55 °C for 15 minutes. However, its activity declined significantly at temperatures above 65 °C (Schreiner and Eikmanns, 2005). Furthermore, PQO exhibited optimal stability within a pH range of 5.5 to 8.5, with substantially diminished activity outside this range (Schreiner and Eikmanns, 2005). The overall reaction catalyzed by PQO is depicted in **Fig. 2**.

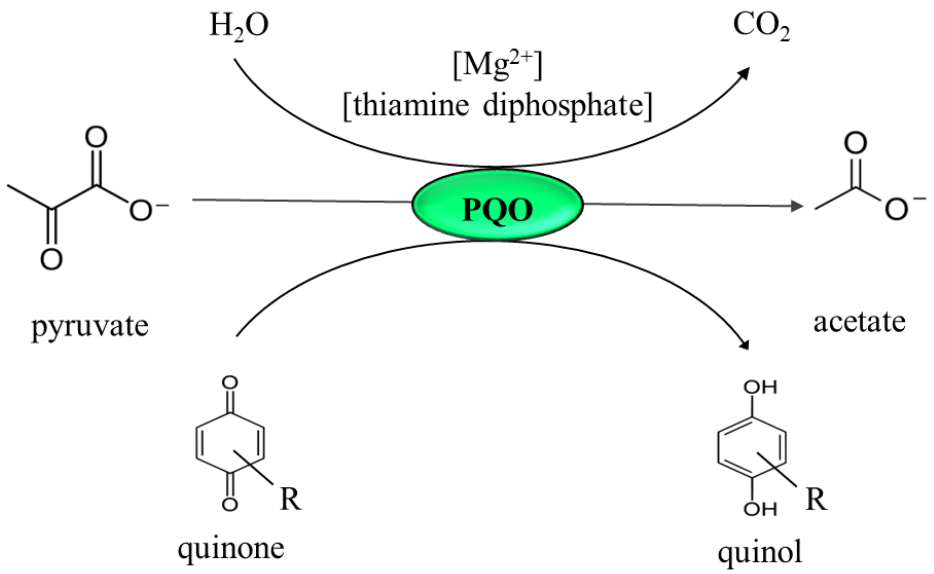


**Fig. 2: Oxidative decarboxylation of pyruvate to acetate, catalyzed by PQO from *C. glutamicum*.**

Further studies focused on the expression of the *pqo* gene. The transcription is initiated 45 bp upstream of the translational start site and the gene is organized in an operon together with genes encoding a putative metal-activated pyridoxal enzyme and a putative activator protein, MapA and TipA, respectively. Deletion of the chromosomal *pqo* gene led to the absence of PQO activity. Nevertheless, the impact of this deletion on growth in various conditions and glutamate production (in glucose minimal medium with Tween60 acting as an inducer), was negligible compared to the wildtype strain (Schreiner *et al*., 2006).

*C. glutamicum* possesses the enzymes acetate kinase and phosphotransacetylase (**Fig. 1**). Given that these enzymes promote the activation of acetate to acetyl-CoA, it was postulated that PQO activity combined with these two acetate-activating enzymes might function as an alternative route to the PDHC reaction (Schreiner and Eikmanns, 2005). This route would enable an alternative for oxidative decarboxylation of pyruvate, resulting in acetyl-CoA, $CO_2$ and reduced quinone (Schreiner and Eikmanns, 2005). However, a PDHC-deficient mutant, *C. glutamicum* Δ*aceE* exhibited restricted growth in both complex medium and in minimal medium with glucose. This suggests that under the tested conditions the PQO activity in the wildtype strain is not sufficient to mimic the PDHC function (Schreiner *et al*., 2006). To investigate whether enhanced PQO activity could offset missing PDHC function, plasmid-bound *pqo* was introduced in a PDHC-deficient *C. glutamicum* strain. The overexpression of the *pqo* gene in

this strain resulted in elevated specific PQO activity and enabled linear growth in complex medium. In contrast, growth experiments on diverse media revealed that the equivalent strain without plasmid showed no growth in complex medium and in glucose minimal medium, unless it was complemented with more than 0.1 % acetate These observations suggest that elevated PQO activity can at least partially substitute PDHC activity in *C. glutamicum* (Schreiner *et al*., 2006).

A later study showed that PQO might have biotechnological significance, as the deletion of the *pqo* gene in a PDHC-deficient *C. glutamicum* strain improved L-lysine accumulation by 13 % and led to an 30 % increased substrate-specific yield $Y_{P/S}$ in fed-batch fermentations with minimal medium supplemented with glucose, acetate and Brain-Heart-Infusion (BHI), compared to the parental strain (Blombach *et al*., 2008). Moreover, the removal of the *pqo* gene in a strain optimized for 2-ketoisovalerate production proved beneficial, i.e. an over twofold higher volumetric productivity and final concentration (Krause *et al*., 2010). Building on this optimized strain, *C. glutamicum* was further engineered for isobutanol synthesis, exploiting 2-ketoisovalerate as an essential precursor for isobutanol production (Blombach *et al*., 2011).

In *Escherichia coli*, a PQO-homologous enzyme, PoxB, exhibits a sequence identity of 47 % with the enzyme of *C. glutamicum*. Whereas soluble pyruvate oxidases (POXs) in *Lactobacillae* mediate the oxidative decarboxylation of pyruvate in the presence of phosphate and oxygen to produce acetyl phosphate, carbon dioxide, and hydrogen peroxide, PoxB in *E. coli* forms acetate instead of the high-energy compound acetyl phosphate (Sedewitz *et al*., 1984; Hager, 1957). In a past study, an artificial minimal respiratory chain comprising PoxB, cytochrome d terminal oxidase, and quinones within phospholipid vesicles, was constructed. This assembly facilitates electron transfer from pyruvate to oxygen in a liposome system, generating a transmembrane potential (Koland *et al*., 1984). This finding suggests that one function of PoxB in *E. coli* is to transfer reducing equivalents through quinols from the cytosol to the respiratory chain located at the membrane (Koland *et al*., 1984). Such functionality categorizes PoxB in *E. coli* as a pyruvate:quinone oxidoreductase (Sousa *et al*., 2023), analogous to the PQO in *C. glutamicum* and the CidC in *Staphylococcus aureus*, which has been demonstrated to efficiently reduce the quinone menadione (Zhang *et al*., 2017).

The mechanism of action for the *E. coli* PoxB has been the subject of significant research, as elucidated through comprehensive biochemical studies and supported by structural data (reviewed in Weidner *et al*., 2009). In the process of converting pyruvate into carbon dioxide and acetate, the first step involves transferring two electrons to an FAD cofactor attached to

PoxB. This reduction in flavin is hypothesized to induce a structural modification in the protein, unmasking a site with high lipid-binding affinity at the C-terminus of the enzyme (Recny and Hager, 1983; Mather and Gennis, 1985). When PoxB associates with the membrane, the electrons from the flavin are transferred to ubiquinone 8 (Q8), an integral component of the electron transport chain (Cunningham and Hager, 1975). PoxB's *in vitro* activity can be determined using reductase assays, where synthetic electron acceptors, such as ferricyanide, replace the physiological quinone Q8. In its "resting" (non-activated) state, the reductase activity of PoxB is modest but can be increased by the incorporation of lipids, detergents (Cunningham and Hager, 1971), or by limited proteolysis with α-chymotrypsin in presence of pyruvate and thiamine diphosphate (Russel *et al*., 1977).

Incorporation of lipids or limited proteolysis of PoxB alters both its turnover number and its affinity for pyruvate. The activation results in a 20-fold increase in its maximum reaction velocity ($V_{max}$) and a tenfold reduction of the Michaelis constant ($K_m$) (Chang and Cronan, 1984). Notably, whether the enzyme is activated through lipid/membrane interactions or proteolytic means, the resultant kinetic constants remain consistent, suggesting these activation processes yield similar enzyme forms in terms of structure and function (Weidner *et al*., 2009). In the context of limited proteolysis, the full-length enzyme undergoes cleavage of a segment encompassing the last 23 residues at its C-terminus (Russel *et al*., 1977), termed the α-peptide (residues 550–572). The removal of this peptide results in the formation of the fully activated $\Delta_{23}$-variant ($PoxB_{\Delta 23}$). Notably, this truncated form exhibits an activity profile comparable to the full-length enzyme but attains such activity without the requisite of lipids or detergents (Neumann *et al*., 2008).

Structural analyses of PoxB revealed that the C-terminal domain is notably well-anchored, with multiple hydrogen bonds and electrostatic interactions holding it in place. Furthermore, this domain obstructs access to the active site of the enzyme (Neumann *et al*., 2008). For the aforementioned α-peptide, which is part of the C-terminal domain, earlier speculations postulated that this peptide, specifically residues G559 to T568, might form an amphipathic α-helix that facilitates the binding of the enzyme to membranes (Recny *et al*., 1985). However, detailed structural examinations revealed that this segment forms an antiparallel two-stranded β-sheet structure, challenging earlier theories (Neumann *et al*., 2008). Nonetheless, when this peptide is synthesized and introduced to SDS micelles (which mimic a biological membrane), it does adopt an α-helical structure, but in the absence of these micelles, the peptide remains largely unstructured (Neumann *et al*., 2008; Weidner *et al*., 2009). Consequently, it is thought that PoxB's activation and membrane binding involve a sequence of structural shifts. Initially,

the reduction of FAD may cause some localized structural rearrangements that release the C-terminus from its interactions with other domains, thus granting access of the active site to the surrounding environment. The formation of the proposed amphipathic helix likely happens only when the C-terminus contacts a biological membrane (Weidner *et al*., 2009) (**Fig. 3**).

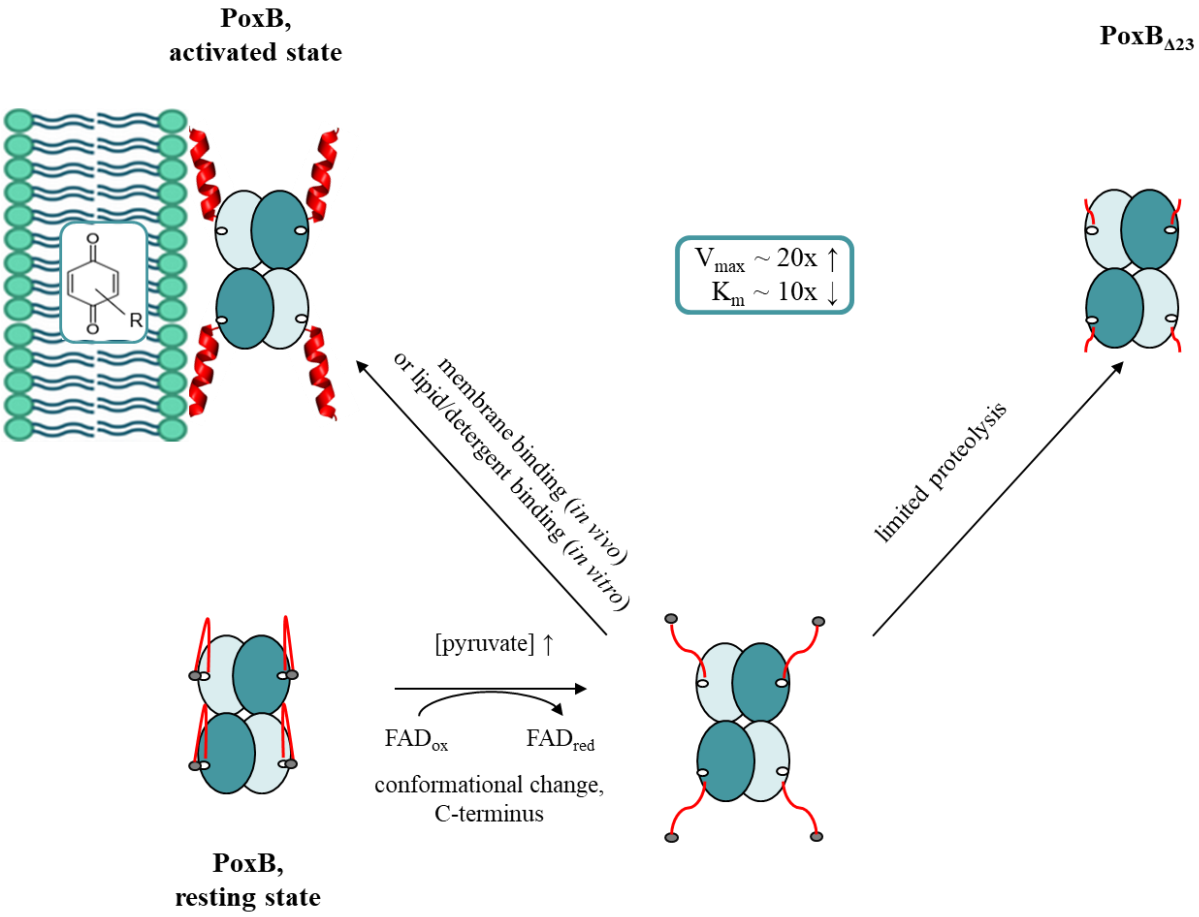


**Fig. 3: Model of activation for PoxB in *E. coli*.**

At lower pyruvate concentrations, PoxB is predominantly cytosolic, showing limited activity and substrate affinity. However, with an increase in pyruvate concentration, there is a reduction of the bound cofactor FAD, initiating a structural transformation that unveils the C-terminus as a primary lipid-binding site, facilitating active site accessibility. *In vivo* membrane interactions (with the C-terminus hypothesized to form an amphipathic α-helix, highlighted in red), *in vitro* associations with lipids/detergents, or specific proteolytic digestion, reinforce this activated configuration, boosting both enzyme activity and substrate affinity (based on Neumann *et al*., 2008).

While PoxB has been extensively characterized at both the biochemical and structural levels, its physiological significance remains elusive. Although its catalytic behavior implies an

important role at high intracellular pyruvate levels, PoxB in *E. coli* has been categorized as a non-essential enzyme, predominantly operational during the stationary phase as a wasteful back-up system to the PDHC. Notably, *poxB* expression is controlled by the sigma factor encoded by *rpoS*, which is transcribed during the late exponential phase. This factor is integral for regulating the expression of stationary-phase-associated genes (Chang *et al*., 1994).

*E. coli* strains devoid of PDHC can sustain growth with overproduced PoxB, even without external acetate supplementation. This observation reinforces prior suggestions that the acetate produced by PoxB is metabolically relevant (Chang and Cronan, 1983; Grabau and Cronan, 1984). Nonetheless, under such conditions, the growth rate is considerably lower, reaching only about 20 % of the rate observed when supplemented with acetate. Such a pattern points to the synthesis of acetyl-CoA from acetate as the potential rate-limiting step in growth (Grabau and Cronan, 1984).

Abdel-Hamid *et al*. (2001) highlighted the significance of PoxB, particularly in the absence of PDHC. When PDHC was absent, PoxB facilitated aerobic growth without reliance on externally added acetate. Under glucose-limited, aerobic conditions during continuous fermentation, the native promoter of PoxB maintained steady-states in PDHC-deficient strains exclusively at dilution rates $\leq 0.05\ h^{-1}$. This selectivity towards lower growth rates suggests a strategic adaptation where *E. coli* capitalizes on the seemingly counter-intuitive route of pyruvate to acetyl-CoA via acetate. Abdel-Hamid *et al*. further showed that aerobic growth efficiency of *E. coli*, encompassing aspects like growth rate, yield, and carbon conversion efficiency, is compromised in the absence of PoxB.

Subsequent research delved deeper into the metabolic implications of *poxB* gene deletion in *E. coli*, focusing on growth dynamics and enzymatic activities pivotal to central carbon metabolism (Li *et al*., 2007). The deletion resulted in overall decreased glucose uptake and growth rates, while also causing an increase in $O_2$ consumption and $CO_2$ release. From an enzymatic perspective, there was an enhancement in glucokinase activity, but this was offset by a decrease in glycolytic flow, attributed to reduced activity of glycolytic enzymes. In cultures grown in LB medium, the PoxB-deficient *E. coli* showed decreased activity of TCA cycle enzymes, such as citrate synthase and malate dehydrogenase. Conversely, the deletion resulted in increased activity of glucose-6-phosphate dehydrogenase and acetyl-CoA synthetase (Li *et al*., 2007).

The role of alternative pyruvate oxidation pathways, exemplified by the PQO reaction in *C. glutamicum*, so far remained enigmatic. While prior research hinted at PQO's non-essential

role (Schreiner and Eikmanns, 2005; Schreiner *et al*., 2006), this investigation took a comprehensive approach, encompassing both biochemistry and structural biology, while also building upon existing knowledge about the physiological role of its *E. coli* counterpart, PoxB.

One of the objectives of this study was the systematic investigation of PQO activities under various conditions, to gain insights into the potential metabolic functions of the enzyme. Building on these findings, another goal was to purify this enzyme natively from *C. glutamicum* for biochemical analysis, focusing on kinetic parameters and post-translational modifications. Additionally, the study aimed to elucidate the three-dimensional structure of the purified enzyme, seeking clues about its function and regulation. The cumulative knowledge from this and previous studies was utilized to conduct comparative experiments with various *C. glutamicum* strains, thereby inferring the physiological role of the enzyme.

Through this integrative approach, the research presented here aimed to elucidate the functional attributes and regulatory details of corynebacterial PQO, further deciphering its potential influence on carbon redistribution at the pivotal PEP-pyruvate-oxaloacetate node in *C. glutamicum*.

# 2 Material and methods

## 2.1 Chemicals

If not stated otherwise, all chemicals used in this thesis were purchased from Carl Roth GmbH & Co. KG (Karlsruhe), Sigma-Aldrich (Seelze), Otto Nordwald (Hamburg) or Merck KGaA (Darmstadt).

## 2.2 Bacterial strains, plasmids, and oligonucleotides

Bacterial strains and plasmids used in this study are listed in **Tab. 1**. Plasmids were constructed either by Gibson assembly (Gibson *et al.*, 2009; see 2.4.6) or via molecular cloning through restriction sites (see 2.4.2). Oligonucleotides used for these cloning procedures are listed in **Tab. 2** and were synthesized externally (Eurofins Genomics, Ebersberg).

**Tab. 1:** Bacterial strains and plasmids used in this study.

| Strain or plasmid | Relevant characteristics and usage | Source or reference |
|---|---|---|
| ***C. glutamicum*** | | |
| ATCC13032 | Wildtype (WT) | Kinoshita *et al.*, 1957 |
| Δ*pqo* | WT, 353 bp deletion within *pqo* gene | Schreiner *et al.*, 2006 |
| Δ*aceE* | WT, 2077 bp deletion within *aceE* gene | Schreiner *et al.*, 2005 |
| Δ*aceE* Δ*pqo* | double mutant, Δ*aceE* Δ*pqo* | Schreiner *et al.*, 2006 |
| ***E. coli*** | | |
| DH5α | $F^-$ Φ80dlacΔ(*lacZ*)M15 Δ(*lacZYA-argF*) U169 *endA1 recA1 hsdR17* ($r_K^-$, $m_K^+$) *deoR thi-1 phoA supE44* $\lambda^-$ *gyrA96 relA1*; used for cloning procedures | Hanahan, 1985 |
| **Plasmids** | | |
| pET-28a (+)-TEV | $Kan^R$, *lacI*$^q$, $P_{lac}$, $P_{T7}$, *ori* pBPR322, *ori* f1, T7term, $His_6$-tag, T7-tag, TEV site | GeneScript |
| pET28a (+)-TEV-*pqo*-$\Delta_{C17}$ | pET-28a(+)-TEV with *pqo*-$\Delta_{C17}$ insert | This work |
| pMiniT | $Amp^R$, $P_{SP6}$, $P_{T7}$, *ori* pMB1, toxic minigene | New England Biolabs |
| pMiniT-*pqo* | pMiniT with *pqo* insert, flanked by *Kpn*I and *Eco*RI restriction sites | This work |

| | | |
|---|---|---|
| pMiniT-*pqo*$^{K121A/E/R}$ | pMiniT-*pqo*, *pqo* mutated via site-directed mutagenesis, K121 replaced by either A, E or R | This work |
| pMiniT-*pqo*$^{K213A}$ | pMiniT-*pqo*, *pqo* mutated via site-directed mutagenesis, K213 replaced by A | This work |
| pMiniT-*pqo*$^{K325A/E}$ | pMiniT-*pqo*, *pqo* mutated via site-directed mutagenesis, K325 replaced by either A or E | This work |
| pMiniT-*pqo*$^{K500A/E}$ | pMiniT-*pqo*, *pqo* mutated via site-directed mutagenesis, K500 replaced by either A or E | This work |
| pJET | $Amp^R$, $P_{lacUV5}$, $P_{T7}$, *ori* pMB1, *eco47IR* | Thermo Scientific |
| pJET-*pqo* | pJET with *pqo* insert, flanked by *Kpn*I and *EcoR*I restriction sites | This work |
| pJET-*pqo*$^{K19A}$ | pJET-*pqo*, *pqo* mutated via site-directed mutagenesis, K19 replaced by A | This work |
| pJET-*pqo*$^{K304A}$ | pJET-*pqo*, *pqo* mutated via site-directed mutagenesis, K304 replaced by A | This work |
| pEKEx2 | $Kan^R$, *lacI*$^q$, $P_{tac}$, *ori* pBL1, *ori* colE1 | Eikmanns *et al.*, 1994 |
| pEKEx2-*pqo* | pEKEx2 with *pqo* insert | Schreiner and Eikmanns, 2005 |
| pEKEx2-*pqo*$^{K19A}$ | pEKEx2 with *pqo*$^{K19}$ | This work |
| pEKEx2-*pqo*$^{K121A/E/R}$ | pEKEx2 with *pqo*$^{K121A}$ or *pqo*$^{K121E}$ or *pqo*$^{K121R}$ | This work |
| pEKEx2-*pqo*$^{K213A}$ | pEKEx2 with *pqo*$^{K213A}$ | This work |
| pEKEx2-*pqo*$^{K304A}$ | pEKEx2 with *pqo*$^{K304A}$ | This work |
| pEKEx2-*pqo*$^{K325A/E}$ | pEKEx2 with *pqo*$^{K325A}$ or *pqo*$^{K325E}$ | This work |
| pEKEx2-*pqo*$^{K500A/E}$ | pEKEx2 with *pqo*$^{K500A}$ or *pqo*$^{K500E}$ | This work |
| pEKEx2-*pqo*-$\Delta_{C17}$ | pEKEx2 with *pqo*-$\Delta_{C17}$ insert | This work |
| pEKEx2-*his*$_6$_TEV-*pqo*-$\Delta_{C17}$ | pEKEx2 with *pqo*-$\Delta_{C17}$ insert, N-terminal $His_6$-tag and TEV site | This work |
| pPBEx2 | pEKEx2 derivative containing a correct *lacI*$^q$ allele and lacking replicate sequences | Bakkes *et al.*, 2020 |
| pPBEx2$^{\dagger}$ | pPBEx2 without *lacI*$^q$ and $P_{tac}$, linearized by *Pst*I and *Pvu*II | Reich, unpublished |
| pPBEx2$^{\dagger}$-*mCherry* | pPBEx2$^{\dagger}$ with *mCherry* insert, $P_{tuf}$ | This work |
| pPBEx2$^{\dagger}$-*mut2* | pPBEx2$^{\dagger}$ with *mut2* insert, $P_{tuf}$ | This work |

**Tab. 2:** Oligonucleotides used in this study.

| Name | Sequence (5' → 3') | Purpose |
|---|---|---|
| pET28a-TEV_lin_fwd | CTCGAGCACCACCACCAC | Amplification and linearization of pET28a-TEV to create vector backbone of pET28a (+)-TEV-*pqo*-$\Delta_{C17}$. |
| pET28a-TEV_lin_rev | TATGGCCCTGAAAATAA AGATTCTCGC | |
| pqo-$\Delta_{C17}$_in28a_fwd | CAGTGGTGGTGGTGGTG GTGCTCGAGTCATACTCC TCCACCAAAGACG | Amplification of the gene coding for PQO-$\Delta_{C17}$, lacking the sequence coding for the last 17 amino acids of PQO, to be inserted in pET-28a (+)-TEV. |
| pqo_in28a_rev | TCTTTATTTTCAGGGCCA TATGGCACACAGCTACGC AG | |
| px2_His-TEV-pqo$\Delta_{C17}$_fwd | GGATCCCCGGGTACCGA GCTTTAACTTTAAGAAGG AGATATACC | Amplification of the gene coding for PQO-$\Delta_{C17}$ containing an N-terminal $His_6$-tag and TEV-cleavage site from pET28a (+)-TEV-*pqo*-$\Delta_{C17}$. To be inserted in pEKEx2, linearized with *Sac*I. |
| px2_His-TEV-pqo-$\Delta_{C17}$_rev | ACGGCCAGTGAATTCGA GCTTCATACTCCTCCACC AA | |
| delta_C1_fwd | CACCCACTAAAAGCGGC ATAAACC CCGTTC | Amplification of part of pEKEx2-*pqo*, without sequence coding for the last 17 amino acids of PQO. To be ligated with Fragment C2, resulting in pEKEx2-*pqo*-$\Delta_{C17}$. |
| delta_C1_rev | TCAATCATCATACTCCTC CACCAAAGACG | |
| delta_C2_fwd | TGGAGGAGTATGATGATT GATACACCTGC | Amplification of part of pEKEx2-*pqo*, without sequence coding for the last 17 amino acids of PQO. To be ligated with Fragment C1, resulting in pEKEx2-*pqo*-$\Delta_{C17}$. |
| delta_C2_rev | TATGCCGCTTTTAGTGGG TGCGAAGAATAG | |
| K19A_fwd | TCAAGGTGTGgcaCGAATT TATGGTTTG | Oligonucleotides for site-directed mutagenesis to replace the codon for K19 to A. The new codon used in the forward oligonucleotide is marked with small letters. |
| K19A_rev | GCTTCCAAAGTGTCAATT AATTG | |
| K121A_fwd | GATTTTGTTTgcaGAATGC TCTGGTTACTGCGAG | Oligonucleotides for site-directed mutagenesis to replace the codon for K121 to either A or R. The new codon used in the forward oligonucleotide is marked with small letters. |
| K121R_fwd | GATTTTGTTTcgaGAATGC TCTGGTTACTGCGAG | |
| K121A_R_rev | TCCGGATGCGTTTCCTGG | |
| K121E_fwd | CGGAGATTTTGTTTgagGA ATGCTCTG | Oligonucleotides for site-directed mutagenesis to replace the codon for K121 to E. The new codon used in the forward oligonucleotide is marked with small letters. |
| K121E_rev | GATGCGTTTCCTGGAAGA AC | |

| | | |
|---|---|---|
| K213A_fwd | TGCGGGCGTGgcaAATGCTCGCG | Oligonucleotides for site-directed mutagenesis to replace the codon for K213 to A. The new codon used in the forward oligonucleotide is marked with small letters. |
| K213A_rev | CCGCAGAACAAAGTGACAGAC | |
| K304A_fwd | TACCACGGTGgcaTATCCGGTGACCGGTG | Oligonucleotides for site-directed mutagenesis to replace the codon for K304 to A. The new codon used in the forward oligonucleotide is marked with small letters. |
| K304A_rev | CGTCGACCAATGTGCGCA | |
| K325A_fwd | TGTGAAGGAAgcaACAGATCGTTC | Oligonucleotides for site-directed mutagenesis to replace the codon for K325 to either A or E. The new codon used in the forward oligonucleotide is marked with small letters. |
| K325E_fwd | TGTGAAGGAAgagACAGATCGTTC | |
| K325A_E_rev | TGAGGCAAAATATTTTCGATTG | |
| K500A_fwd | TGCGGGTATCgcaTCGGTACGCATCACC | Oligonucleotides for site-directed mutagenesis to replace the codon for K500 to either A or E. The new codon used in the forward oligonucleotide is marked with small letters. |
| K500E_fwd | TGCGGGTATCgagTCGGTACGCATC | |
| K500A_E_rev | GCCGCCGCAATCTCTGCG | |
| $P_{tuf}$_fwd | CGGGAAACCTGTCGTGCCAGCTGCCACAGGGTAGCTGG | Oligonucleotides for amplification of $P_{tuf}$, to be inserted in pPBEx2†. |
| $P_{tuf}$_rev | TGCTCACCATGGTATGTCCTCCTGGACTTC | |
| mCherry_fwd | AGGACATACCATGGTGAGCAAGGGCGAG | Oligonucleotides for amplification of *mCherry,* to be inserted in pPBEx2†. |
| mCherry_rev | TCCTCTAGAGTCGACCTGCATTACTTGTACAGCTCGTCCATG | |
| mut2_fwd | AGGACATACCATGAGTAAAGGAGAAGAAC | Oligonucleotides for amplification *mut2,* to be inserted in pPBEx2†. |
| mut2_rev | TCCTCTAGAGTCGACCTGCATTATTTGTATAGTTCATCCATGC | |

## 2.3 Media and cultivation conditions

All media used in this work for the cultivation of *C. glutamicum* or *E. coli* were prepared in deionized water and were sterilized by autoclaving at 121 °C for 20 min. Solid media were obtained by addition of Bacto$^{TM}$ agar at 15 g/L to the medium. If needed, the antibiotics kanamycin (50 µg/mL) or ampicillin (100 µg/mL) were added in the given concentrations. For strains carrying the pEKEx2 plasmid, gene overexpression was induced by adding sterile 0.5 mM isopropyl-β-D-thiogalactopyranoside (IPTG) to the culture, 2 h after growth. For cultivation in complex medium, 2xTY medium was used with the following composition: 16 g Bacto$^{TM}$ Tryptone /L, 10 g Bacto$^{TM}$ Yeast Extract /L and 5 g NaCl /L (Sambrook and Russell, 2001). Cultivations of *C. glutamicum* in minimal medium were carried out in modified CGXII medium (Eikmanns *et al.*, 1991; **Tab. 3**).

**Tab. 3:** Composition of modified CGXII medium (based on Eikmanns *et al.*, 1991).

| Name | Concentration (g/L) |
|---|---|
| MOPS | 21 |
| $(NH_4)_2SO_4$ | 10 |
| Urea | 5 |
| $K_2HPO_4$ | 1 |
| $KH_2PO_4$ | 1 |
| $MgSO_4$ x 7 $H_2O$ | 0.25 |
| $CaCl_2$ x $H_2O$ | 0.01 |
| Biotin | $0.2 * 10^{-3}$ |
| **TES (1000x)** | 1 mL/L |
| $FeSO_4$ x 7 $H_2O$ | 16 |
| $MnSO_4$ x 7 $H_2O$ | 10 |
| $ZnSO_4$ x 7 $H_2O$ | 1 |
| $CuSO_4$ x 5 $H_2O$ | 0.2 |
| $NiCl_2$ x $H_2O$ | 0.02 |

The chemicals ammonium sulfate, urea, both potassium phosphates and 3-(N-morpholino)propanesulfonic acid (MOPS) were dissolved in deionized water and the pH adjusted to 7.0 for cultivation with glucose, to 6.5 for cultivations with glucose and acetate and to 6.3 for cultivations with acetate by adding appropriate amounts of 5 M potassium hydroxide. Calcium chloride and magnesium sulfate were prepared as sterile 1000-fold stock solutions and added after pH adjustment. Biotin, sterilized via filtration, and trace element solution (TES, **Tab. 3**) were added after autoclaving, each were prepared as 1000-fold stock solutions. Both glucose and (potassium) acetate were prepared as sterile filtered 50 % (w/v) stock solutions and added after autoclaving to either 2xTY or modified CGXII medium, if needed. For cultivations in the DASGIP® fermentation plant (see section 2.3.1), MOPS and urea were omitted.

For cultivation of either *C. glutamicum*- or *E. coli* strains, the organisms were streaked out from glycerol stocks (30 % (v/v)) to 2xTY medium agar plates and incubated for two days at 30 °C (*C. glutamicum*) or one day at 37 °C (*E. coli*). After incubation of the plates, single colonies were used to inoculate a glass tube containing 5 mL 2xTY medium and incubated aerobically for about 8 h at 150 rpm.

For growth experiments with *C. glutamicum* strains in shake flasks, pre-cultures were generated by transferring the whole content of the inoculated glass tube to 50 mL of 2xTY medium in 500 mL baffled shake flasks. These pre-cultures were cultivated aerobically at 130 rpm over night at 30 °C. The pre-culture was transferred to a 50 mL tube and the cells were harvested by centrifugation (3,200 g, 10 min). For cultivations in CGXII minimal medium, cells were washed once with 0.9 % (w/v) sodium chloride and resuspended in a small volume before inoculation. For cultivations in 2xTY medium, the cells were resuspended in a small volume directly before inoculation. This suspension was used to inoculate 50 mL of the desired medium in 500 mL baffled shake flasks to an $OD_{600}$ between 1 to 1.5. Cultivations were performed aerobically at 130 rpm at 30 °C and growth of the cultures was monitored by measuring the $OD_{600}$.

### 2.3.1 Cultivation in bioreactor (Münßinger, 2022)

**General setup**

As depicted in **Fig. 4**, the overall setup of the DASGIP® Parallel Bioreactor System (Eppendorf, Jülich) was composed by a GA2 controlling module for the analysis of the off-gases carbon dioxide and oxygen (in two out of four reactors), a PH4PO4 module for the analysis of pH and dissolved oxygen (DO) value, a TC4SC4 module for temperature control and agitation (stirrer

control in dependency from the setpoint for DO), a MP8 pumping module for eight peristaltic pumps for acid/base control, a Bioblock with an integrated DASGIP® CWD4 distributer for cooling water, a RX2/4 module for the regulated fumigation with pressured air and a bioprocess computer. All process parameters were set and monitored with the program DASGIP® Control 4 and cultivations were performed in 1.4 L bioreactors. Within the lid of the bioreactor vessel there are three ports, each for a sensor monitoring the parameters mentioned above: a DO sensor (InPro 6000 series, Mettler Toledo), a pH sensor (Type 465, Mettler Toledo) and a temperature sensor (DASGIP®).

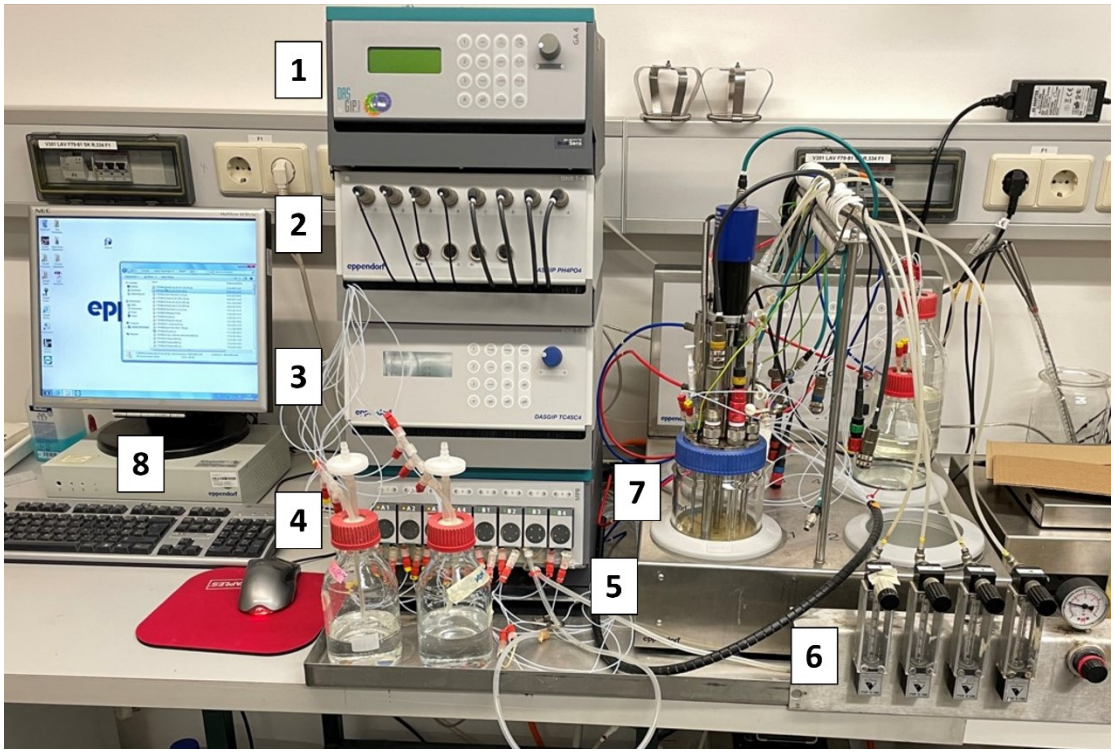


**Fig. 4: General setup of the DASGIP® Parallel Bioreactor System.**

The system is composed by a GA2 module (1) for off-gas analysis, a PH4PO4 module for the analysis of pH and dissolved oxygen (DO) value (2), a TC4SC4 module for temperature control and agitation (3), a MP8 pumping module for eight peristaltic pumps for acid/base control (4), a bioblock with an integrated CWD4 distributer for cooling water (5), a RX2/4 module for the regulated fumigation with pressured air (6) and a bioprocess computer (8). Cultivations were carried out in 1.4 L bioreactors containing 700 mL medium (7).

**Batch fermentation**

For batch fermentations, 700 mL CGXII medium with 1 % (w/v) glucose (without MOPS and urea) were inoculated with *C. glutamicum* strains to an $OD_{600}$ of 1.5, pre-cultivation was performed as described before for shake flask experiments. If not stated otherwise, cultivation was carried out at pH 7, adjusted automatically with 2 M $H_2SO_4$ and 2 M KOH, a constant DO level of 30 %, controlled via a stirrer cascade (400 – 1,200 rpm), and at 30 °C. To circumvent foam over, Struktol® J 647 (Schill+Seilacher GmbH, Böblingen) was added dropwise manually, if needed.

**Continuous fermentation**

The setup described for batch fermentations was expanded with two external pumps. One pump was used for a continuous feed from a 10 L bottle with CGXII medium with 1 % (w/v) glucose and 30 µg protocatechuic acid /mL, connected through a short sampling tube of the 3-way port of the lid of the bioreactor. The pump rate was set according to the desired growth rate at which *C. glutamicum* should grow. To keep the reaction volume within the bioreactor constant, a second external pump to harvest was connected through a long sampling tube of the 3-way port. The level of the tube was adjusted depending on the filling level of the reactor vessel and the pump rate was set higher than the pump rate of the feed. Due to the relatively constant agitation during the cultivation, no deviations in the harvesting volumes were observed over time. The harvested cell suspension was pumped into a second 10 L bottle.

For the cultivation process itself, first a batch process in CGXII medium with 1 % (w/v) glucose (i.e., without the external pumps) and 30 µg protocatechuic acid /mL acid was performed to generate the necessary concentration of biomass. The switch to the continuous mode was performed in the time after the appearance of the ’hunger-peak’ of the DO signal. This peak appeared when the cells consumed all glucose in the medium, hence no growth and oxygen consumption took place. However, due to the consumption of secondary metabolites in the medium, *C. glutamicum* was again able to grow aerobically, hence the DO levels fell again for a short period. The switch to continuous mode was started manually by turning on the external pumps. All continuous fermentations were performed at a constant pH of 7, a constant DO level of 30 %, controlled via a stirrer cascade (150 – 900 rpm) at 30 °C. For all fermentations, five volume exchanges with fresh medium were conducted. After every exchange, sterile controls were done to confirm whether the whole process was free of contaminants.

## 2.4 Molecular biology

### 2.4.1 Polymerase chain reaction (PCR) (Mullis *et al*., 1986)

Amplification of DNA through PCR for cloning purposes was performed with the Q5 DNA polymerase according to manufacturer's instructions (New England Biolabs, Frankfurt), using a 25 µL reaction setup. Annealing temperatures for the oligonucleotides were calculated using the online tool '$T_m$ calculator' (New England Biolabs). For initial screening of putative positive transformants after transformation of competent *E. coli* or *C glutamicum* strains with plasmids or ligation reactions (see section 2.4.5 and 2.4.6), 'Colony PCR' with single colonies was performed using 'RedMastermix' according to manufacturer's instructions (Genaxxon, Ulm).

### 2.4.2 Agarose gel electrophoresis

DNA fragments were separated and visualized using agarose gel electrophoresis and ethidium bromide staining followed by UV light detection. Depending on the size of the DNA fragments, agarose was dissolved in TAE buffer (40 mM tris(hydroxymethyl)aminomethane [Tris, pH 7.5], 20 mM acetic acid and 1 mM ethylenediaminetetraacetic acid [EDTA]) to a final concentration of either 1 or 2 % (w/v). The electrophoretic separation was performed in TAE buffer at 130 V for 35 min in gel chambers. GeneRuler™ 1 kb DNA Ladder or 50 bp DNA ladder (Thermo Scientific; Dreieich) were used as markers.

### 2.4.3 DNA isolation

DNA fragments obtained after PCR and separated via agarose gel electrophoresis were isolated with the 'NucleoSpin® Gel and PCR clean-up-Kit' (Macherey-Nagel, Düren) according to the manufacture's instruction. Plasmid DNA was isolated using the 'NucleoSpin® Plasmid Kit' (Macherey-Nagel). For this purpose, 5 mL 2xTY medium was inoculated with single colonies from agar plates of *E. coli* or *C. glutamicum* strains harboring the plasmid of interest. Plasmid DNA from this culture was isolated according to the manufacture's instructions.

### 2.4.4 Restriction digest of DNA

Restriction digest of DNA was performed with 'Fast digest' restriction enzymes according to manufacturer's instructions (Thermo Scientific). DNA fragments were afterwards separated and verified via agarose gel electrophoresis.

### 2.4.5 Site directed *pqo* mutagenesis and ligation of DNA fragments with T4 ligase

Site directed mutagenesis was performed with the 'NEB Q5 Site Directed Mutagenesis Kit' (New England Biolabs) according to manufacturer's instructions. As template, *pqo* flanked with restriction sites for *Kpn*I and *EcoR*I within the sub-cloning vectors pJET or pMiniT was used. Mutations for codons were introduced through oligonucleotides listed in **Tab. 2**. For the transfer of mutated *pqo* genes from pMiniT or pJET vectors to the pEKEx2 vector, the gene was isolated from these plasmids via restriction digestion with *Kpn*I and *EcoR*I and subsequent agarose gel electrophoresis of the DNA fragments. The mutated genes were ligated with *Sac*I-linearized pEKEx2 via T4 DNA ligase (Thermo Fisher Scientific) according to manufacturer's instructions. *E. coli* DH5α was then transformed with 5 µL of this ligation reaction as described in section 2.5. All plasmids were verified via sequencing (Eurofins Genomics, Ebersberg).

### 2.4.6 Gibson assembly (Gibson *et al*., 2009)

For the ligation of genes in linearized plasmids (except plasmids constructed as described in section 2.4.5, site directed mutagenesis), Gibson assembly was performed. Oligonucleotides were designed with the 'NEBuilder®' online tool (New England Biolabs). For the reaction, a master mix was prepared according to manufacturer's instructions and stored at -20 °C until further use. The reaction was prepared on ice by mixing 50 ng of linearized plasmid, a threefold molar excess of insert and 10 µL of the twofold concentrated master mix in a total volume of 20 µL, nuclease-free water was added if appropriate. The mixture was incubated at 50 °C for 1 h and up to 10 µL were used for transformation of competent *E. coli* DH5α cells.

## 2.5 Preparation of competent cells and transformation

*E. coli*

Chemo-competent *E. coli* DH5α cells were prepared based on Inoue *et al*., 1990. A single colony from an agar plate was used to inoculate a glass tube with 5 mL of 2xTY medium. Next day, this pre-culture was used to inoculate 200 mL SOB medium (20 g Bacto™ Trypton /L, 5 g Bacto™ Yeast extract /L, 0.5 g NaCl /L, 0.186 g KCl /L; after autoclaving: $MgCl_2$ [stock 250 g/L]: 1 mL/L and $MgSO_4$ x 7 $H_2O$ [stock: 250 g/L]: 1 mL/L). The culture was grown under shaking at 130 rpm and 30 °C until an approximate $OD_{600}$ of 0.4. The culture was incubated afterwards for 10 min on ice and harvested via centrifugation (3,200 g, 4 °C, 10 min). The

sedimented cells were resuspended in 80 mL ice cold TB buffer (10 mM 4-(2-hydroxyethyl)-1-piperazineethanesulfonic acid [HEPES, pH 6.7], 250 mM KCl, 15 mM $CaCl_2$, 55 mM $MnCl_2$) and the suspension was incubated on ice for 10 min. Next, cells were sedimented again via centrifugation (3,200 g, 4 °C, 10 min) and resuspended in 20 mL ice-cold TB buffer. After drop-wise addition of 1.4 mL dimethyl sulfoxide (DMSO), the bacterial suspension was aliquoted in 50 µL portions in test tubes and frozen immediately in liquid nitrogen. Until use, the aliquots were stored at -80 °C.

For transformation, the aliquots were thawed on ice for 15 min and mixed gently with up to 10 µL of plasmid or ligation reaction. Next to another incubation on ice for 15 min, a heat-shock (incubation for 45 s at 42 °C) was performed. Subsequently, the cells regenerated by adding 1 mL 2xTY medium and incubating them under constant shacking for 30 min at 37 °C. Recombinant cells were selected by platting the culture on agar plates with appropriate antibiotics.

*C. glutamicum*

Electro-competent *C. glutamicum* cells were obtained as described by Liebl *et al*., 1989. 2 mL of a *C. glutamicum* pre-culture was used to inoculate 200 mL BHIS medium (37 g brain heart infusion /L, 91 g sorbitol /L). The culture was grown to an approximate $OD_{600}$ of 1.6, harvested via centrifugation (3,200 g, 4 °C, 20 min) and resuspended in 20 mL ice-cold TG buffer (1 mM Tris, pH 7.4, 10 % (v/v) glycerol). This step was repeated except that the cells were resuspended in 10 mL TG buffer. The suspension was centrifuged again, and the cells were resuspended in 10 mL 10 % (w/v) glycerol. Finally, centrifugation was repeated, and the sediment was resuspended in 2 mL 10 % (v/v) glycerol. Aliquots of 150 µL were prepared and frozen immediately in liquid nitrogen. Until use, the aliquots were stored at -80 °C.

For transformation, the cells were thawed on ice for 15 min. After adding 6 µL of plasmid, the sample was incubated on ice for 15 min. The cells were transferred to an ice-cold electroporation cuvette and electroporated in the 'Micro PULSER™' apparatus at a 2.5 kV pulse. Adding 1 mL of 2xTY medium, the bacterial suspension was passed to a reaction tube and then incubated for 6 min at 46 °C. For regeneration, the suspension was pipetted to a glass tube with 4 mL 2xTY medium and incubated under continuous shaking for 1 h at 30 °C. Recombinant cells were selected by platting the culture on agar plates with appropriate antibiotics.

## 2.6 Biochemical methods

### 2.6.1 Preparation of cell-free extracts (Schreiner, 2004)

Pyruvate:quinone oxidoreductase (PQO) activity measurements were performed with cell-free extracts of *C. glutamicum*. For disruption, *C. glutamicum* cultures were harvested, the cells washed at least once in 0.9 % (w/v) NaCl and resuspended to a total volume of 1 mL in in 100 mM 2-(n-morpholino)ethanesulfonic acid (MES) (pH 6.0) with 10 % (v/v) glycerol, additionally 1 mM phenylmethylsulphonyl fluoride was added as protease inhibitor. The cell suspension was transferred to a 2 mL micro tube filled with 250 mg glass beads and subsequently the cells were disrupted in a cell homogenizer (FastPrep-24™ 5G, M.P. Biomedicals, Santa Ana California, USA) at 6,500 rpm and 4 °C in four cycles. Separation of cell debris and glass beads from cell extract was achieved by centrifugation at 11,000 g at 4 °C for 45 min. The supernatant was transferred subsequently in a new reaction tube and was immediately measured for enzyme activity or stored at -20 °C until further use.

### 2.6.2 Determination of protein concentrations

The protein concentration within cell-free extracts was determined with the 'Pierce™ BCA Protein Assay Kit' (Thermo Scientific) according to manufacturer's instructions. The concentration of a pure protein solution was determined using the fluorescence based 'Qubit™ Protein Assay Kit' according to the manufacturer's instructions (Thermo Scientific).

### 2.6.3 Purification of PQO and PQO variants

#### 2.6.3.1 Purification of PQO and PQO variants with Triton X-114 extraction

The purification of PQO (and variants) natively from *C. glutamicum* strains was achieved based on a protocol established by M. Schreiner and the works of Zhang and Hager with the *E. coli* homologue of PQO, the PoxB (Schreiner, 2004; Zhang and Hager, 1987). Briefly, the protocol exploits the characteristic that in presence of its substrate and cofactors, PQO binds to the detergent Triton X-114, contrarily to other cytosolic proteins in *C. glutamicum*. This property is reversible when substrate and cofactors are absent, and thus PQO can be extracted back in aqueous phase to homogeneity.

Beginning with cell-free extracts (see section 2.6.1), ultracentrifugation was performed (180,000 g, 1.5 h) and the supernatant was collected. A heat precipitation step (49 °C, 3 min)

was performed and the sample was ultracentrifuged again (100,000 g, 50 min). With the resulting supernatant, the Triton X-114 extraction method was used, as described in detail in Scheiner and Eikmanns, 2005. Purified samples were kept in 100 mM MES (pH 6.0) with 10 % glycerol.

#### 2.6.3.2 Purification of $His_6$-PQO-$\Delta_{C17}$

For purification of His-tagged PQO-$\Delta_{C17}$ from *C. glutamicum* Δ*pqo* (pEKEx2-$his_6$_TEV-*pqo*-$\Delta_{C17}$), cells were disrupted as described before, except that the cells were resuspended in binding buffer (20 mM sodium phosphate buffer [pH 7.4], 500 mM sodium chloride, 40 mM imidazole). Cell extracts were ultracentrifuged and heat precipitation was performed as described before (see section 2.6.3.1). Next, nickel-affinity chromatography was conducted by applying the sample through a 50 mL super-loop to a pre-equilibrated (with binding buffer) 1 ml HisTrapFF column (Cytiva, Freiburg) on an 'ÄKTA pure™' system (Cytiva). His-tagged PQO-$\Delta_{C17}$ was eluted by applying 100 % of elution buffer (20 mM sodium phosphate buffer [pH 7.4], 500 mM sodium chloride, 500 mM imidazole). To remove imidazole, a 30 kDa cut-off filter (Amicon Ultra-15, Merck) was used and the retained sample was resuspended in 25 mM sodium phosphate buffer (pH 7.4), 125 mM sodium chloride, and 5 mM dithiothreitol (DTT). The His-Tag was consequently removed with TEV-protease and a 100 kDa cut-off filter (Vivaspin 2, Sartorius) was used to separate PQO-$\Delta_{C17}$ from the His-tag and the TEV-protease. The retained sample was resuspended in 100 mM MES (pH 6.0) with 10 % glycerol.

### 2.6.4 PQO assay (Schreiner and Eikmanns, 2005)

Cell extracts (see section 2.6.1) or pure protein solutions were analyzed for PQO activity using the test buffer mentioned below. The decrease in absorption at 600 nm was photometrically monitored over time in a photometer (Ultrospec 2100 pro UV/Vis Spectrophotometer, Pharmacia Biotech). All activity measurements were performed at 30 °C and samples were pre-heated in cuvettes at 30 °C for at least 5 min before measurement. Enzyme activity is represented in units per milligram of protein, where 1 U is defined as 1 mol of substrate reduced per minute. To calculate the specific enzyme activity, the following formula was used.

Specific activity [U/mg] = ($\Delta E$ / ($\Delta t$ * $V_{Total}$)) / ($\varepsilon$ * d * $V_{Sample}$ * $concentration_{Protein}$)

**$concentration_{Protein}$** = concentration of sample (mg/mL)

**d** = layer thickness of the cuvette (1 cm)

**$\varepsilon$** = extinction coefficient of substance measured during test ($mM^{-1}$ * $cm^{-1}$)

**$\Delta E$** = change in absorbance in the cuvette

**$\Delta t$** = period of the measurement ($min^{-1}$)

**$V_{Sample}$** = volume of cell extract or pure protein solution used, variable (1 mL)

**$V_{Total}$** = total volume in cuvette (1 mL)

The reaction catalyzed by PQO is the oxidative decarboxylation of pyruvate to acetate, where presumably *in vivo* a quinone is reduced to a quinol. Specific activity of the PQO enzyme was quantified *in vitro* by measuring the absorption change of 2,6-dichloroindophenol (DCPIP) at 600 nm, with $\varepsilon_{600}$ = 22 $mM^{-1}$ * $cm^{-1}$. Upon reduction, the absorption of DCPIP decreases (also observable by color change from blue to white). As test buffer, 100 mM MES (pH 6.0), 10 mM $MgCl_2$, 0.1 mM thiamine diphosphate (TPP), 0.5 % (w/v) n-dodecyl-β-D-maltoside (DDM) and 0.3 mM DCPIP were used in the given final concentrations. As change from the original reference, DDM instead of Triton X-100 was used as an activator of PQO. Adding a varying amount of protein sample, the reaction was started by adding pyruvate to a final concentration of 100 mM.

### 2.6.5 SDS-PAGE (Laemmli, 1970) and Western blot (adapted from Towbin *et al.*, 1979)

Analytical separation of proteins according to mass was performed via sodium dodecyl sulfate polyacrylamide gel electrophoresis (SDS-PAGE). 10 % polyacrylamide gels were formed with the 'TGX™ FastCast™ Acrylamide Starter Kit' based on manufacturer's instructions (Bio-Rad Laboratories Inc., Feldkirchen). Sample were prepared by mixing with loading buffer (final concentration of 62.5 mM Tris [pH 6.8], 2 % (w/v) SDS, 10 % (v/v) glycerol, 5 % (w/v) β-mercaptoethanol and 0.001 % (w/v) bromophenol blue) and incubating them for 5 min at 95 °C. 5 µg of protein mixtures or 1 µg of a pure protein solution were applied per well in a gel. Electrophoretic separation was performed in a Mini-PROTEAN® Tetra System (Bio-Rad Laboratories Inc.) filled with running buffer (25 mM Tris [pH 8.8], 192 mM glycine, 0.1 % (w/v) SDS) at 15 mA per gel. As a marker, the PageRuler™ Prestained Protein Ladder

(Thermo Scientific) was used. Gels were silver stained using 'Pierce™ Silver Stain Kit' (Thermo Scientific) according to manufacturer's instructions.

For detection of His-tagged proteins, transfer of proteins to a PVDF membrane from SDS-PAGE gels was performed in a 'Trans-Blot® Turbo™' device (Bio-Rad Laboratories Inc.) for 20 min at 1 A and 25 V according to manufacturer's instructions. To avoid unspecific binding of antibodies, the membrane was blocked overnight at 4 °C in 3 % bovine serum albumin (BSA) in TBST buffer (50 mM Tris [pH 7.5], 0.9 % (w/v) NaCl, 0.1 % (v/v) Tween20). Next to washing the membrane for 5 min in TBST buffer, the primary antibody (Anti-6-His antibody [mouse], Sigma-Aldrich, diluted 1:3000) was added and incubated with the membrane for 1 h at room temperature. Before adding the secondary antibody (Anti-Mouse IgG-HRP [goat], Sigma-Aldrich, diluted 1:2000), the membrane was washed three times for 5 min each in TBST. After incubation for 1 h at room temperature, the membrane was washed again three times as described before. Protein bands were detected by incubating the membrane with the 'SuperSignal™ West Femto Maximum Sensity Substrate' and visualizing it in the iBright FL1000 device (both Thermo Scientific).

## 2.7 Miscellaneous

### 2.7.1 Fluorescence measurements

Fluorescence measurements for the co-culture experiments were conducted by washing the harvested cells (1 mL of culture) in 0.9 % NaCl and resuspending them again in 1 mL of 0.9 % NaCl. The bacterial suspension was transferred to a black 96-well microtiter plate (Sarstedt AG & Co. KG, Nümbrecht) and fluorescence was determined in an infinite® 200 plate reader (Tecan Group AG, Männedorf). For detection of the red fluorescent protein mCherry, emission at 610 nm was measured with an excitation wavelength of 570 nm. For detection of the green fluorescent protein Mut2, excitation and emission wavelengths were at 450 and 530 nm, respectively. All detected signals were normalized to the $OD_{600}$ of the respective co-culture.

### 2.7.2 Bioinformatics

DNA sequences (plasmids, sequencing data, *in silico* PCR, *in silico* restriction digest) were visualized and analyzed in 'CLC Main Workbench 8' (Qiagen, Hilden, DE). Alignment of protein sequences were performed with the 'Basic Local Alignment Search Tool' (BLAST) and ClustalΩ (Thompson *et al.*, 1994) and visualized using Jalview (Clamp *et al.*, 2004). Sequences of genes coding for proteins of *C. glutamicum* ATCC 13032 were retrieved from the sequenced

genome, available online (Kalinowski *et al.*, 2003). Evaluation of enzyme activity data and growth experiments were performed with ‘Microsoft Excel’ (Microsoft, Redmond), visualization of these data was done in ‘GraphPad Prism 8’ (GraphPad Software Inc., Boston). Three dimensional structures of proteins were analyzed and visualized with ‘PyMol’ (Schrödinger Inc., New York), predictions of protein structures were performed using ‘AlphaFold 2’ (Jumper *et al.*, 2020).

# 3 Results

The pyruvate branching point encompasses a series of reactions that link the main pathways of carbon metabolism and determines the distribution of carbon flow between catabolism and anabolism (reviewed in Sauer and Eikmanns, 2005, see also **Fig. 1**). The conversion of pyruvate to acetyl-CoA for fueling the TCA cycle in aerobic bacteria is primarily accomplished through oxidative decarboxylation by the PDHC. The function of alternative pyruvate oxidation routes, such as the PQO reaction in *C. glutamicum*, remains to date unclear. Despite previous studies revealing no observable phenotype associated with the presence or absence of PQO (Schreiner and Eikmanns, 2005; Schreiner *et al.*, 2006), this research sought to delve deeper into this topic by utilizing a multi-disciplinary approach that combines experiments in biochemistry and structural biology. By utilizing these techniques, the aim of this research was to analyze the characteristics and regulatory mechanisms of PQO and to determine the potential role of PQO in the regulation of carbon flow at the pyruvate node in *C. glutamicum*.

## 3.1 Carbon source and growth phase modulate PQO activity in *C. glutamicum*

To gain a comprehensive understanding of the regulation of PQO activities under various conditions, *C. glutamicum* wildtype, a PQO-deficient and a PQO overproducer strain (*C. glutamicum* Δ*pqo* and *C. glutamicum* Δ*pqo* (pEKEx2-*pqo*), respectively) were cultivated either in 2xTY complex medium or in CGXII minimal medium with or without 1 % acetate or 1 % glucose. Under the conditions tested, no growth phenotype was observed between the wildtype, PQO-deficient and the PQO overproducer strains (data not shown).

Specific PQO activities in cell extracts of the three *C. glutamicum* strains were determined in both the mid-exponential and late stationary phase (24 h of cultivation) (**Fig. 5**). The *pqo* deletion strain showed no detectable activity under all conditions tested, while the wildtype strain displayed the highest overall activity in 2xTY medium at the stationary phase (approximately 0.08 U/mg protein) and the lowest overall activity in acetate minimal medium at both the exponential and stationary phase (less than 0.01 U/mg protein). The addition of either 1 % glucose or 1 % acetate to 2xTY medium led to a stepwise decrease in specific PQO activities at the stationary phase (lowest in 2xTY medium with 1 % acetate with 0.038 U/mg protein). At the exponential phase, the activities in 2xTY medium-grown cells with or without additional carbon source were up to fourfold lower compared to the activities in the stationary phase. The cultivation of the wildtype in acetate minimal medium resulted in a twofold decrease

in activity compared to that seen in cells grown in glucose minimal medium, with values less than 0.01 U/mg protein and approximately 0.025 U/mg protein, respectively. These findings suggest that the activity of corynebacterial PQO is influenced by both the type of carbon source and the growth phase.

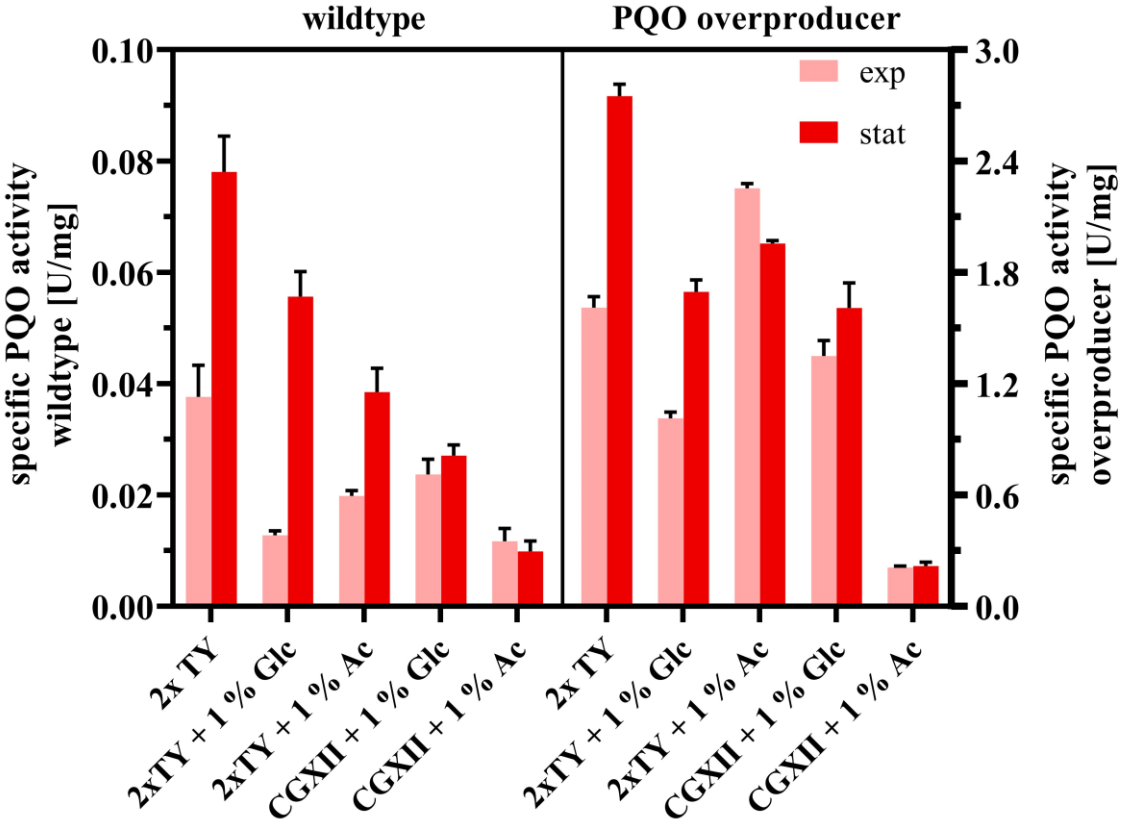


**Fig. 5: PQO activity patterns.**

PQO activities in cell extracts of *C. glutamicum* (wildtype, left) or *C. glutamicum* Δ*pqo* (pEKEx2-*pqo*) (PQO overproducer, right) cultivated in different media and harvested at both the exponential (**exp, light red**) and stationary phase (**stat, 24 h, red**) (N ≥ 3). TY, tryptone yeast; Ac, acetate; Glc, glucose.

For the PQO overproducer, the activity pattern is similar to that of the wildtype, but with up to 30-fold higher specific activities. The growth phase had a less pronounced effect in cultivations with 2xTY medium and an additional carbon source, with the largest difference in specific activity observed between exponential and stationary phase cells grown in 2xTY medium without an additional carbon source (ranging from approximately 1.6 to 2.8 U/mg protein). The highest PQO activity was found in stationary phase cells grown in 2xTY medium (approximately 2.8 U/mg protein), while the lowest activity was observed in both growth phases of cells grown in acetate minimal medium (approximately 0.2 U/mg protein).

The differences in specific activity under various conditions cannot be attributed to transcriptional regulation, as the *pqo* gene expression in the PQO overproducer strain of *C. glutamicum* is solely controlled by the artificial $P_{tac}$ promoter in the pEKEx2 plasmid. It is therefore suggested that these differences in specific activity under various conditions are attributed to post-translational modification, leading to different PQO enzymes with varying biochemical properties, rather than transcriptional regulation.

## 3.2 Investigating PQO activity in *C. glutamicum*: Purification of the enzyme and effects of cultivation conditions and post-translational modifications

### 3.2.1 Purification and kinetic analysis of PQO enzyme activity

The difference in the specific activity of PQO in cells of the PQO overproducer strain when cultivated in either 2xTY (highest activity) or acetate minimal medium (lowest activity) was further analyzed. The PQO enzyme was purified from *C. glutamicum* Δ*pqo* (pEKEx2-*pqo*) cells using the protocol established by Schreiner and Eikmanns (2005). The protocol relies on the ability of PQO to specifically bind to the detergent Triton X-114 in the presence of its substrate (pyruvate) and cofactors ($Mg^{2+}$ cations and TPP). This property is reversible, allowing PQO to be extracted back into the aqueous phase when the substrate and cofactors are absent. As shown in **Fig. 6**, the protein was purified to homogeneity after SDS-PAGE.

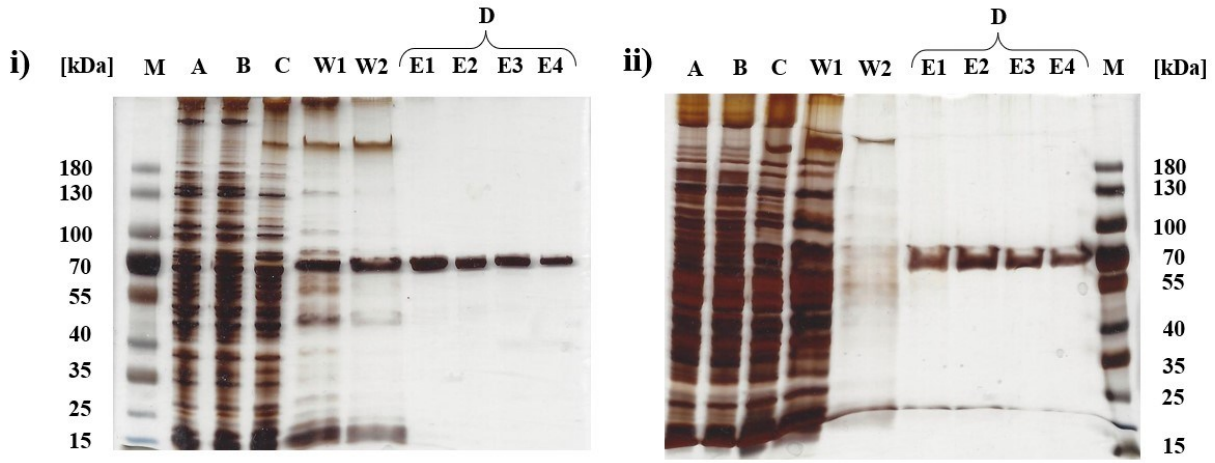


**Fig. 6: Purification of PQO via Triton X-114 extraction.**

SDS-PAGE-analysis of different purification steps of PQO from *C. glutamicum* Δ*pqo* (pEKEx2-*pqo*) cells grown in 2xTY medium (i) or CGXII minimal medium with 1 % acetate (ii), harvested after 24 h. Lane M, Prestained Protein Ladder™; lane A, cell extract; lane B, supernatant after ultracentrifugation; lane C, supernatant after heat precipitation; lanes W1 and W2, waste fractions during Triton X-114 extraction; lanes E1 – E4, samples after Triton X-114 extraction (D).

**Tab. 4** shows that the protein was enriched from both cell extracts nearly 30-fold, with different specific activities in all purification steps. The PQO from 2xTY medium-grown cells showed a specific activity of 72.3 U/mg protein, while the PQO from acetate minimal medium-grown cells had one of 11.9 U/mg protein. The recovery rates differed slightly between the two: up to the heat precipitation step, 67 % of the PQO from 2xTY medium-grown cells was recovered, while for the PQO from acetate minimal medium-grown cells, the figure was 87 %. However, post the final purification step, 4.3 % of PQO from the 2xTY medium and 1.9 % from the acetate minimal medium were retrieved. When considering the net protein yield, both in relative and absolute terms, a more substantial recovery was observed for PQO from 2xTY medium-grown cells compared to the acetate minimal medium, registering 0.60 mg versus 0.32 mg, respectively.

**Tab. 4: Purification of PQO from *C. glutamicum* Δ*pqo* (pEKEx2-*pqo*).**

Purification of PQO from *C. glutamicum* Δ*pqo* (pEKEx2-*pqo*) cultivated in either 2xTY medium (left values) or CGXII minimal medium with 1 % acetate as carbon source (right values) and harvested in the stationary phase.

| purification step | total amount of protein (mg) | total activity (U) | specific activity (U/mg) | recovery of activity (%) | purification (fold) |
|---|---|---|---|---|---|
| cell extract | 393 \|\| 503 | 1016 \|\| 196 | 2.6 \|\| 0.4 | 100 \|\| 100 | 1 \|\| 1 |
| ultra-centrifugation | 262 \|\| 470 | 850 \|\| 190 | 3.2 \|\| 0.4 | 84 \|\| 97 | 1.3 \|\| 1.1 |
| heat precipitation | 128 \|\| 209 | 678 \|\| 171 | 5.3 \|\| 0.8 | 67 \|\| 87 | 2.0 \|\| 2.0 |
| Triton X-114 extraction | 0.60 \|\| 0.32 | 43.4 \|\| 3.8 | 72.3 \|\| 11.9 | 4.3 \|\| 1.9 | 27.8 \|\| 29.8 |

**Tab. 5: Steady-state kinetics of PQO.**

Kinetic parameters of PQO from *C. glutamicum* Δ*pqo* (pEKEx2-*pqo*), cultivated in 2xTY medium and in CGXII with 1 % acetate, harvested after 24 h. For the calculation of the $k_{cat}$ values, a molecular weight of 247.8 kDa was assumed, corresponding to a tetramer of the enzyme.

| PQO variant | $K_m$ (mM) | $k_{cat}$ ($s^{-1}$) | $k_{cat}/K_m$ ($s^{-1}$ $M^{-1}$) |
|---|---|---|---|
| full-length (2xTY) | 53 | 440 | 8301 |
| full-length (CGXII + 1 % Ac) | 58 | 78 | 1344 |

$K_m$ and $k_{cat}$ values were determined for both PQO variants with pyruvate as the substrate (**Tab. 5**). Although the PQO enzymes purified from cells grown under the two different conditions showed very similar $K_m$ values (53 mM and 58 mM, respectively), the $k_{cat}$ values differed significantly, with the PQO from 2xTY medium-grown cells showing about sixfold higher value (440 $s^{-1}$ vs. 78 $s^{-1}$). In conclusion, these results indicate that the activity of PQO is regulated based on the cultivation condition of the respective *C. glutamicum* strain, through post-translational modifications.

However, the mechanism of regulation of PQO activity through post-translational modifications remains to date unclear. Previous studies in *C. glutamicum* on the analysis of the phosphoproteome (Bendt *et al*., 2003) or changes in the acylome during glutamate overproduction (entirety of proteins that are either succinylated and/or acetylated) (Mizuno *et al*., 2016) have identified PQO as a modified protein. In the work by Mizuno *et al*. (2016), the specific lysine residues (K) to be modified were identified as K19, K213 and K304. Considering all these findings, three altered alleles of the *pqo* gene were generated to assess the impact of acylation at these lysine residues on PQO, which resulted in the substitution of the respective K residue with the neutral, non-acylable residue alanine (A) (K19A, K213A and K304A) in the resultant PQO enzyme. These modified alleles were overexpressed in the *C. glutamicum* Δ*pqo* background and the strains cultured in 2xTY complex medium or in CGXII acetate or glucose minimal medium. Under the conditions tested, all overexpression strains did not exhibit a phenotype compared to the *C. glutamicum* wildtype or *pqo* deletion strain. The activity patterns of $pqo^{K19A}$, $pqo^{K213A}$, and $pqo^{K304A}$ overexpression strains, as conducted by K. Zauner and by J. Sacik in their bachelor theses, were not significantly different from the wildtype *pqo* overexpression strain (data not shown). This suggests that these residues are not pertinent to PQO activity under the experimental conditions conducted thus far.

### 3.2.2 Corynebacterial PQO is abundantly acylated

The present study aimed to elucidate the catalytic diversity observed in PQO enzymes when *C. glutamicum* strains were grown in either 2xTY medium or CGXII acetate minimal medium. Previous literature data and experiments were inconclusive in this regard (see section 3.2.1). To address this issue, PQO was purified from cells grown in either 2xTY complex medium or in CGXII acetate or glucose minimal medium, and subjected to mass spectrometry analysis at the Core Unit Mass Spectrometry and Proteomics facility at the University of Ulm. The results revealed that PQO undergoes post-translational modifications (PTMs) depending on the cultivation conditions of the respective *C. glutamicum* strain, with specific lysine residues being particularly susceptible to succinylation and acetylation. These findings are summarized in **Tab. 6a** and **6b**.

**Tab. 6a: Relative abundance of succinylated lysine residues within PQO.**

PQO was purified natively from *C. glutamicum* Δ*pqo* (pEKEx2-*pqo*) cells, which were cultivated in either 2xTY medium, CGXII 1 % acetate or CGXII 1 % glucose medium. n.d., not detectable

| succinylation position | PQO from cells in 2xTY | PQO from cells in CGXII with 1 % acetate | PQO from cells in CGXII with 1 % glucose |
|---|---|---|---|
| K19 | ~ 0.1 % | ~ 0.2 % | ~ 0.3 % |
| K151 | < 0.01 % | n.d. | n.d. |
| K225 | ~ 5 % | ~ 6 % | ~ 6 % |
| K304 | n.d. | ~ 0.2 % | ~ 0.4 % |
| K323 | ~ 0.5 % | ~ 0.6 % | n.d. |
| K325 | ~ 5 % | ~ 41 % | ~ 28 % |
| K341 | n.d. | < 0.1% | n.d. |
| K500 | n.d. | ~ 15 % | ~ 31 % |

**Tab. 6b: Relative abundance of acetylated lysine residues within PQO.**

PQO was purified natively from *C. glutamicum* Δ*pqo* (pEKEx2-*pqo*) cells, which were cultivated in either 2xTY medium, CGXII 1 % acetate or CGXII 1 % glucose medium. n.d., not detectable

| acetylation position | PQO from cells in 2xTY | PQO from cells in CGXII with 1 % acetate | PQO from cells in CGXII with 1 % glucose |
|---|---|---|---|
| K19 | ~ 1 % | < 0.1 % | ~ 2.5 % |
| K93 | ~ 6 % | ~ 56 %. | ~ 50 %. |
| K151 | ~ 3 % | ~ 6 % | ~ 6 % |
| K225 | ~ 18 % | ~ 17 % | ~ 21 % |
| K304 | n.d. | ~ 0.2 % | ~ 0.4 %. |
| K323 | ~ 1 % | ~ 0.4 % | ~ 1 % |
| K341 | < 0.1%. | ~ 0.1 % | ~ 0.2 % |
| K457 | n.d. | n.d. | ~ 6 % |
| K500 | n.d. | n.d. | ~ 11 % |

A variety of lysine residues were identified that are prone to succinylation and acetylation. Among these, K19 and K304 were previously reported to be modified in previous works (Mizuno *et al*., 2016). Interestingly, the identified lysine residues were found to be more prone to succinylation in cells cultivated in CGXII minimal medium compared to cells cultivated in 2xTY complex medium.

The most abundantly succinylated lysine residues were identified as K325 (approximately 41 % are succinylated in PQO from acetate minimal medium grown cells) and K500 (approximately 31 % are succinylated in PQO from glucose minimal medium grown cells). It was also found that some of the lysine residues that are partly succinylated are also partly acetylated. Specifically, K19, K225, and K500 were found to be acetylated at abundances above 1 % in at least one of the three conditions tested.

Lysine acetylation analysis revealed that K93 was the most abundantly modified residue, with up to 56 % of PQO from cells grown in acetate minimal medium exhibiting acetylation at this site. Another lysine residue that was abundantly modified was K225, with a roughly equal distribution of acetylation among all three tested conditions, ranging from around 20 %. These findings suggest that PQO's lysine succinylation and acetylation patterns are influenced by the growth media used, and specific lysine residues are more susceptible to these modifications than others.

### 3.2.3 Sequence analysis of corynebacterial PQO and mutant characterization

The most abundantly modified lysine residues in PQO from *C. glutamicum* were identified as K93, K325, and K500 (see section 3.2.2). To investigate the potential significance of these residues to PQO activity in *C. glutamicum*, a sequence data analysis was performed using the amino acid sequence of PQO and the ‘Basic Local Alignment Search Tool’ (BLAST). The top hits identified putative PQOs from various bacterial species, including *Dietzia timorensis* (71 % identity), *Nocardia jejuensis* (62 % identity), *Mycobacterium tuberculosis* (60 % identity), *Rhodococcus equi* (56 % identity), and *Mycobacterium smegmatis* (48 % identity), in addition to previously characterized PQO homologues from *E. coli* (PoxB, 47 % identity) and *Staphylococcus aureus* (CidC, 33 % identity). A comparison of the amino acid sequences of these putative PQOs and PQO homologues is presented in **Fig. 7**.

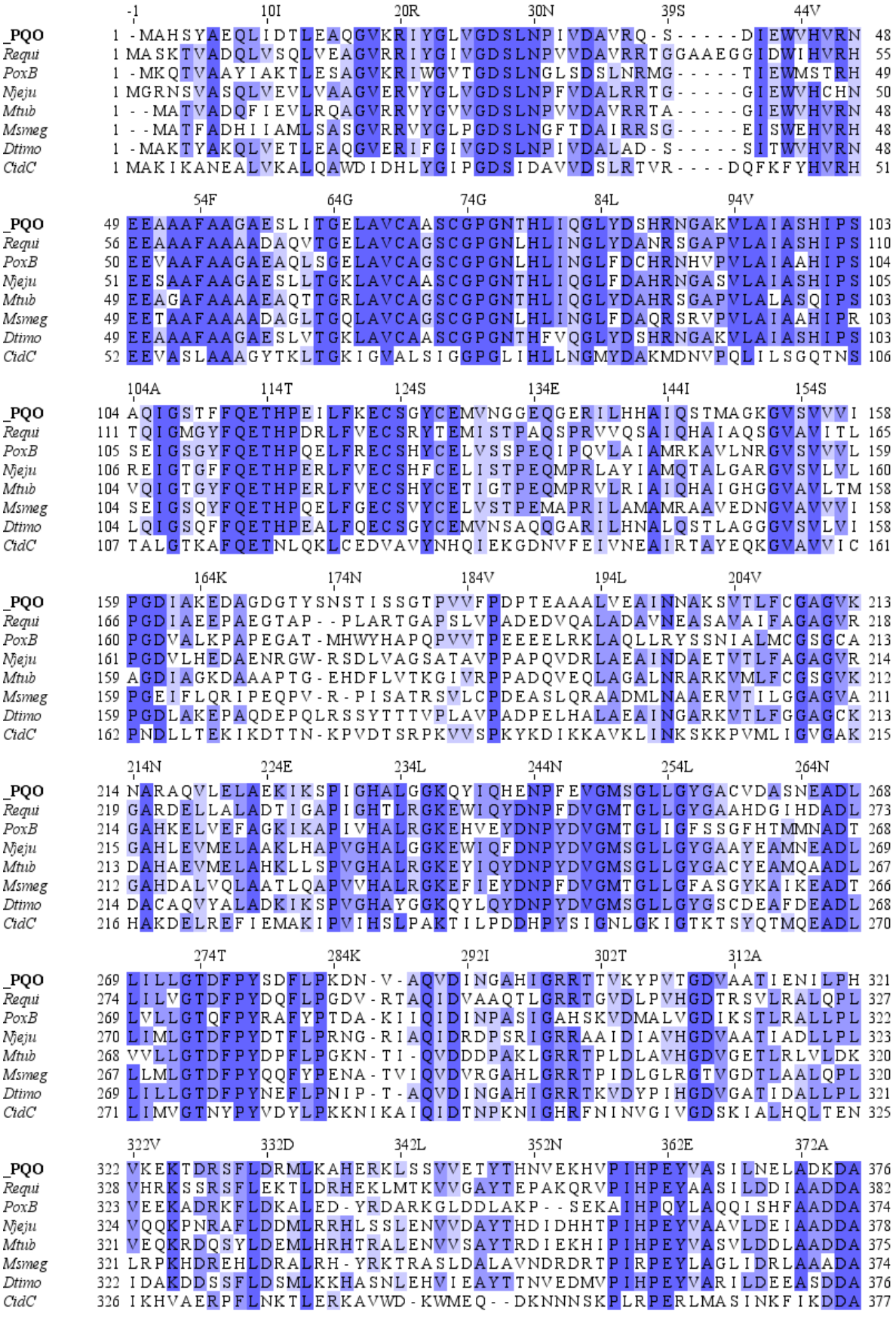
-1 10I 20R 30N 39S 44V
_PQO 1 -MAHSYAEQLIDTLEAQGVKRIYGLVGDSLNPIVDAVRQ-S-----DIEWVHVRN 48
Requi 1 MASKTVADQLVSQLVEAGVRRIYGIVGDSLNPVVDAVRRTGGAAEGGIDWIHVRH 55
PoxB 1 -MKQTVAAYIAKTLESAGVKRIWGVTGDSLNGLSDSLNRMG-----TIEWMSTRH 49
Njeju 1 MGRNSVASQLVEVLVAAGVERVYGLVGDSLNPFVDALRRTG-----GIEWVHCHN 50
Mtub 1 --MATVADQFIEVLRQAGVRRVYGVVGDSLNPVVDAVRRTA-----GIEWVHVRN 48
Msmeg 1 --MATFADHIIAMLSASGVRRVYGLPGDSLNGFTDAIRRSG-----EISWEHVRH 48
Dtimo 1 -MAKTYAKQLVETLEAQGVERIFGIVGDSLNPIVDALAD-S-----SITWVHVRN 48
CidC 1 MAKIKANEALVKALQAWDIDHLYGIPGDSIDAVVDSLRTVR----DQFKFYHVRH 51
54F 64G 74G 84L 94V
_PQO 49 EEAAAFAAGAESLITGELAVCAASCGPGNTHLIQGLYDSHRNGAKVLAIASHIPS 103
Requi 56 EEAAAFAAAADAQVTGELAVCAGSCGPGNLHLINGLYDANRSGAPVLAIASHIPS 110
PoxB 50 EEVAAFAAGAEAQLSGELAVCAGSCGPGNLHLINGLFDCHRNHVPVLAIAAHIPS 104
Njeju 51 EESAAFAAGAESLLTGKLAVCAASCGPGNTHLIQGLFDAHRNGASVLAIASHIPS 105
Mtub 49 EEAGAFAAAAEAQTTGRLAVCAGSCGPGNTHLIQGLYDAHRSGAPVLALASQIPS 103
Msmeg 49 EETAAFAAAADAGLTGQLAVCAGSCGPGNLHLINGLFDAQRSRVPVLAIAAHIPR 103
Dtimo 49 EEAAAFAAGAESLVTGKLAVCAASCGPGNTHFVQGLYDSHRNGAKVLAIASHIPS 103
CidC 52 EEVASLAAAGYTKLTGKIGVALSIGGPGLIHLLNGMYDAKMDNVPQLILSGQTNS 106
104A 114T 124S 134E 144I 154S
_PQO 104 AQIGSTFFQETHPEILFKECSGYCEMVNGGEQGERILHHAIQSTMAGKGVSVVVI 158
Requi 111 TQIGMGYFQETHPDRLFVECSRYTEMISTPAQSPRVVQSAIQHAIAQSGVAVITL 165
PoxB 105 SEIGSGYFQETHPQELFRECSHYCELVSSPEQIPQVLAIAMRKAVLNRGVSVVVL 159
Njeju 106 REIGTGFFQETHPERLFVECSHFCELISTPEQMPRLAYIAMQTALGARGVSVLVL 160
Mtub 104 VQIGTGYFQETHPERLFVECSHYCETIGTPEQMPRVLRIAIQHAIGHGGVAVLTM 158
Msmeg 104 SEIGSQYFQETHPQELFGECSVYCELVSTPEMAPRILAMAMRAAVEDNGVAVVVI 158
Dtimo 104 LQIGSQFFQETHPEALFQECSGYCEMVNSAQQGARILHNALQSTLAGGGVSVLVI 158
CidC 107 TALGTKAFQETNLQKLCEDVAVYNHQIEKGDNVFEIVNEAIRTAYEQKGVAVVIC 161
164K 174N 184V 194L 204V
_PQO 159 PGDIAKEDAGDGTYSNSTISSGTPVVFPDPTEAAALVEAINNAKSVTLFCGAGVK 213
Requi 166 PGDIAEEPAEGTAP--PLARTGAPSLVPADEDVQALADAVNEASAVAIFAGAGVR 218
PoxB 160 PGDVALKPAPEGAT-MHWYHAPQPVVTPEEEELRKLAQLLRYSSNIALMCGSGCA 213
Njeju 161 PGDVLHEDAENRGW-RSDLVAGSATAVPPAPQVDRLAEAINDAETVTLFAGAGVR 214
Mtub 159 AGDIAGKDAAAPTG-EHDFLVTKGIVRPPADQVEQLAGALNRARKVMLFCGSGVK 212
Msmeg 159 PGEIFLQRIPEQPV-R-PISATRSVLCPDEASLQRAADMLNAAERVTILGGAGVA 211
Dtimo 159 PGDLAKEPAQDEPQLRSSYTTTVPLAVPADPELHALAEAINGARKVTLFGGAGCK 213
CidC 162 PNDLLTEKIKDTTN-KPVDTSRPKVVSPKYKDIKKAVKLINKSKKPVMLIGVGAK 215
214N 224E 234L 244N 254L 264N
_PQO 214 NARAQVLELAEKIKSPIGHALGGKQYIQHENPFEVGMSGLLGYGACVDASNEADL 268
Requi 219 GARDELLALADTIGAPIGHTLRGKEWIQYDNPFDVGMTGLLGYGAAHDGIHDADL 273
PoxB 214 GAHKELVEFAGKIKAPIVHALRGKEHVEYDNPYDVGMTGLIGFSSGFHTMMNADT 268
Njeju 215 GAHLEVMELAAKLHAPVGHALGGKEWIQFDNPYDVGMSGLLGYGAAYEAMNEADL 269
Mtub 213 DAHAEVMELAHKLLSPVGHALRGKEYIQYDNPYDVGMSGLLGYGACYEAMQAADL 267
Msmeg 212 GAHDALVQLAATLQAPVVHALRGKEFIEYDNPFDVGMTGLLGFASGYKAIKEADT 266
Dtimo 214 DACAQVYALADKIKSPVGHAYGGKQYLQYDNPYDVGMSGLLGYGSCDEAFDEADL 268
CidC 216 HAKDELREFIEMAKIPVIHSLPAKTILPDDHPYSIGNLGKIGTKTSYQTMQEADL 270
274T 284K 292I 302T 312A
_PQO 269 LILLGTDFPYSDFLPKDN-V-AQVDINGAHIGRRTTVKYPVTGDVAATIENILPH 321
Requi 274 LILVGTDFPYDQFLPGDV-RTAQIDVAAQTLGRRTGVDLPVHGDTRSVLRALQPL 327
PoxB 269 LVLLGTQFPYRAFYPTDA-KIIQIDINPASIGAHSKVDMALVGDIKSTLRALLPL 322
Njeju 270 LIMLGTDFPYDTFLPRNG-RIAQIDRDPSRIGRRAAIDIAVHGDVAATIADLLPL 323
Mtub 268 VVLLGTDFPYDPFLPGKN-TI-QVDDDPAKLGRRTPLDLAVHGDVGETLRLVLDK 320
Msmeg 267 LLMLGTDFPYQQFYPENA-TVIQVDVRGAHLGRRTPIDLGLRGTVGDTLAALQPL 320
Dtimo 269 LILLGTDFPYNEFLPNIP-T-AQVDINGAHIGRRTKVDYPIHGDVGATIDALLPL 321
CidC 271 LIMVGTNYPYVDYLPKKNIKAIQIDTNPKNIGHRFNINVGIVGDSKIALHQLTEN 325
322V 332D 342L 352N 362E 372A
_PQO 322 VKEKTDRSFLDRMLKAHERKLSSVVETYTHNVEKHVPIHPEYVASILNELADKDA 376
Requi 328 VHRKSSRSFLEKTLDRHEKLMTKVVGAYTEPAKQRVPIHPEYAASILDDIAADDA 382
PoxB 323 VEEKADRKFLDKALED-YRDARKGLDDLAKP--SEKAIHPQYLAQQISHFAADDA 374
Njeju 324 VQQKPNRAFLDDMLRRHLSSLENVVDAYTHDIDHHTPIHPEYVAAVLDEIAADDA 378
Mtub 321 VEQKRDQSYLDEMLHRHTRALENVVSAYTRDIEKHIPIHPEYVASVLDDLAADDA 375
Msmeg 321 LRPKHDREHLDRALRH-YRKTRASLDALAVNDRDRTPIRPEYLAGLIDRLAAADA 374
Dtimo 322 IDAKDDSSFLDSMLKKHASNLEHVIEAYTTNVEDMVPIHPEYVARILDEEASDDA 376
CidC 326 IKHVAERPFLNKTLERKAVWD-KWMEQ--DKNNNSKPLRPERLMASINKFIKDDA 377

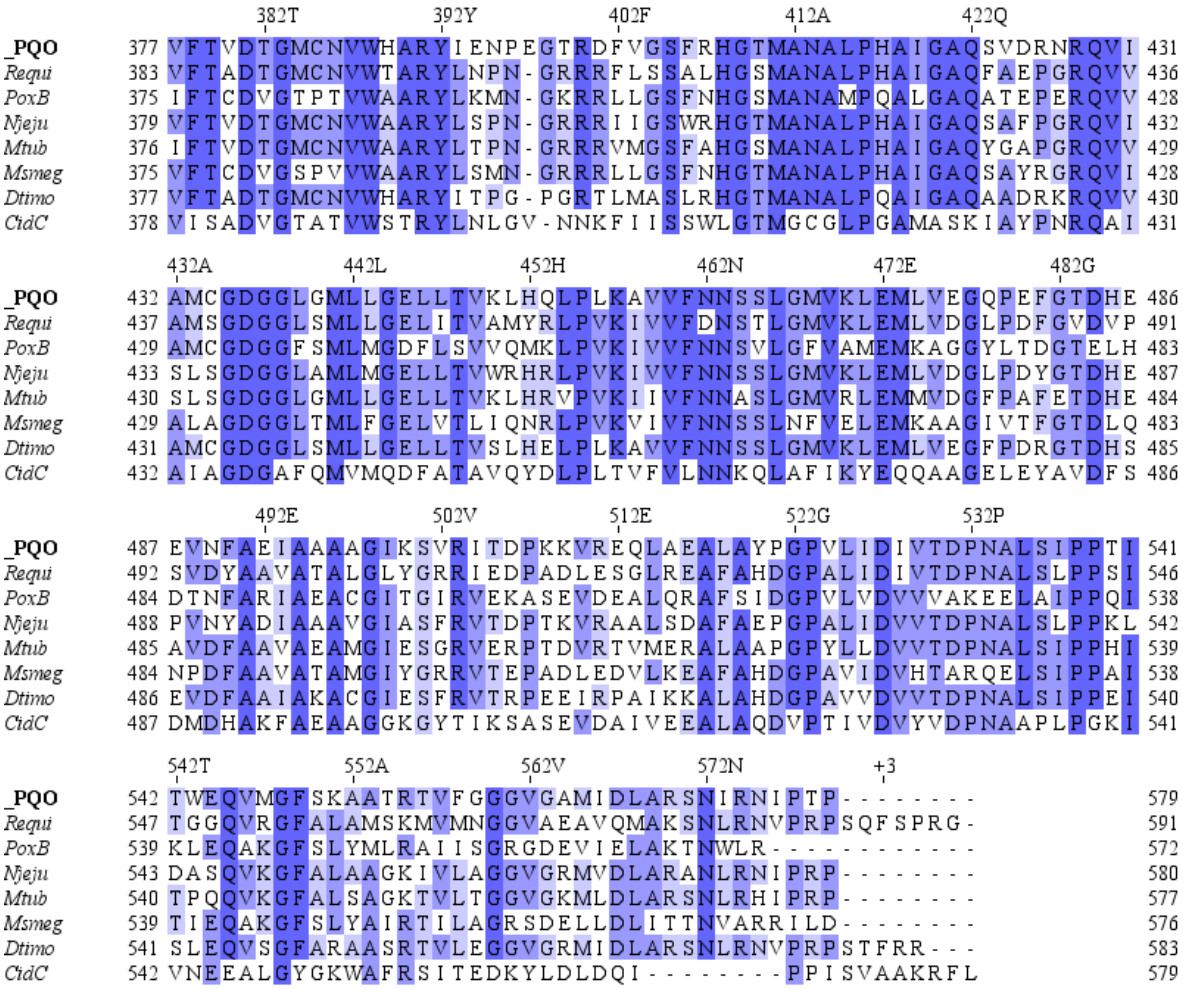


**Fig. 7: Amino acid sequence alignment of different (putative) PQO enzymes.**

Amino acid sequence comparison of PQO from *Corynebacterium glutamicum* (_PQO, accession number: CAF21272.1) with (putative) PQOs from *Rhodococcus equi* (Requi, WP_084962976.1), *Escherichia coli* (PoxB, CAD6018048.1), *Nocardia jejuensis* (Njeju, WP_067691424.1), *Mycobacterium tuberculosis* (Mtub, CND64251.1), *Mycobacterium smegmatis* (Msmeg, WP_011728276.1), *Dietzia timorensis* (Dtimo, HJE91135.1) and *Staphylococcus aureus* (CidC, WP_001062648.1). Conserved amino acids are depicted in blue. The scale above the alignment is referring to the sequence of the PQO from *C. glutamicum*.

As later shown in the crystallographic structure of the corynebacterial PQO (section 3.3), the *C. glutamicum* enzyme exhibits a conserved domain arrangement similar to PoxB and other enzymes in its family. This organization consists of three distinct domains: a pyrimidine-binding domain located at the N-terminus (Pyrimidine, residues 1-164), a central FAD-binding domain (FAD, residues 188-350), and a pyrophosphate binding domain (PP, residues 360-532). Within these domains, the conservation is on average lowest in the FAD-binding domain

(between 32 to 63 % identity) and highest in the pyrimidine-binding domain (between 33 to 82 % identity).

The sequence analysis revealed that K325 within the FAD-binding domain is conserved, as this residue is shared between all analyzed PQOs, except for CidC from *S. aureus*. For K93 and K500, the respective lysine residue is only shared with the putative PQO from *D. timorensis* and CidC from *S. aureus*, respectively. These findings suggest that K325 may play an important role in PQO catalytic activity or structural integrity, while K93 and K500 may be less critical for PQO function.

### 3.2.4 Modifying lysine residues in PQO: Effects on enzyme activity in *C. glutamicum*

PQO was found to be abundantly acylated based on the mass spectrometry analysis (see section 3.2.2), which led to the creation of three sets of two slightly modified alleles of the *pqo* to investigate the effect of PQO modification at the respective lysine residue. This involved the replacement of K93, K325 or K500 by either the neutral residue alanine (K to A) or the negatively charged amino acid glutamate (K to E) in the resulting PQO enzyme. These variants were overproduced in a *C. glutamicum* Δ*pqo*-background and cultivated in 2xTY medium, as well as in glucose- or acetate minimal medium. No growth phenotypes associated with alterations within the PQO enzymes were observed (data not shown). PQO activity patterns were determined at both the exponential and late stationary phase (24 h) and are presented in **Fig. 8**, related to the activity of the native PQO overproducer.

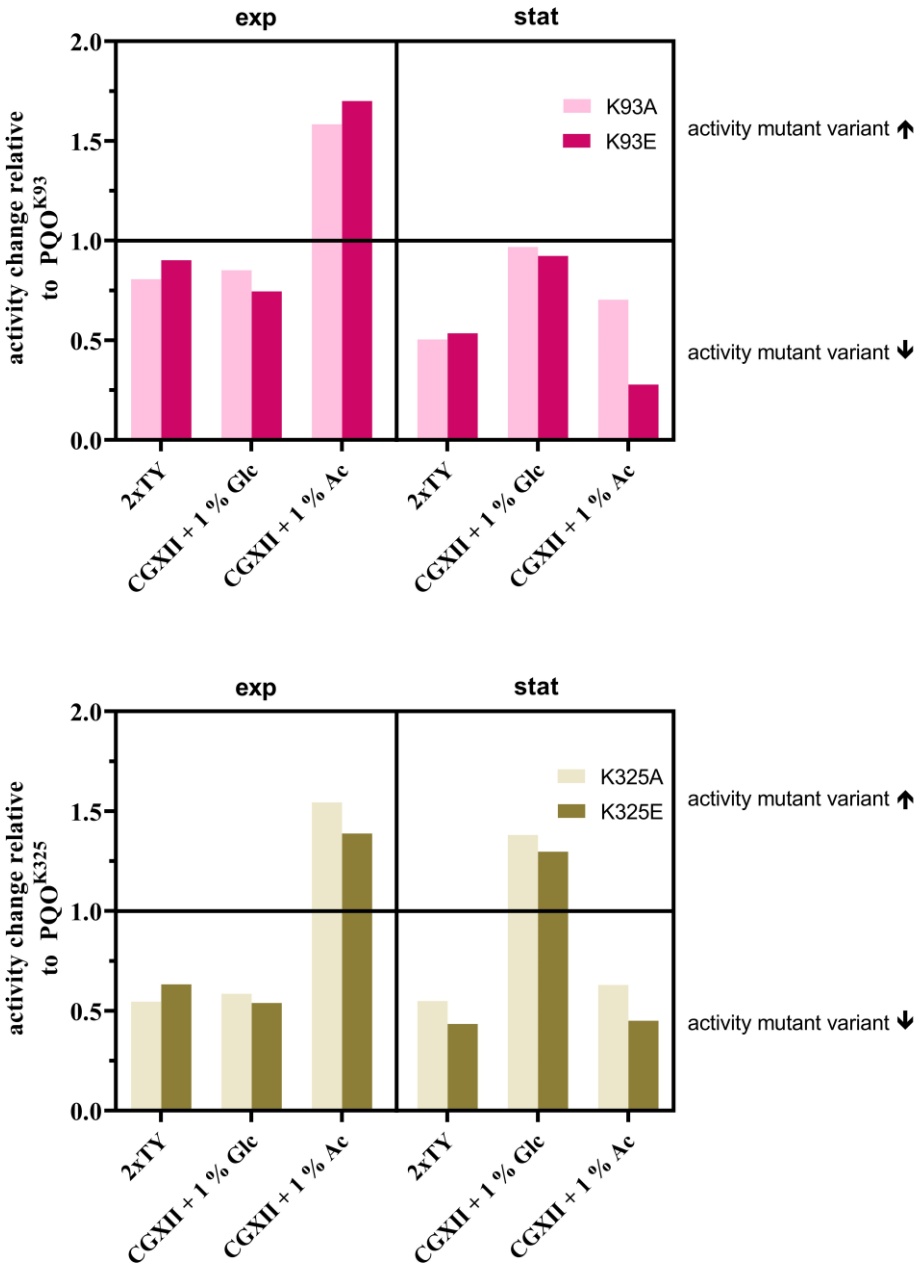


**Fig. 8: Relative specific activity of PQO K93 and K325 variants compared to wildtype PQO.**

The relative specific PQO activity of *C. glutamicum* Δ*pqo* (pEKEx2-*pqo*$^{K93A/E}$, magenta) and of *C. glutamicum* Δ*pqo* (pEKEx2-*pqo*$^{K325A/E}$, gold) was determined using cell extracts and normalized to the specific PQO activity of *C. glutamicum* Δ*pqo* (pEKEx2-*pqo*). The strains were cultivated in different media and harvested at both the exponential and stationary phase (24 h). The specific activities of the mutant variants were normalized to the specific activities in 2xTY medium, CGXII minimal medium with 1 % glucose, and CGXII minimal medium with 1 % acetate, which were 2.8 U/mg, 1.6 U/mg, and 0.22 U/mg protein, respectively. The presented data are mean values obtained from three independent experiments for wildtype PQO, and three independent experiments for all mentioned mutants. Ac, acetate; Glc, glucose.

For both K93 mutant variants at the exponential growth phase, the strongest effect was observed in acetate minimal medium-grown cells, with a 1.5-fold higher specific activity than wildtype PQO. However, the effect was negligible for cells grown in 2xTY or glucose minimal medium. At the stationary phase, both an effect was observed in extracts from 2xTY and acetate minimal medium-grown cells, with 0.5-fold and 0.2-fold lower activity, respectively. For the K325 mutant variants, effects on PQO activity were detected in every condition tested. At the exponential phase, 0.5-fold lowered activities were detected in extracts from 2xTY and glucose minimal medium-grown cells, whereas a 1.5-fold higher specific activity than wildtype PQO was observed in acetate minimal medium-grown cells. At the stationary phase, activity change compared to wildtype PQO were high for 2xTY- and acetate minimal medium grown cells, with 0.5-fold lowered activities. Mutations introduced at K500 (both K500A and K500E) were characterized in the master thesis of D. Haberbosch under my supervision and revealed similar effects as observed for the mutant variants at K93 and K325, respectively.

In conclusion, these experiments demonstrate that modifications to specific lysine residues of the PQO enzyme have a significant impact on its activity. The K93 and K325 mutant variants exhibited distinct activity profiles, particularly when grown in acetate minimal medium. Specifically, K93 mutants showed increased activity in this medium during the exponential phase, while K325 mutants demonstrated both increased and decreased activities across the different growth phases. Overall, it is evident that the specific growth medium and the growth phase play a crucial role in influencing the activity of the PQO enzyme, especially when certain mutations are present. These findings provide insight into the role of acylation in regulating PQO activity and may have implications for understanding the metabolic processes in which PQO is involved.

## 3.3 Structural analysis of PQO from *C. glutamicum*

The findings detailed in this work highlight the unique biochemical properties of PQO from *C. glutamicum*, which stands out within the pyruvate oxidase family. In this section, the aim is to elucidate the three-dimensional structure of this enzyme to comprehend the post-translational modifications that PQO undergoes, their potential influence on structural transformations, and to deepen the understanding of PQO activity regulation via acylation. Particular attention is given to the structural examination that might identify specific lysine residues subject to modifications, and provide comprehensive insight into their role in the catalytic functionality of PQO. The three-dimensional structure could also shed light on the structural reasons behind

the diverse biochemical properties of PQO. Therefore, this investigation is anticipated to contribute information about the not-yet-defined physiological role of PQO in *C. glutamicum*.

### 3.3.1 The corynebacterial PQO contains a structurally unique C-terminus

PQO crystals were procured under varying conditions from protein purified via Triton X-114 extraction from cells cultivated in 2xTY medium and harvested in the stationary phase. The crystal structure was initially deciphered from a 2.5 Å resolution dataset (M. Bellinzoni, manuscript in preparation), collected from a crystal cultivated in the presence of 1 mM FAD, employing the structure of a truncated variant of the *E. coli* pyruvate oxidase PoxB (PDB: 3EYA) as the search model. Following this, isomorphous crystals were harvested from protein purified identically, however, from cells grown in a minimal acetate medium, and these crystals diffracted up to a 1.26 Å resolution (M. Bellinzoni, manuscript in preparation). Hence, this high-resolution dataset was used to refine the final model, as depicted in **Fig. 9**.

Overall, the enzyme demonstrates a homotetrameric 222 symmetrical arrangement similar to that observed for PoxB. It includes a solitary monomer in the asymmetric unit and four protomers interconnected by crystallographic symmetry, in which one dimer is made up of two mirror-symmetric monomers (**Fig. 9a**). The *C. glutamicum* PQO reflects the domain organization of PoxB and related enzymes, namely, an N-terminal pyrimidine-binding domain (Pyrimidine; residues 1-164), a central FAD-binding domain (FAD; residues 188-350), and a pyrophosphate binding domain (PP; residues 360-532), all connected via flexible linkers. Attention is drawn to the amphipathic α-helix within the C-terminal region of *C. glutamicum* PQO (residues 560-572), as illustrated in **Fig. 9b** and examined in detail below (**Fig. 13**).

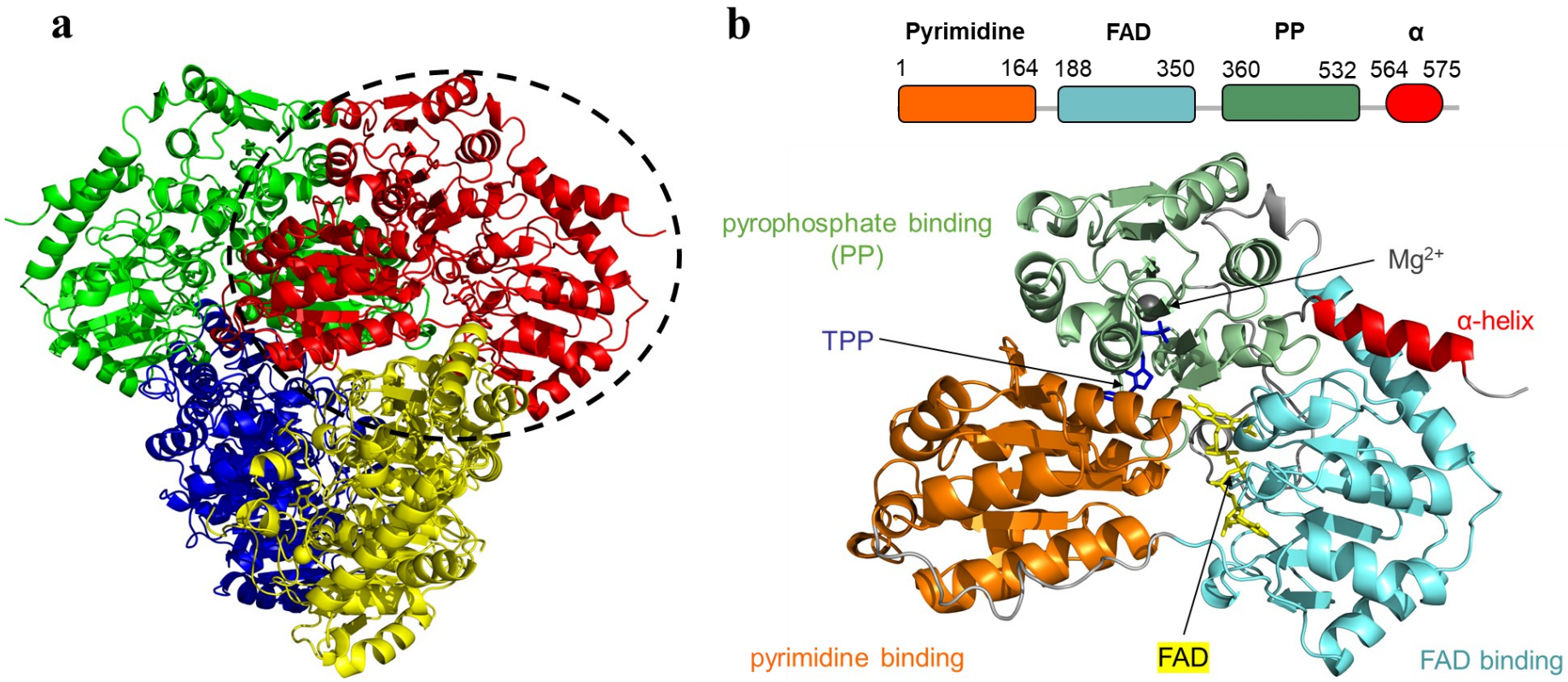


**Fig. 9: Cartoon overview of PQO, purified natively from *C. glutamicum* Δ*pqo* (pEKEx2-*pqo*).**

(a) Schematic representation of the homotetrameric structure of *C. glutamicum* PQO. Each chain within the tetramer is depicted in a distinct color (green, red, deep blue, yellow). The arrangement of the individual protomers follows a crystallographic 222 symmetry. Furthermore, in (b), the detailed structure of the monomer, indicated by a dashed circle in the overall cartoon overview in (a), is highlighted. The cofactors FAD (yellow) and TPP (deep blue) are represented as sticks, the divalent cation $Mg^{2+}$ as a grey sphere. Resolution = 1.26 Å.

An examination of the high-resolution electron density map revealed a bound FAD molecule within the central domain, occupying a position identical to the one found in *E. coli* PoxB (**Fig. 10**). The FAD isoalloxazinic group exhibits the characteristic 'butterfly' bent conformation of the three-ring system, marked by a deviation of approximately 15° from planarity (**Fig. 10**). This observation aligns with earlier studies involving *E. coli* PoxB and *Lactobacillus plantarum* pyruvate oxidase POX, which postulated that this bent conformation might be key in elevating the FAD reduction potential (Wille *et al*., 2005).

Furthermore, despite the absence of TPP in the sample and crystallization drops, the Fourier difference Fo-Fc map analysis revealed the existence of a TPP molecule at a low occupancy level, in complex with $Mg^{2+}$. This molecule could be modeled in a conformation mirroring that seen in *E. coli* PoxB (**Fig. 10**).

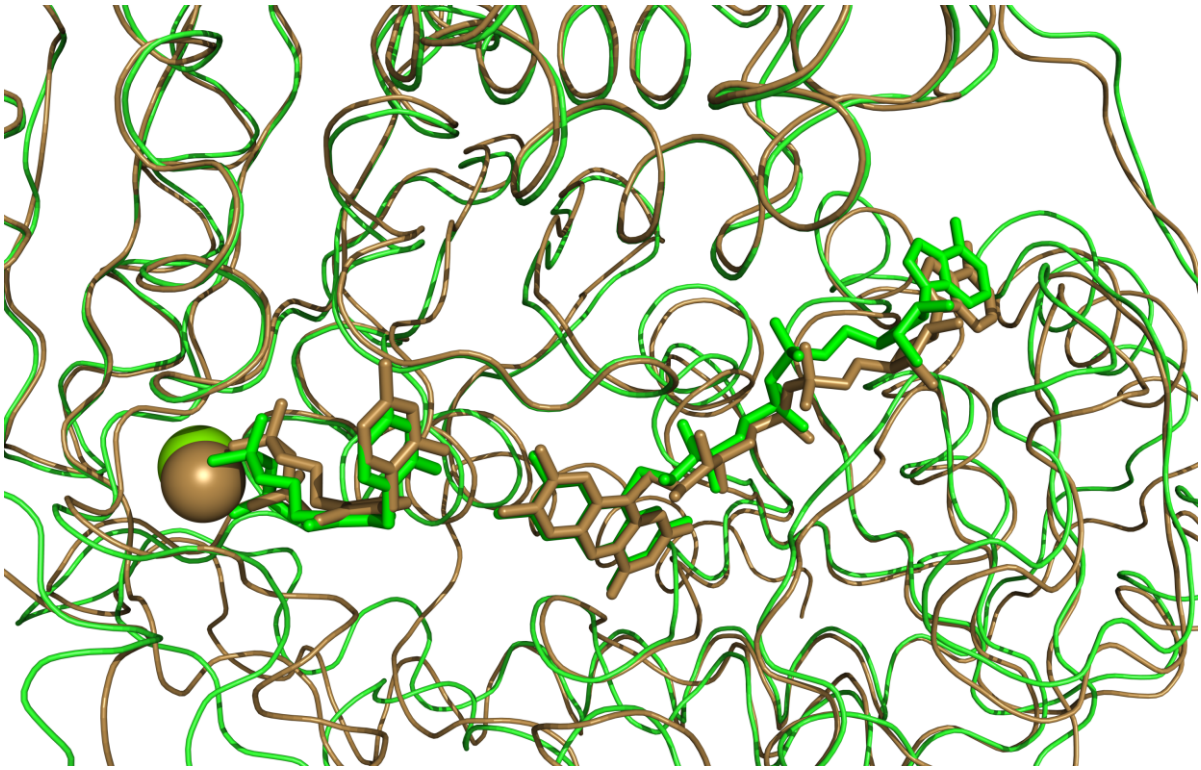

**Fig. 10: Schematic overview of bound cofactors in both *C. glutamicum* PQO and *E. coli* PoxB**

Superimposed image of *C. glutamicum* PQO (sand, identical structure as shown in Fig. 9) and *E. coli* PoxB (green, PDB: 3EY9), both being represented as ribbons. The cofactors FAD and TPP are represented as sticks, and $Mg^{2+}$ as a sphere.

The active site of PQO from *C. glutamicum*, depicted in **Fig. 11**, features both cofactors bound in close proximity, approximately 7.7 Å apart, between TPP-N4 and FAD-C7M. Within this site, there are residues that stabilize the position of TPP, highlighted in blue, including M411 and L466. The M411 side chain establishes a cation–π interaction with the pyrimidine and thiazolium ring moiety, at a distance of approximately 3 Å, aligning the ring systems to allow for T-shaped π-π-stacking. Furthermore, the side chain of L466 interacts with the methyl group of the thiazolium ring via van der Waals forces, approximately 3.8 Å apart. The position of $Mg^{2+}$, in complex with the pyrophosphate group of TPP, is stabilized via electrostatic interactions with the side chains of N463 and D436. The residues that potentially mediate the interaction between PQO and FAD are emphasized in yellow. The hydroxyphenyl group of Y278 is arranged to enable T-shaped π-π-stacking with the isoalloxazinic moiety of FAD at a distance of around 3.5 Å. R407 engages with the negatively charged phosphate group, an interaction facilitated by surrounding water molecules. The side chain of D291 contributes to the stability through hydrogen bond formation with the hydroxyl groups of the ribityl group of FAD. Additionally, the side chain of D310, through the mediation of surrounding water molecules, forms a hydrogen bond with the adenine group of FAD.

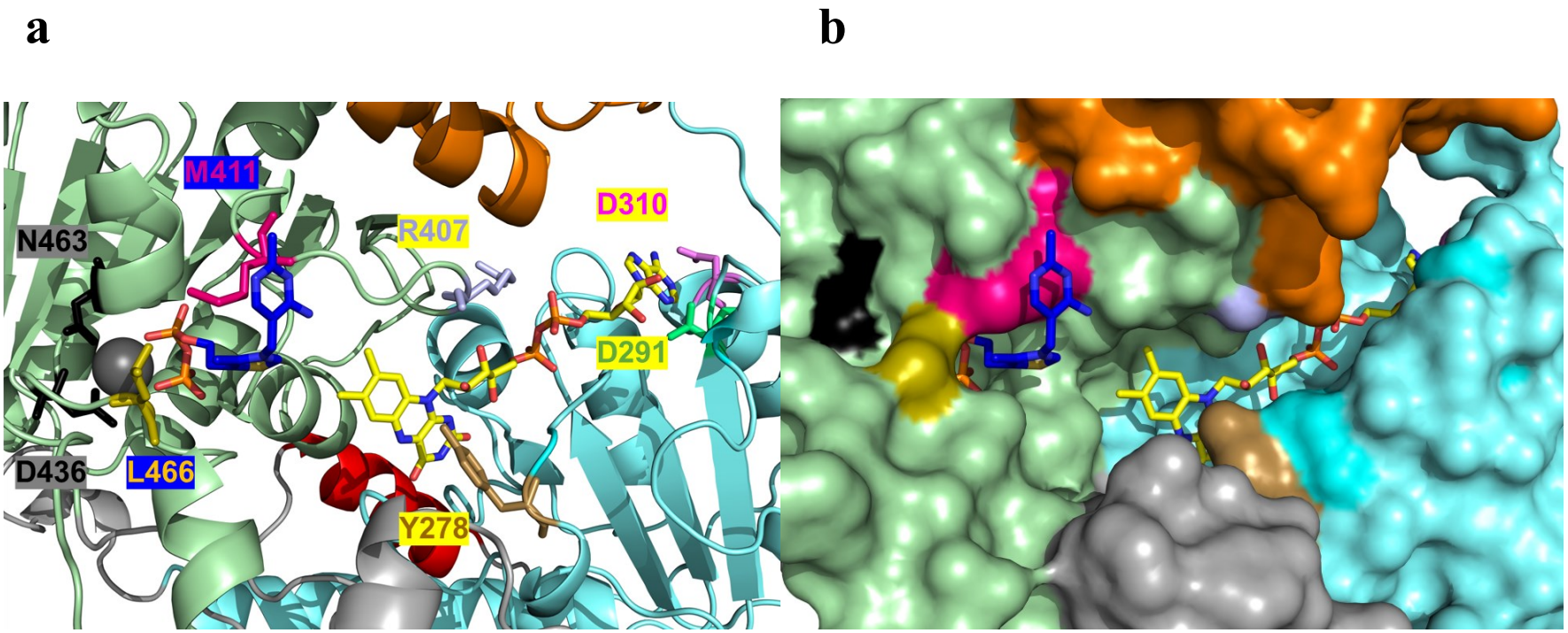


**Fig. 11: Active site of a PQO monomer, purified natively from *C. glutamicum* Δ*pqo* (pEKEx2-*pqo*).**

(a) Cartoon overview of a *C. glutamicum* PQO monomer, providing a schematic representation of its active site, with bound cofactors FAD and TPP depicted as sticks and $Mg^{2+}$ as a sphere. The coloring scheme follows the coloring of the domains as depicted in Fig. 9. Residues likely stabilizing the position of $Mg^{2+}$ are highlighted in grey, residues stabilizing TPP are highlighted in blue and residues likely stabilizing the interaction of PQO with FAD are highlighted in yellow, respectively. (b) The same overview as in (a), except that the structure is depicted as a surface model.

Despite these findings, the active site of PQO is actually situated at the dimer interface, with other significant residues contributing to its structure, as detailed in **Fig. 12**. The active site is primarily composed of the FAD-binding and PP-binding domain of one monomer and the Pyrimidine-binding domain of the neighboring monomer. As noted above, the cofactors maintain a close proximity. Electron transfer, from the adduct formed by TPP and pyruvate to FAD is likely conducted via the residues G76, P75, G74, and C73. The intermediate cysteine-radical may be stabilized by Q112. The resultant final radical, formed by the transfer of one electron to FAD, is possibly stabilized through a variety of T-shaped π-π-stacking interactions involving the side chains of the residues Y278, F110, F111, and the isoalloxazinic moiety of FAD.

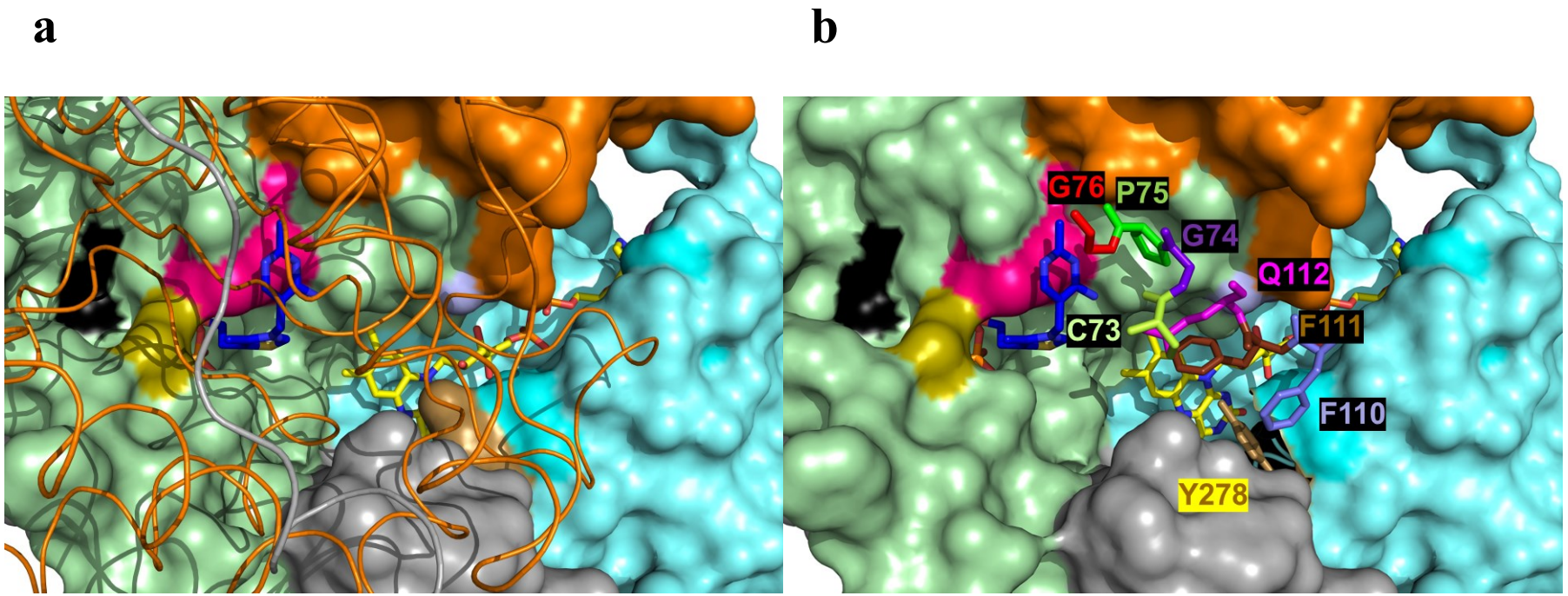


**Fig. 12: Active site of a PQO dimer, purified natively from *C. glutamicum* Δ*pqo* (pEKEx2-*pqo*).**

(a) Schematic representation of a *C. glutamicum* PQO dimer, depicting the "full" active site of *C. glutamicum* PQO, with bound cofactors. One monomer is represented in a surface model, the adjacent monomer is shown in the ribbon model. The coloring scheme follows the coloring of the domains as depicted in Fig. 9. (b) The same overview as in (a), where residues likely contributing to the electron transfer during pyruvate oxidation from the cofactors TPP to FAD are highlighted in different colors each. The remaining residues of the adjacent monomer where hidden.

With its structural and functional aspects comprehensively elucidated, pyruvate oxidase PoxB of *E. coli* provides an established model for studying this family of enzymes. Hence, an overall comparison of the structure was performed with the structure of the homologue in *C. glutamicum*, the PQO (**Fig. 13**). As already hinted by the fact that the cofactors were positioned within the structure in almost identical positions (**Fig. 10**), both enzymes share a very similar overall fold (**Fig. 13a, left**).

Nonetheless, a notable difference is observed in the general structure of the C-terminal domain (**Fig. 13a, right**). In PoxB, this domain contains the 'α-peptide' (M550-R572), instrumental for the catalytic activation of the enzyme due to its interaction with the membrane, as summarized in Weidner *et al*., 2009. In PQO, part of the corresponding residues are structured as an amphipathic α-helix (residues A564-N575) and are positioned 'above' a lengthy α-helix (residues R328-Y349), a sharp contrast to the conformation seen in PoxB. Within PoxB, these C-terminal residues are part of an antiparallel β-sheet instead, with the corresponding residues pointing 'below' the long α-helix mentioned previously. **Fig. 13b** offers a detailed visualization of the aligned structures of the C-terminal regions of both proteins. Specifically, in PQO, the 26-residue segment originating from the PP-binding domain (A534-F558) adopts an extended conformation, forming a lengthy cap that closes over the FAD-binding domain. In stark contrast with PoxB, no β-sheet structure is visible. Instead, a short α-helix is present from W543 to M547, aligned similarly to the PoxB sequence from S547-L551. Additionally, the Gly-rich sequence GGGVG, positioned between residues 559-563, runs beneath the elongated R328-Y349 α-helix, as previously noted. This positioning prompts the C-terminal amphipathic α-helix to extend out from the other side, taking an opposite direction. The helix begins at A564 and continues until N575, concluding with a short flexible tail that reaches the C-terminal end.

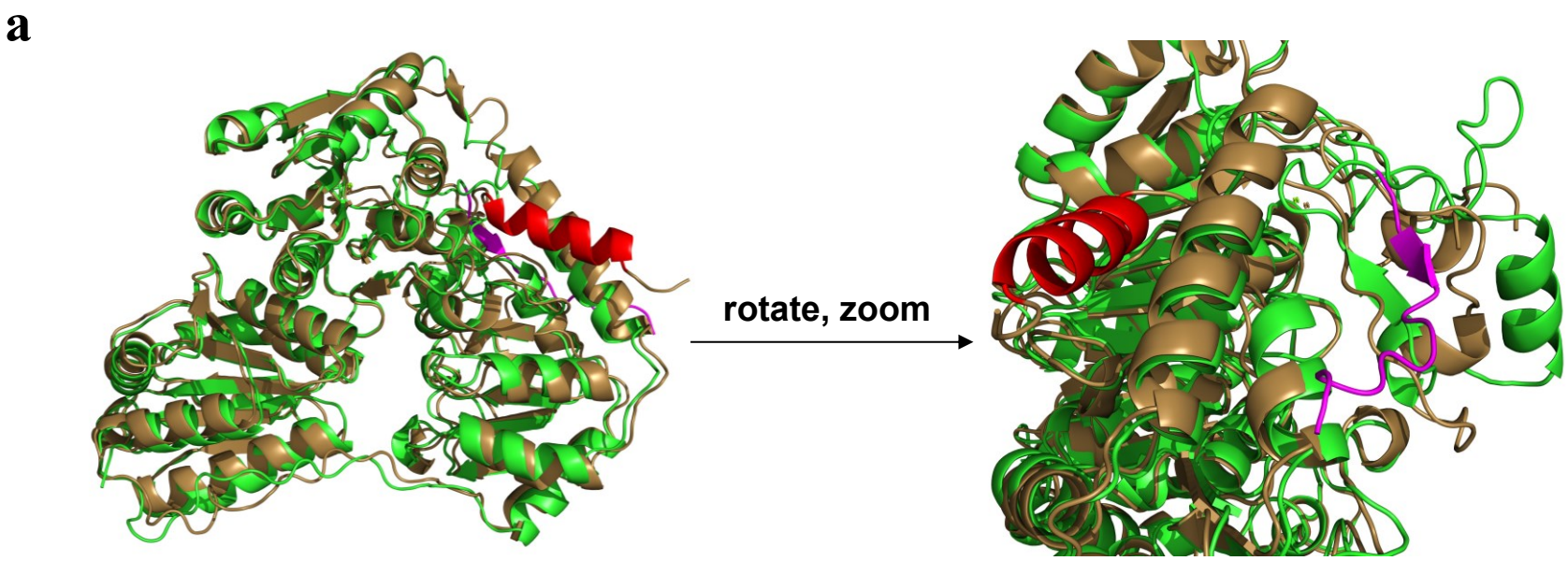


**Fig. 13: Structural alignment of PQO from *C. glutamicum* and PoxB from *E. coli*.**

(a) Cartoon overview of PQO (sand) upon superimposition to full-length PoxB (green; PDB 3EY9) (left). Zoomed view of the C-terminal, membrane-interacting domain of PQO (red) and of PoxB (magenta) (right). The α-helix composed by R328-Y349 in PQO is positioned in the center of the image.

(b) Detailed, superimposed cartoon overview of the C-terminal region of PQO (A534-T578) and PoxB (E531-R572). In PQO, residues A564-N575 fold to an amphipathic α-helix (red), the equivalent residues in PoxB are marked in magenta. In PoxB, residues A553-E564 form an antiparallel β-sheet structure.

For PoxB from *E. coli*, the positioning of the residues A553-E564, which form an antiparallel β-sheet, is critical to block the access to the active site with the cofactor TPP, as depicted in **Fig. 14b**, as the residues L253, L254, V385, F465, L532 and L548 form a hydrophobic pore. For the homologue in *C. glutamicum* (PQO), the corresponding residues do not block any "pore", nor does the large proportion of the C-terminal region, as shown in **Fig. 14a**.

In conclusion, multiple residues within the active site of PQO that interact with and stabilize the cofactors, TPP and FAD, have been identified and might play critical roles in the catalytic process. Despite substantial similarities between PQO and the homologue in *E. coli*, PoxB, critical structural differences were highlighted specifically in the C-terminal region of PQO. The absence of a closing β-sheet structure, as observed in PoxB, suggests a different regulation and/or function of PQO.

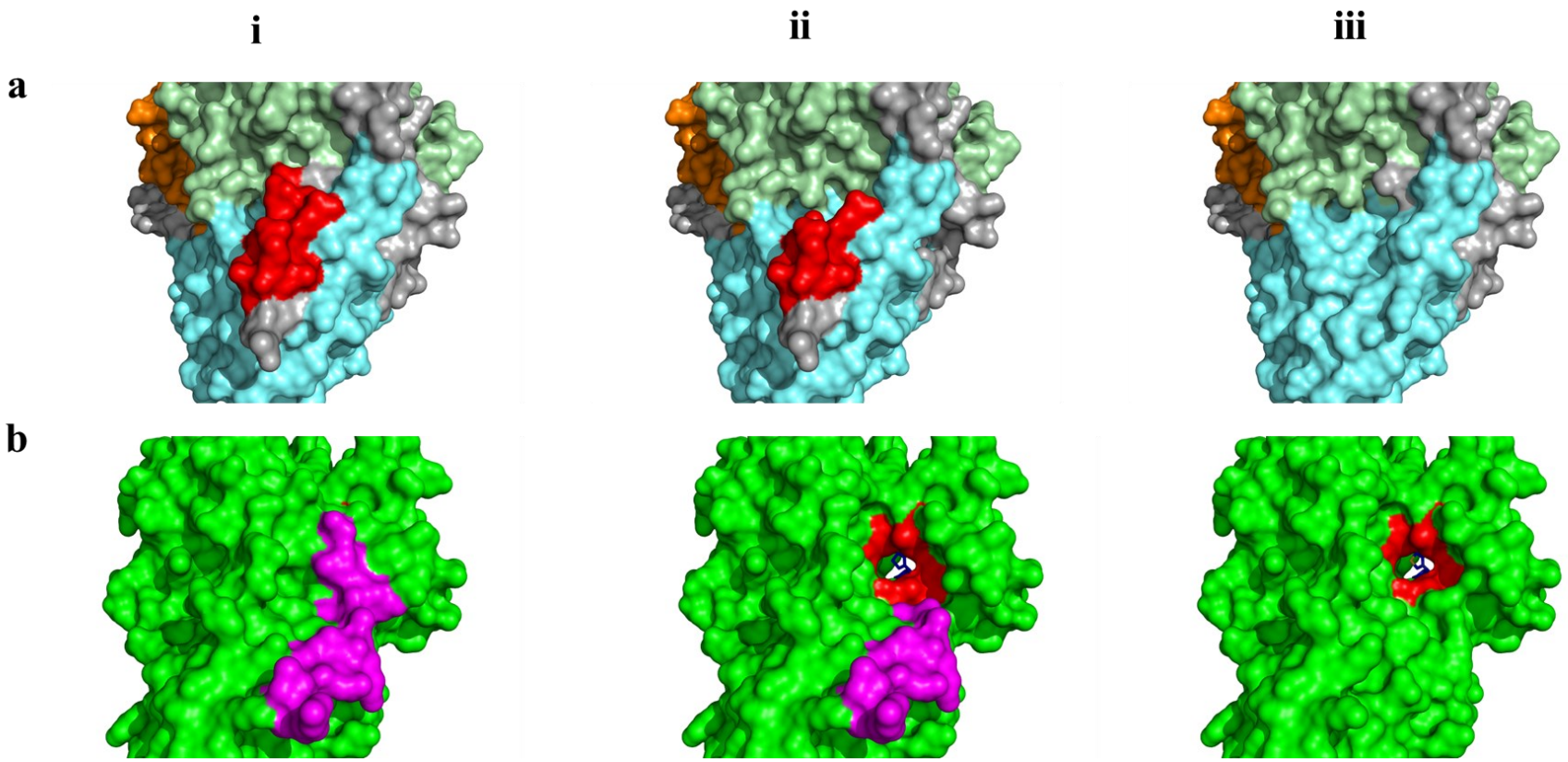


**Fig. 14: Position of the 'α-helix' in *C. glutamicum* PQO and 'α-peptide' in *E. coli* PoxB, at the C-terminus of the respective protein.**

(a) Different surface models of *C. glutamicum* PQO, with the same coloring representing the domain structure as shown in Fig. 9. From left to right: i) full-length PQO, ii) residues T556-D567 hidden, and iii) like ii), additionally all remaining residues from the α-helix hidden. (b) Different surface models of *E. coli* PoxB (green; PDB 3EY9), with residues equivalent to the ones in PQO forming an amphipathic α-helix at the C-terminus, marked in magenta. From left to right: i) full-length PoxB, ii) residues hidden at C-terminus, which do form an antiparallel β-sheet structure, and iii) residues I554-R572 hidden. To note the hydrophobic pore formed by L253, L254, V385, F465, L532 and L548, marked in red, enabling access to the active site with the cofactor TPP (stick, blue) if the antiparallel β-sheet structure is absent.

### 3.3.2 A C-terminal truncated PQO exhibits detergent-independent activity

Section 3.3.1 clarifies that *C. glutamicum* PQO possesses a distinctive conformation at its membrane-binding C-terminus. Since the Triton X-114 extraction method utilized in this study for native purification of the enzyme from *C. glutamicum* is based on its catalytic activation (Schreiner and Eikmanns, 2005), it was important to evaluate whether this distinctive conformation of PQO resulted from a conformational change provoked by the Triton X-114 extraction method. For this purpose, a recombinant N-terminal $His_6$-tagged PQO was overproduced in *E. coli* (M. Bellinzoni and co-workers). The enzyme underwent subsequently purification via $Ni^{2+}$-affinity chromatography, with the $His_6$-tag excised through TEV cleavage, and further purification was achieved by size exclusion chromatography. This purified recombinant protein readily crystallized, yielding crystals that were isomorphous to those obtained from the native protein (M. Bellinzoni, data not shown).

The entire structure of the PQO monomer was essentially indistinguishable to the high-resolution model derived from crystals of the native protein, exhibiting a root-mean-square deviation no greater than 0.3 Å (data not shown). This similarity extends to the entire C-terminal domain, which retains the same conformation described above, regardless of the presence of the bound cofactor TPP. This indicates that the conformation is not influenced by the detergent extraction procedure (M. Bellinzoni, data not shown).

As there is clear evidence that the distinct positioning and secondary structure of the amphipathic α-helix (residues A564-N575) is an intrinsic property of *C. glutamicum* PQO, this prompted further investigation into the role of this α-helix in the enzyme function and its enzymatic properties. Hence, a PQO variant that lacked the final 17 amino acids (corresponding to a cut at the Gly-rich region GGGVG, which precedes the α-helix) was constructed and overproduced in *C. glutamicum* Δ*pqo* (pEKEx2-*pqo*-$\Delta_{C17}$).

This PQO-$\Delta_{C17}$ overproducer strain was cultivated under a range of conditions and the specific PQO activity was assessed during both the exponential and the stationary phase (24 h of cultivation) and compared with the overproducer strain carrying the plasmid-encoded native *pqo* gene. No notable growth phenotype for *C. glutamicum* Δ*pqo* (pEKEx2-*pqo*-$\Delta_{C17}$) was observed under the tested conditions, but interestingly, excluding extracts of cells grown in the presence of acetate, enzyme activities detected in extracts of stationary phase cells were more than twofold higher for the PQO-$\Delta_{C17}$ variant (**Fig. 15**).

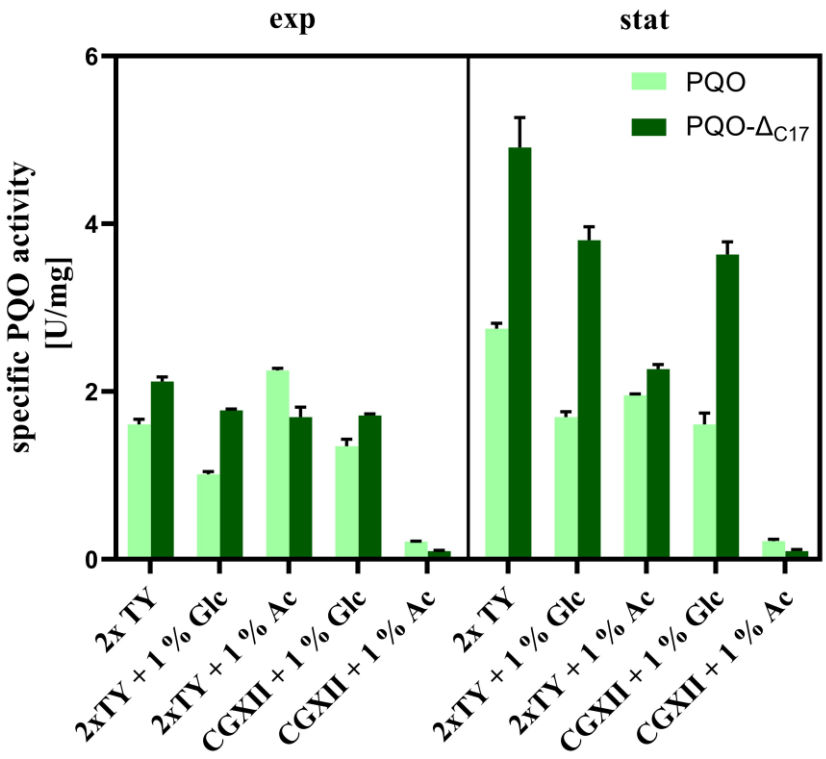


**Fig. 15: Comparative analysis of specific activity patterns for PQO and PQO-$\Delta_{C17}$ in cell extracts from PQO overproducing strains with a Δ*pqo* background.**

The PQO activity was assessed in cell extracts of two strains: *C. glutamicum* Δ*pqo* (pEKEx2-*pqo*) (represented in light green) and *C. glutamicum* Δ*pqo* (pEKEx2-*pqo*-$\Delta_{C17}$) (represented in dark green). These strains were cultivated in different media and harvested during both the exponential and stationary growth phases. (N = 3). TY, tryptone yeast extract; Ac, acetate; Glc, glucose.

Considering the observed alterations in activity on cell extract level of PQO-$\Delta_{C17}$, the decision was made to proceed with further purification and characterization of this enzyme variant. Hence, the PQO-$\Delta_{C17}$ overproducer strain was cultivated in 2xTY medium until the late stationary phase and the enzyme purified with the Triton X-114 extraction method mentioned above. The truncation of the last 17 amino acids in PQO-$\Delta_{C17}$ resulted in a significantly lower recovery of protein. The recovery rate of the full-length PQO post-Triton X-114 extraction was approximately 0.15 % (0.60 mg from 393 mg protein), whereas that of PQO-$\Delta_{C17}$ was around fourfold lower (0.04 %; 0.12 mg from 304 mg total protein) (**Tab. 7**). This probably implies that the truncated variant has reduced binding capacity to the Triton X-114 detergent.

**Tab. 7: Purification of PQO and PQO-$\Delta_{C17}$ with the Triton X-114 extraction method.**

Purification of PQO-$\Delta_{C17}$ from stationary phase *C. glutamicum* Δ*pqo* (pEKEx2-*pqo*-$\Delta_{C17}$) cells, grown in 2xTY medium. Comparison with full-length PQO purification under identical conditions, values in brackets, are also shown in Tab. 4.

| Purification step | total amount of protein (mg) | total activity (U) | specific activity (U/mg) | recovery of activity (%) | purification (fold) |
|---|---|---|---|---|---|
| harvesting of cell extract | 304 (393) | 1480 (1016) | 4.3 (2.6) | 100 (100) | 1 (1) |
| ultra-centrifugation | 288 (262) | 1191 (850) | 4.1 (3.2) | 80 (84) | 0.95 (1.3) |
| heat precipitation | 76 (128) | 780 (678) | 10.3 (5.3) | 53 (67) | 2.4 (2.0) |
| triton X-114 extraction | 0.12 (0.60) | 2.4 (43.4) | 20.0 (72.3) | 0.16 (4.3) | 4.6 (27.8) |

In cell extracts, the truncated PQO variant displayed higher specific activity (4.3 U/mg protein) relative to the full-length PQO (2.6 U/mg protein). This increased activity did not require the presence of the DDM detergent, a prerequisite for the full-length PQO which showed approximately a 4.5-fold activation in the *in vitro* enzymatic assay used in this study (**Fig. 16**). However, once purified, the full-length PQO demonstrated an elevated specific activity of 72.3 U/mg protein, in contrast to the truncated variant which showed a significantly reduced specific activity of 20.0 U/mg protein. This difference suggests potential stability issues for the PQO-$\Delta_{C17}$ when removed from the *C. glutamicum* cell extract environment.

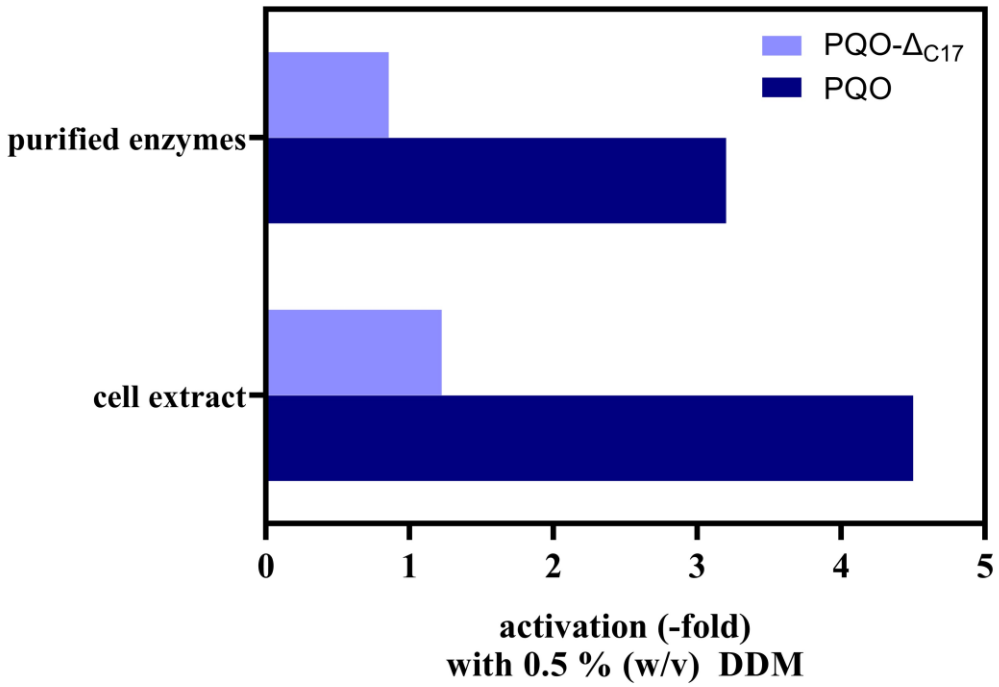


**Fig. 16: DDM-induced activation of *C. glutamicum* PQO.**

Enzyme activity was examined in cell extracts of *C. glutamicum* Δ*pqo* (pEKEx2-*pqo*) and *C. glutamicum* Δ*pqo* (pEKEx2-*pqo*-$\Delta_{C17}$) that were grown in 2xTY medium. Enzyme activity was assessed using the DCPIP reductase assay both in the presence and absence of the detergent DDM, and also analyzed the effect of DDM on the activation of purified PQO and PQO-$\Delta_{C17}$.

The specific activities of PQO and PQO-$\Delta_{C17}$ in cell extracts, in the absence of DDM, were 0.58 U/mg and 3.52 U/mg protein, respectively. For the purified enzymes, their specific activities, in the absence of DDM, were 22.6 U/mg and 23.4 U/mg protein, respectively.

The kinetic properties of PQO-$\Delta_{C17}$ revealed an approximately fivefold lower $k_{cat}$ (89 $s^{-1}$ vs. 440 $s^{-1}$) and a 1.5-fold lower $K_m$ value (35 mM vs. 53 mM) compared to the full-length PQO from 2xTY medium-grown cells (**Tab. 8**). These results strongly suggest that the C-terminal 17 amino acids within the PQO enzyme are critical for detergent/lipid binding and this binding appears to mediate enzyme activation. In the absence of these amino acids, the enzyme maintains full activity and does not require the presence of detergents *in vitro*, at least within the context of a *C. glutamicum* cell extract environment.

**Tab. 8: Steady-state kinetics of PQO compared to PQO-$\Delta_{C17}$.**

Kinetic parameters of PQO from *C. glutamicum* Δ*pqo* (pEKEx2-*pqo*) and PQO-$\Delta_{C17}$, cultivated in 2xTY medium, harvested after 24 h. For the calculation of the $k_{cat}$ values, a molecular weight of 247.8 kDa was assumed, corresponding to a tetramer of the enzyme.

| PQO variant | $K_m$ (mM) | $k_{cat}$ ($s^{-1}$) | $k_{cat}/K_m$ ($s^{-1}$ $M^{-1}$) |
|---|---|---|---|
| full-length (2xTY) | 53 | 440 | 8301 |
| $\Delta_{C17}$ (2xTY) | 35 | 89 | 2514 |

Given the observed changes in the kinetic properties of the truncated PQO variant together with its modified binding behavior with detergents, it was decided to structurally characterize PQO-$\Delta_{C17}$ to shed light on the underlying reasons for these alterations. The mutant protein was purified as an N-terminal $His_6$-tagged variant from an overexpressing *C. glutamicum* strain, followed by TEV cleavage of the tag (**Fig. 17**). Crystallization of the purified PQO-$\Delta_{C17}$ was only successful when the protein was supplemented with 2 mM TPP and 5 mM $MgCl_2$. This suggests that the absence of the thiamine cofactor could result in decreased stability of the enzyme.

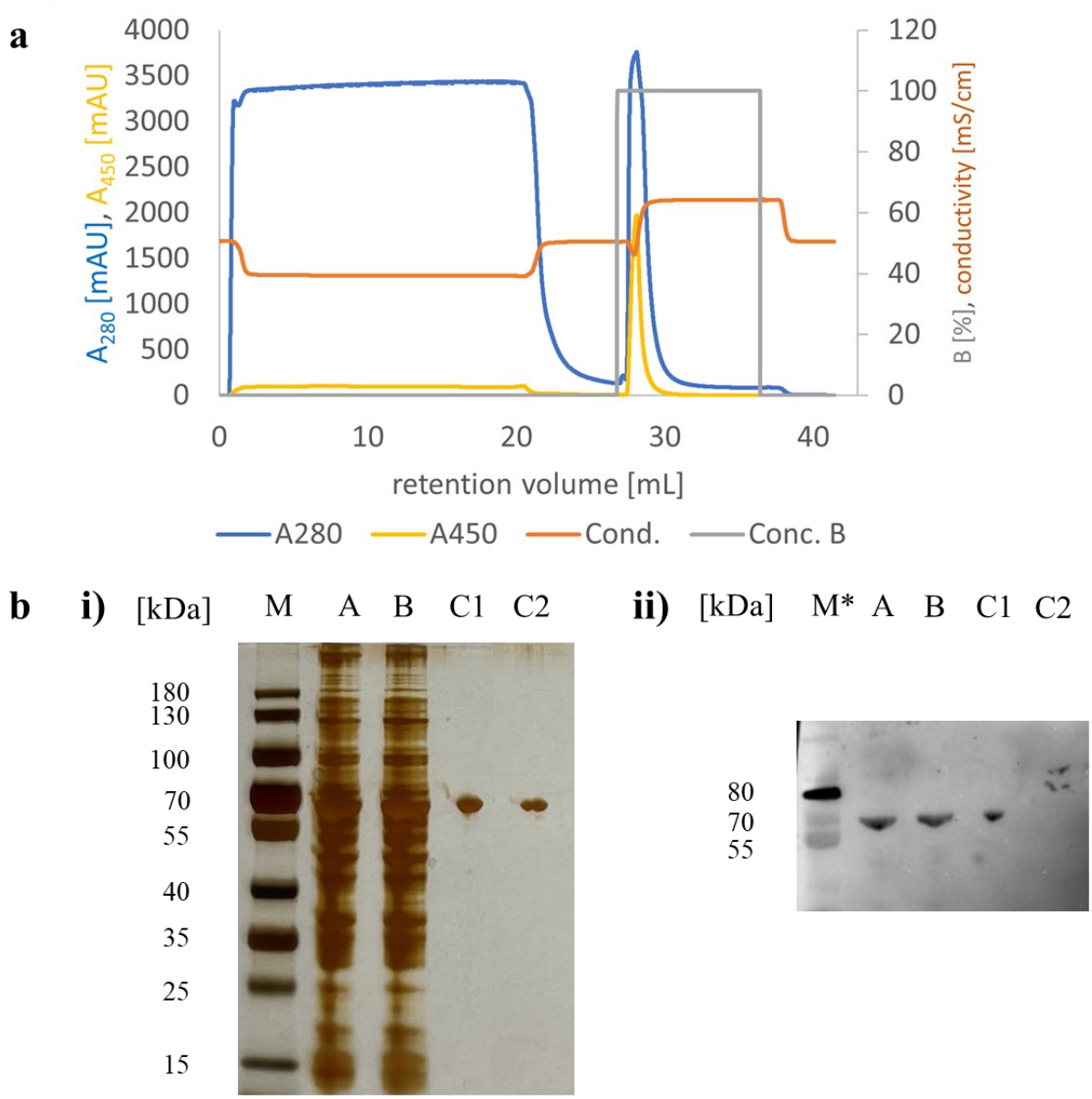


**Fig. 17: Purification of a N-terminal $His_6$-tagged PQO-$\Delta_{C17}$ variant from *C. glutamicum* Δ*pqo* (pEKEx2-*his*$_6$_TEV-*pqo*-$\Delta_{C17}$) by $Ni^{2+}$-NTA chromatography.**

(a) represents the purification process of $His_6$-tagged PQO-$\Delta_{C17}$ from cell extracts of *C. glutamicum* Δ*pqo* (pEKEx2-*his*$_6$_TEV-*pqo*-$\Delta_{C17}$), cultivated in 2xTY medium and harvested after 24 hours. The graph illustrates the absorbance at 280 nm (blue, left y-axis) and 450 nm (yellow, left y-axis). The percentage of applied elution buffer (grey, right y-axis) and conductivity (orange, right y-axis) are also depicted. (b) displays the SDS-PAGE analysis (i) and Western blot against the $His_6$-tag (ii) of different purification stages of $His_6$-tagged PQO-$\Delta_{C17}$. Lane labels are as follows: M, Prestained Protein Ladder™; M*, iBright™ Prestained Protein Ladder; A, cell extract; B, supernatant after ultracentrifugation; C1, sample after $Ni^{2+}$-NTA chromatography; C2, sample after TEV-protease treatment and separation via a 100 kDa cut-off filter.

For structural analysis, the purified enzyme was crystallized (M. Bellinzoni, manuscript in preparation). The crystal structure of PQO-$\Delta_{C17}$, solved at a resolution of 1.9 Å, displays the typical tetramer in association with FAD and a TPP-$Mg^{2+}$ complex (**Fig. 18a**). The polypeptide chain was visible up to the C-terminal end of the PP-binding domain, terminating at residue P538 for subunit D (**Fig. 18a**, yellow). However, the electron density map did not provide evidence for the rest of the C-terminal domain. This result suggests the cap section preceding the amphipathic α-helix may become excessively flexible when lacking the Gly-rich sequence that normally anchors it beneath the α-helix from R328 to Y349. Apart from this difference, no significant conformational changes were observed, with individual PQO-$\Delta_{C17}$ monomers superimposed on the high-resolution full-length structure exhibiting root-mean-square deviation values between 0.43 and 0.66 Å (**Fig. 18b**).

The characterization of the PQO-$\Delta_{C17}$ variant, which lacks the last 17 amino acids, provided insights into the structural and functional role of the C-terminal α-helix in the PQO enzyme from *C. glutamicum*. Despite showing full enzymatic activity in cell extracts without the need for detergents, PQO-$\Delta_{C17}$ exhibited a notably lower recovery of protein using the activation-dependent Triton X-114 extraction method. Further, especially outside of the cell extract environment, it obviously displays reduced stability, the purified PQO-$\Delta_{C17}$ showed a significant drop in specific activity compared to the full-length PQO. The kinetic properties of purified PQO-$\Delta_{C17}$ revealed a substantially lower turnover rate ($k_{cat}$) and a slightly lower $K_m$ value.

In conclusion, the C-terminal 17 amino acids in the PQO enzyme, which do include the amphipathic α-helix, are crucial for the stability of the enzyme, lipid/detergent binding, and potentially its enzymatic activation.

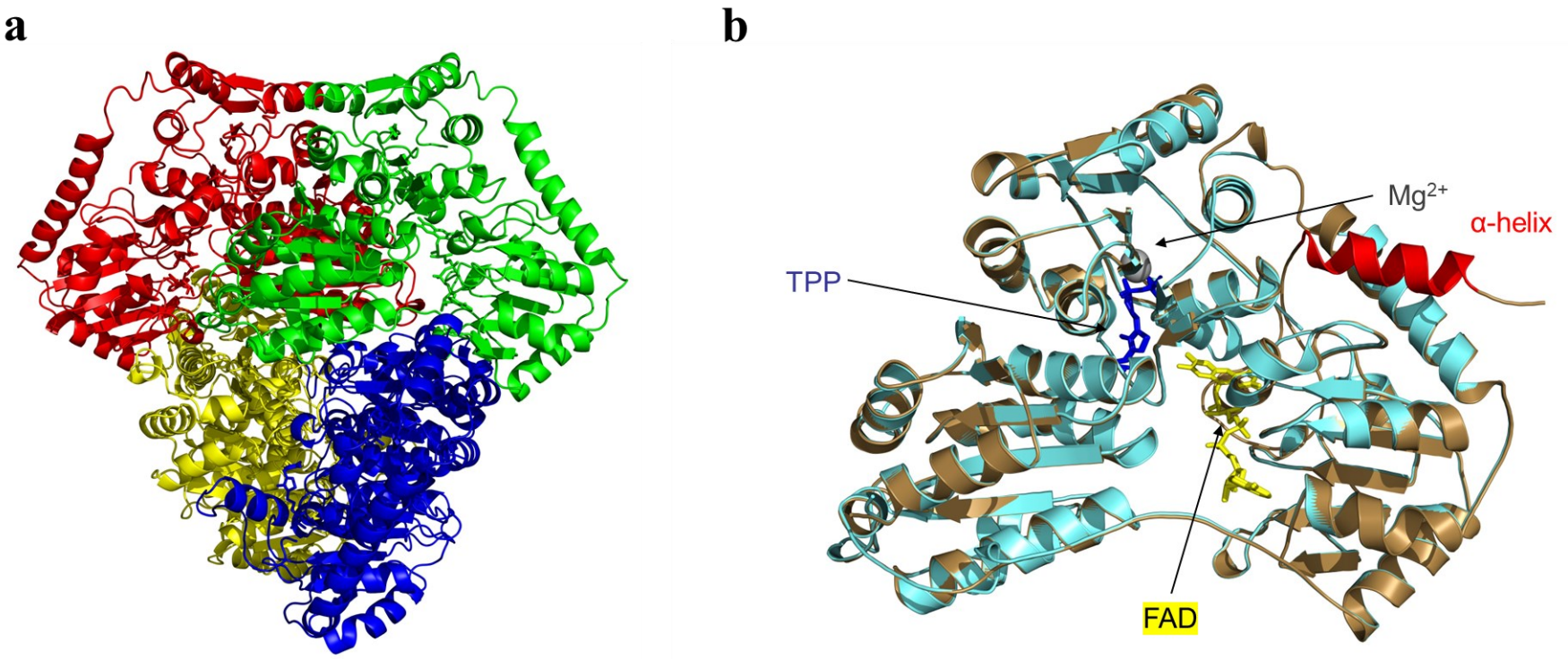


**Fig. 18: Cartoon overview of PQO-$\Delta_{C17}$, and structural alignment with the monomer of the full-length variant**

(a) Cartoon overview of *C. glutamicum* PQO-$\Delta_{C17}$, providing a schematic representation of its homotetrameric structure. Each chain within the tetramer is depicted in a distinct color (green, red, deep blue, yellow). The arrangement of the individual protomers follows a crystallographic 222 symmetry. (b) Cartoon overview of PQO (sand) upon superimposition to the truncated PQO-$\Delta_{C17}$ variant (cyan). The cofactors FAD (yellow) and TPP (deep blue) are represented as sticks, the divalent cation $Mg^{2+}$ as a grey sphere. The α-helix of the full-length variant, marked in red, was deleted in PQO-$\Delta_{C17}$. Resolution = 1.9 Å.

### 3.3.3 Lysine residues found to be post-translationally modified are located at the surface of PQO

Upon clarification of the PQO structure, a deeper analysis was conducted to determine if the lysine residues identified as acylated in the mass spectrometry study (see section 3.3.2) were also modified in the structure, which could potentially induce structural changes. Additionally, the structure was examined to discern whether these modified residues contribute to the catalytic functionality of PQO.

Upon examination of the crystal structures, potential modifications were observed on lysine residues K121 and K325 in the high-resolution structure of the full-length PQO originating from acetate minimal-medium grown cells (M. Bellinzoni, personal communication). For K121, the precise type of PTM could not be unequivocally determined, though the electron density map suggests propionylation (M. Bellinzoni, personal communication). Yet, this residue was not identified to be modified in the mass spectrometry study. Nevertheless, three slightly modified *pqo* gene alleles were created to analyze the influence of K121 post-translational modification on PQO. The resulting PQO enzyme variants, namely K121A (neutral amino acid), K121E (negatively charged amino acid), and K121R (positively charged amino acid) were overproduced from plasmid pEKEx2 in *C. glutamicum* Δ*pqo*. The strains were cultivated in 2xTY medium, glucose, and acetate minimal medium, and PQO activity patterns were determined during both exponential and late stationary phase (24 h) (**Fig. 19**). Construction, cultivation and the activity measurements of the strains described in the following were performed by D. Vogel in his bachelor thesis under my supervision.

Most notable were the changes observed for the K121A variant in extracts from 2xTY medium-grown cells, which showed 0.5-fold lower specific activity in both growth phases, and for the K121R variant in extracts from acetate minimal medium-grown cells, which exhibited up to twofold higher specific activity compared to the wildtype PQO at the stationary phase. Specifically, it is worth noting that the K121R mutant variant generally displayed similar or higher activity compared to the wildtype enzyme, while the K121A and K121E mutants generally showed similar or lower activities. These findings indicate that the K121 residue in the native PQO may play a significant role in the regulation of enzyme activity, and that this regulatory role can be influenced by the cultivation conditions of the strain.

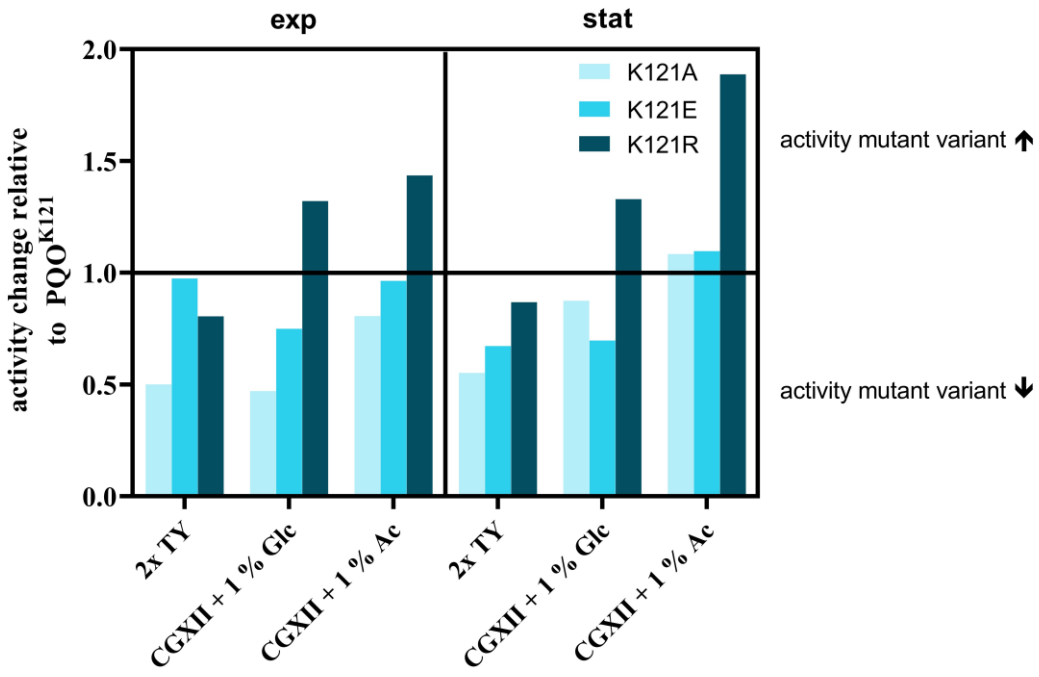


**Fig. 19: Relative specific activity of PQO K121 variants compared to wildtype PQO.**

The relative specific PQO activity of *C. glutamicum* Δ*pqo* (pEKEx2-*pqo*$^{K121A/E/R}$) was determined using cell extracts and normalized to the specific PQO activity of *C. glutamicum* Δ*pqo* (pEKEx2-*pqo*), represented from light to dark blue. The strains were cultivated in different media and harvested at both the exponential and stationary phase (24 h). The specific activities of the mutant variants were normalized to the specific activities in 2xTY medium, CGXII minimal medium with 1 % glucose, and CGXII minimal medium with 1 % acetate, which were 2.8 U/mg, 1.6 U/mg, and 0.22 U/mg protein, respectively. The presented data are mean values obtained from three independent experiments for wildtype PQO, and three independent experiments for all mentioned mutants. Ac, acetate; Glc, glucose.

Given the evidence of modifications at lysine residues K93, K121, K325 and K500, which are also potentially crucial for the catalytic function of the PQO enzyme (see sections 3.2.2 and 3.2.4), it was deemed necessary to examine the structure of PQO at these specific residues. A structural rationale may exist for the significant impact that mutations at these specific residues appear to have.

**Fig. 20** illustrates the structure of the PQO monomer, with particular attention to the highlighted lysine residues: K93, K121, K325, and K500. K93 and K121 are situated within the Pyrimidine-binding domain, K325 is within the FAD-binding domain, and K500 is found in the PP-binding domain. All of these residues are exposed to the protein's surface.

K93, in its unmodified state, is roughly 10 Å apart from the adenine ring of the bound FAD cofactor. This distance shrinks when the residue is acetylated. The negative charge of the acetyl group might instigate an electrostatic interaction with the positively charged adenine moiety of the FAD cofactor. Therefore, a mutation at this residue that impedes post-translational modifications could affect the stability of the bound cofactor.

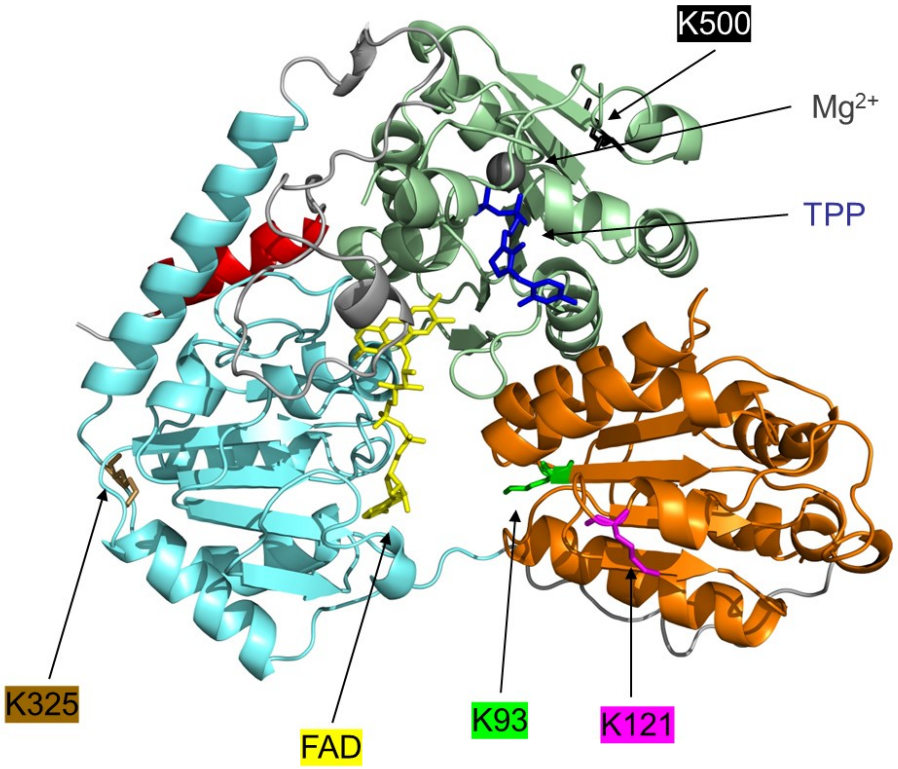


**Fig. 20: PQO monomer as purified natively from *C. glutamicum* Δ*pqo* (pEKEx2-*pqo*). Lysine residues prone to post-translational modifications are highlighted.**

Cartoon overview of a *C. glutamicum* PQO monomer, with bound cofactors FAD and TPP depicted as sticks and $Mg^{2+}$ as a sphere. The coloring scheme follows the coloring of the domains as depicted in Fig. 9. Lysine residues identified in this work to be potentially acetylated, succinylated or propionylated are highlighted and also depicted as sticks.

In contrast, K121 does not appear to influence the binding of the cofactors according to the structure, nor does it interact with residues within the individual monomer. However, as illustrated in **Fig. 21**, K121 is positioned such that two K121 residues are relatively close to each other within the tetrameric assembly, at a distance of 10.5 Å.

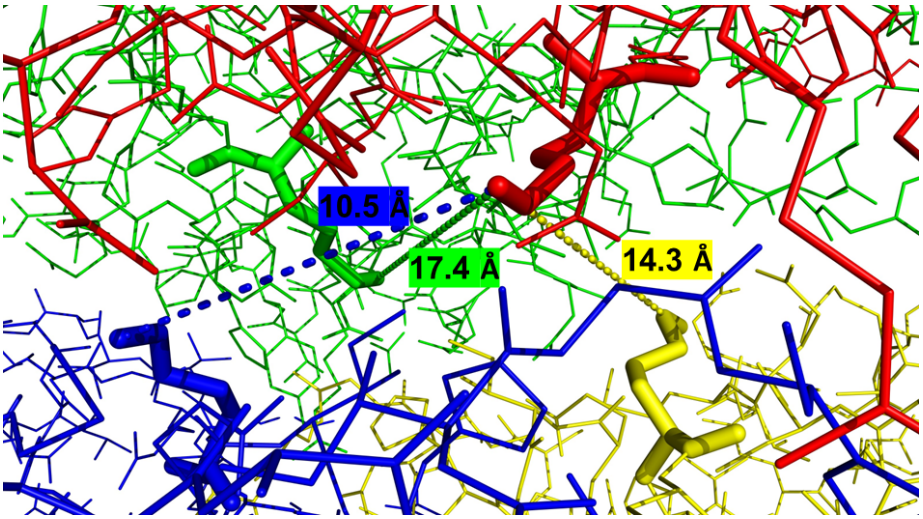


**Fig. 21: PQO tetramer as purified natively from *C. glutamicum* Δ*pqo* (pEKEx2-*pqo*). Distance of K121 of each individual monomer is highlighted.**

Schematic overview of a *C. glutamicum* PQO tetramer, depicted in lines. The coloring scheme follows the coloring of the individual monomers as depicted in Fig. 9. K121 identified in this work to be either acetylated, succinylated or propionylated, is represented in stick model.

Consequently, alterations to this residue that prevent post-translational modifications could potentially affect the stability and formation of the PQO tetrameric assembly. Changes to this specific residue might interfere with the natural positioning and interaction of the subunits, thereby compromising the structural integrity of the PQO tetramer or strengthen it.

K325, when unmodified, is situated close to K202, with an approximate separation of 7.0 Å. Additionally, N199 is also in its vicinity. In the event of succinylation at K325, the electronic charge dynamics with these residues would shift from repulsion, due to their similar charges, to attraction, as the succinyl group introduces an overall negative charge to K325. Furthermore, the inclusion of a succinyl group reduces the inter-residue distance. Hence, succinylation at K325 could enhance the structural integrity of PQO, particularly within the FAD-binding domain, by improving the inter-residue interaction and stability.

In its unmodified state, K500 could engage in an electrostatic interaction with Y520, given that the negatively charged oxygen atom of Y520 and the positively charged amino group of K500 are only 5.6 Å apart. However, if K500 is succinylated, it would introduce a negative charge, resulting in electrostatic repulsion between K500 and Y520. This suggests that succinylation at this residue may alter the protein's conformation or stability by disrupting this interaction.

## 3.4 Physiological role of PQO in *C. glutamicum*

In actinobacteria, sugar metabolism typically proceeds via glycolysis and subsequent oxidative decarboxylation of pyruvate to acetyl-CoA by the pyruvate dehydrogenase complex (reviewed in Sauer and Eikmanns, 2005). However, the alternative pyruvate oxidation route catalyzed by PQO in *C. glutamicum* is poorly understood in terms of its genetic regulation and physiological role. As evidenced from the crystal structure of PQO from *C. glutamicum* (see section 3.3), corynebacterial PQO is a homotetrameric flavoprotein containing FAD, thiamine pyrophosphate, and $Mg^{2+}$ as essential cofactors. It is activated by Triton X-100, phosphatidylglycerol, and dipalmitoyl-phosphatidylglycerol, and uses menaquinone as the physiological electron acceptor (Schreiner and Eikmanns, 2005). Alternatively, it is also activated up to fivefold by the detergent DDM (see section 3.3.2). The *pqo* gene is organized as an operon with two further genes located downstream of *pqo* and so far, not further investigated (Schreiner *et al*., 2006). The PQO protein is well characterized under biochemical aspects, yet, the physiological role of it in *C. glutamicum* remains unknown. The following section depicts attempts to elucidate possible physiological roles of the PQO enzyme.

### 3.4.1 Overproduction of PQO-$\Delta_{C17}$ enables pyruvate decarboxylase-deficient *C. glutamicum* strains to use glucose partially for biomass generation

Apart from PQO, the wildtype of *C. glutamicum* possesses the acetate activating enzymes acetate kinase (ACK) and phosphotransacetylase (PTA) and thus, a theoretical bypass of the pyruvate dehydrogenase complex (PDHC) reaction (see Introduction and **Fig. 1**). Although a *pqo*-deficient mutant of *C. glutamicum* did not show any phenotype under all conditions tested, the overexpression of *pqo* was able to partially complement the growth phenotype of the *aceE*-deficient strain (E1 subunit of the PDHC, E1p/AceE) in 2xTY complex medium, indicating that PQO in principle can complement a PDHC deficiency (Schreiner *et al*., 2006; see **Fig. 22** and **Fig. 23**). However, Schreiner *et al*. also showed that the *aceE*-deficient strain is not able to grow on glucose as a sole carbon source. Despite the presence of PQO, ACK and PTA, it needs to be supplemented with e.g. acetate (see **Fig. 22**).

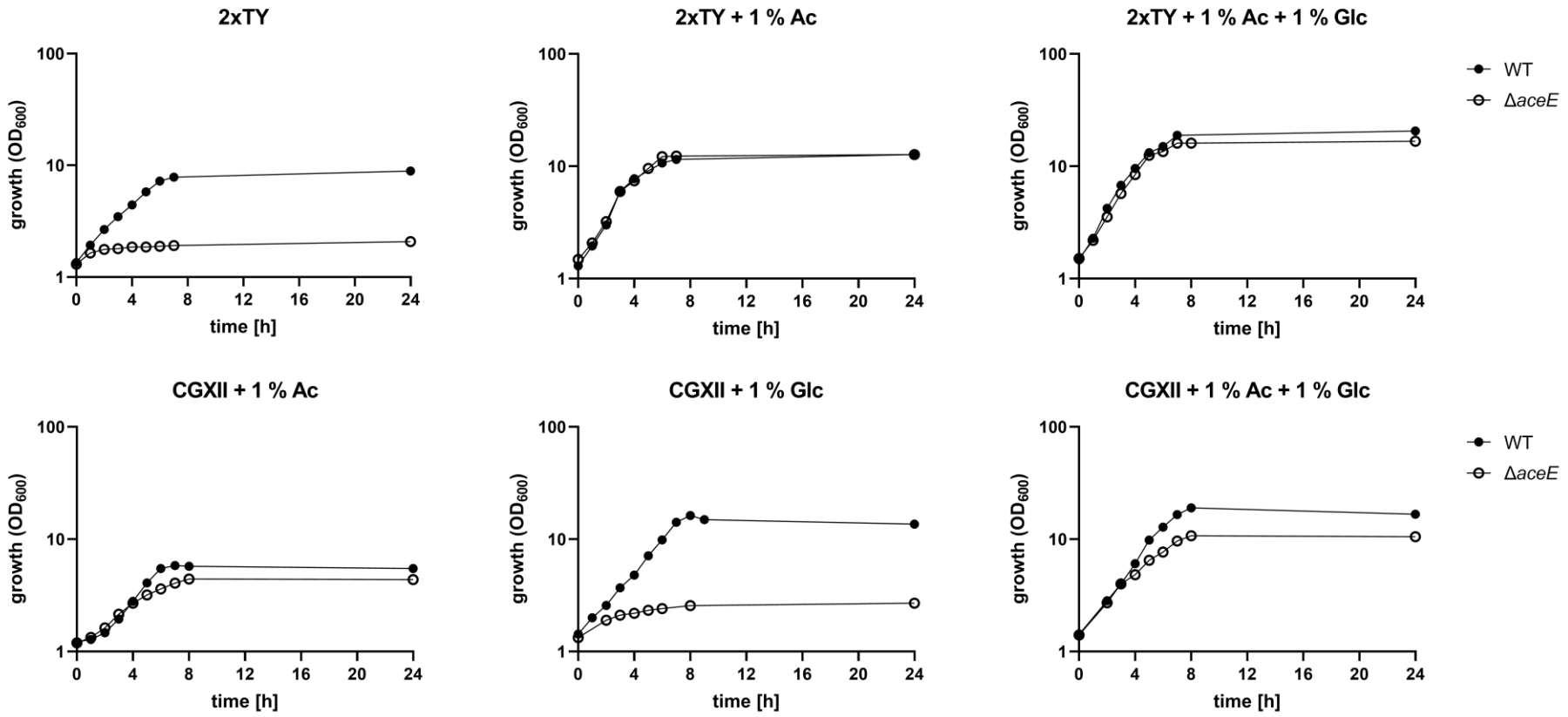


**Fig. 22: Growth of *C. glutamicum* versus growth of *C. glutamicum* Δ*aceE*.**

Growth of *C. glutamicum* WT (filled circles) and *C. glutamicum* Δ*aceE* (open circles) cultivated in different media. The presented data displays the mean values obtained from three independent cultures, with standard deviations below 10 %. Ac, acetate; Glc, glucose.

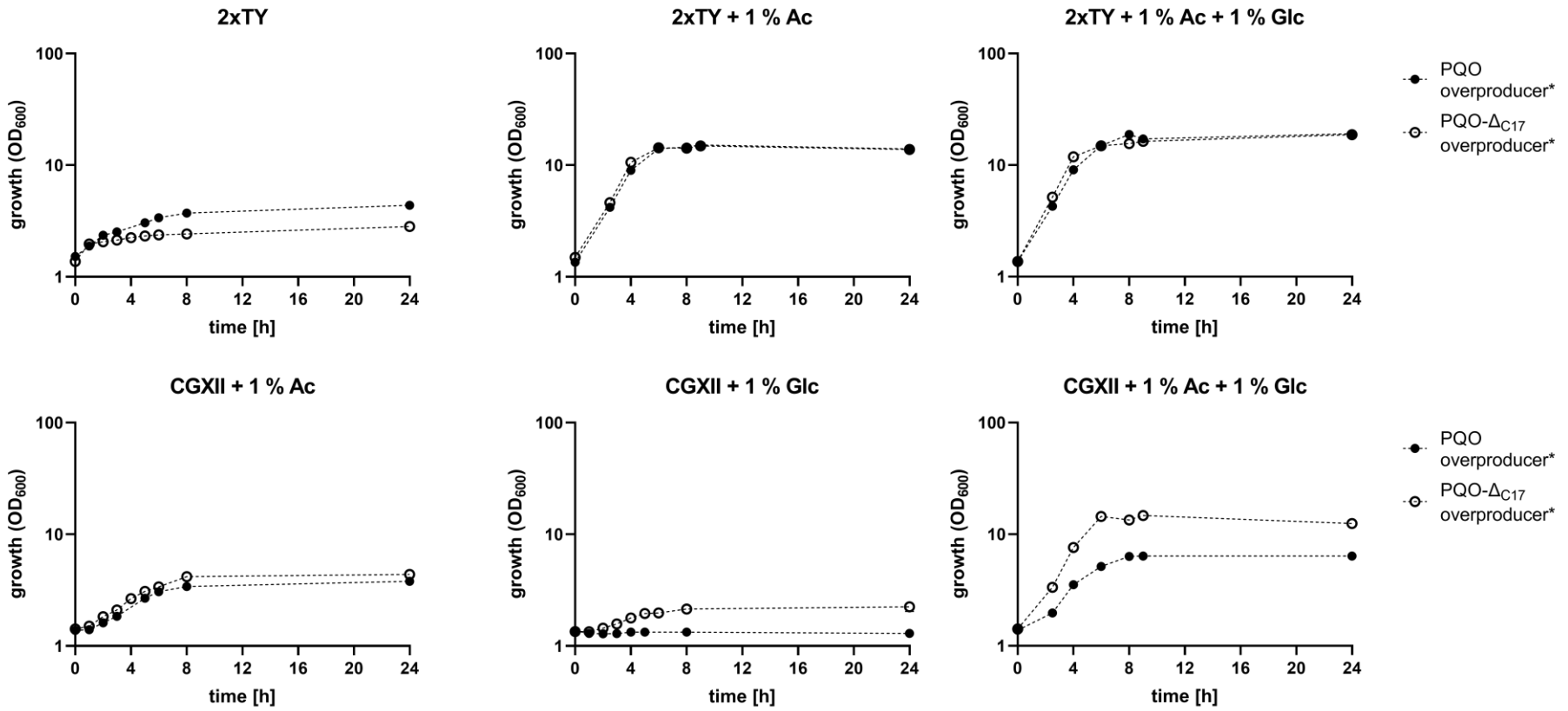


**Fig. 23: Growth of *C. glutamicum* PQO overproducer strains in a Δ*aceE* Δ*pqo*-background.**

Growth of *C. glutamicum* Δ*aceE* Δ*pqo* (pEKEx2-*pqo*) (filled circles, PQO overproducer*) and *C. glutamicum* Δ*aceE* Δ*pqo* (pEKEx2-*pqo*-$\Delta_{C17}$) (open circles, PQO-$\Delta_{C17}$ overproducer*) cultivated in different media. The presented data displays the mean values obtained from three independent cultures, with standard deviations below 10 %. Ac, acetate; Glc, glucose.

Here, it was tested whether overexpression of the native and the truncated version of *pqo* restores the growth of the *aceE*-deficient mutant of *C. glutamicum* in minimal medium with glucose as sole carbon source. For this purpose, *C. glutamicum* Δ*aceE* Δ*pqo* (pEKEx2-*pqo*) and *C. glutamicum* Δ*aceE* Δ*pqo* (pEKEx2-*pqo*-$\Delta_{C17}$) were grown in different media and their growth was analyzed (**Fig. 23**). To point out the difference to the PQO overproducer strains described before in this thesis, these strains with the Δ*aceE* Δ*pqo*-background are designated as PQO overproducer* and PQO-$\Delta_{C17}$ overproducer*, respectively. As depicted in **Fig. 23**, both these strains showed very restricted growth in 2xTY medium and in minimal medium containing glucose as carbon source, similar to the *aceE*-deficient strain (**Fig. 22**). In contrast, both the PQO overproducer* and PQO-$\Delta_{C17}$ overproducer* were growing well in 2xTY medium containing acetate or acetate plus glucose (**Fig. 23**). In acetate minimal medium, both strains grew slower and to lower final cell densities ($OD_{600}$ < 4.0) than the wildtype strain, similar to the *aceE*-deficient strain. Almost no growth of both PQO overproducer* strains was observed in glucose minimal medium. In minimal medium with acetate plus glucose, the maximum $OD_{600}$ reached by the PQO-$\Delta_{C17}$ overproducer* was more than twice as high as the one reached by the PQO overproducer* (14.5 to 6.4). For comparison, the *aceE*-deficient strain reached a maximum $OD_{600}$ of 10.7. This result suggests that under the conditions applied here the altered structural-biochemical properties of PQO-$\Delta_{C17}$ enable the strain to use glucose, at least partially for biomass generation.

To check whether altered PQO activity patterns led to the observed phenotype, cell extracts of the PQO overproducer* and the PQO-$\Delta_{C17}$ overproducer* at both the mid-exponential and the late stationary growth phase (24 h) were analyzed for PQO activity (**Fig. 24**). Contrarily to cell extracts of the full-length variant overproducer*, the cell extracts of the PQO-$\Delta_{C17}$ overproducer* showed in general higher specific PQO activities at the exponential phase, and *vice versa* in the stationary phase. The exception to this trend was observed in cells of the PQO overproducer* when grown in acetate minimal medium. These results indicate that the last 17 amino acids of PQO play an important role in modulating the growth phase-dependent activity of the enzyme when the E1p subunit of the PDHC is absent in *C. glutamicum*.

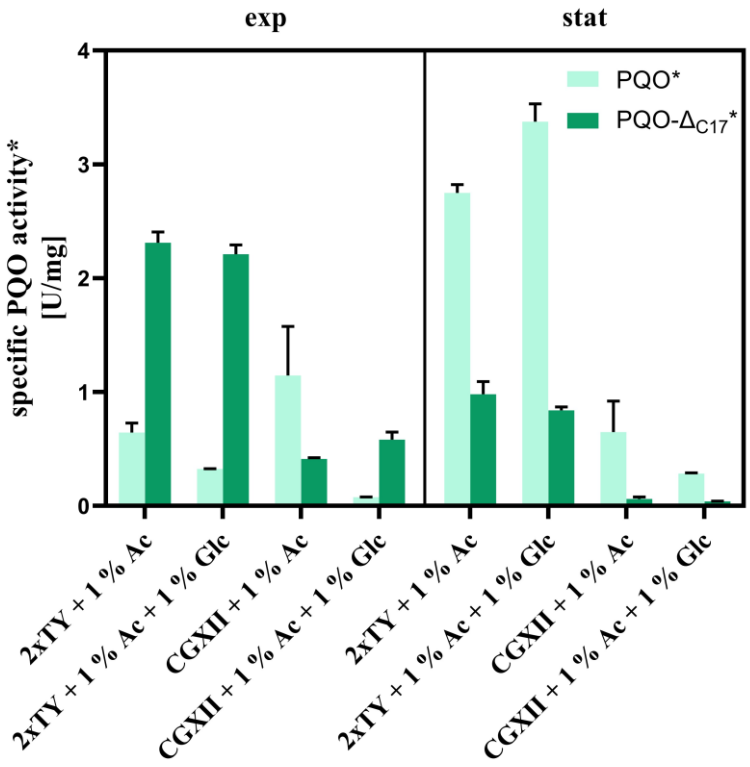


**Fig. 24: Comparative analysis of specific activity patterns for PQO and PQO-$\Delta_{C17}$ in cell extracts from PQO overproducers strains with Δ*aceE* Δ*pqo*-background.**

PQO activity in cell extracts of *C. glutamicum* Δ*aceE* Δ*pqo* (pEKEx2-*pqo*), represented in light green, and *C. glutamicum* Δ*aceE* Δ*pqo* (pEKEx2-*pqo*-$\Delta_{C17}$), represented in dark green, cultivated in different media and harvested at both the exponential (**exp**) and stationary phase (**stat, 24 h**). In all activity measurements, n-dodecyl-β-D-maltoside (DDM) was included in the test buffer (N = 3). Ac, acetate; Glc, glucose.

## 3.4.2 PQO presence in *C. glutamicum* is detrimental in Penicillin G induced glutamate producing conditions

### 3.4.2.1 PQO activity is comparatively high in Penicillin G induced glutamate producing conditions

Considering the work conducted by Mizuno *et al*. (2016), which suggested altered acetylation or succinylation of lysine residues in the PQO enzyme under non-producing or glutamate producing conditions (see section 3.2.1), PQO activity patterns were determined systematically under conditions with and without the addition of Penicillin G. Penicillin G inhibits transpeptidase activity, leading to the inhibition of cross-linking of cell wall peptidoglycan (reviewed by Walsh, 1989). Moreover, alterations in membrane composition have been shown

to be a necessary precursor to trigger glutamate production by *C. glutamicum* (Hoischen and Krämer, 1990).

To obtain a comprehensive understanding of PQO regulation under glutamate producing conditions, *C. glutamicum* wildtype, the PQO-deficient strain *C. glutamicum* Δ*pqo*, and the PQO overproducer strain *C. glutamicum* Δ*pqo* (pEKEx2-*pqo*) were cultivated in CGXII minimal medium containing either 1 % or 6 % glucose, with or without the addition of Penicillin G (60 U/mL). Addition of Penicillin G at 3.6 h of cultivation resulted in a drastic effect on the growth phenotype of all strains, with growth ceasing after 2 h and final $OD_{600}$ values ranging only between 1.6 and 3 (**Fig. 25**).

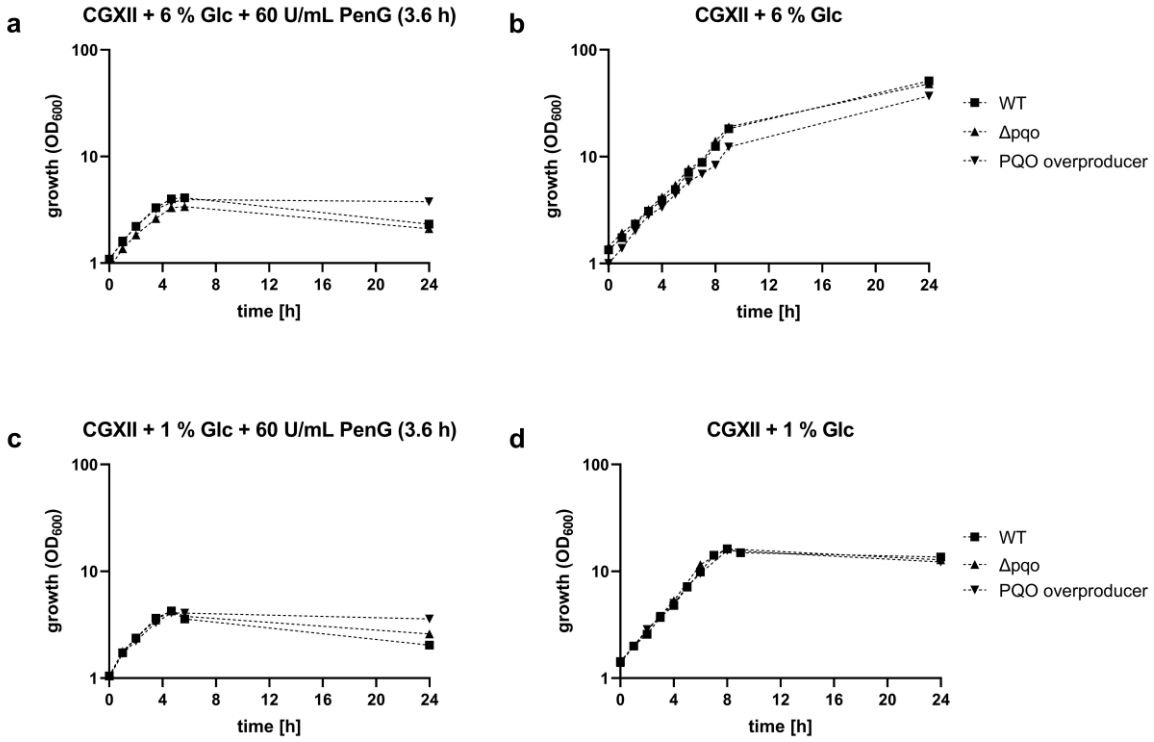


**Fig. 25: Growth of *C. glutamicum* strains in glucose minimal medium with or without addition of Penicillin G (PenG).**

Growth of *C. glutamicum* WT (squares), *C. glutamicum* Δ*pqo* (triangles) and *C. glutamicum* Δ*pqo* (pEKEx2-*pqo*) (inverted triangles, PQO overproducer), cultivated in CGXII minimal medium with 6 % glucose (upper row; a and b) or 1 % glucose (bottom row; c and d). Penicillin G at a concentration of 60 U/mL was either added (left; a and c) or omitted (right; b and d). The presented data display the mean values obtained from three independent cultures, with standard deviations below 10 %. Glc, glucose.

All strains produced between 3 to 6 g/L glutamate after 24 h of cultivation (data not shown). Notably, the PQO overproducer strain exhibited higher final $OD_{600}$ values under these conditions compared to the wildtype and the PQO-deficient strain. However, if Penicillin G was omitted from the cultivations, no significant differences between the strains were observed.

PQO activities of cell extracts from the three *C. glutamicum* strains after 24 h of cultivation were analyzed (**Fig. 26**). The *pqo* deletion strain exhibited no detectable activity under all tested conditions (data not shown).

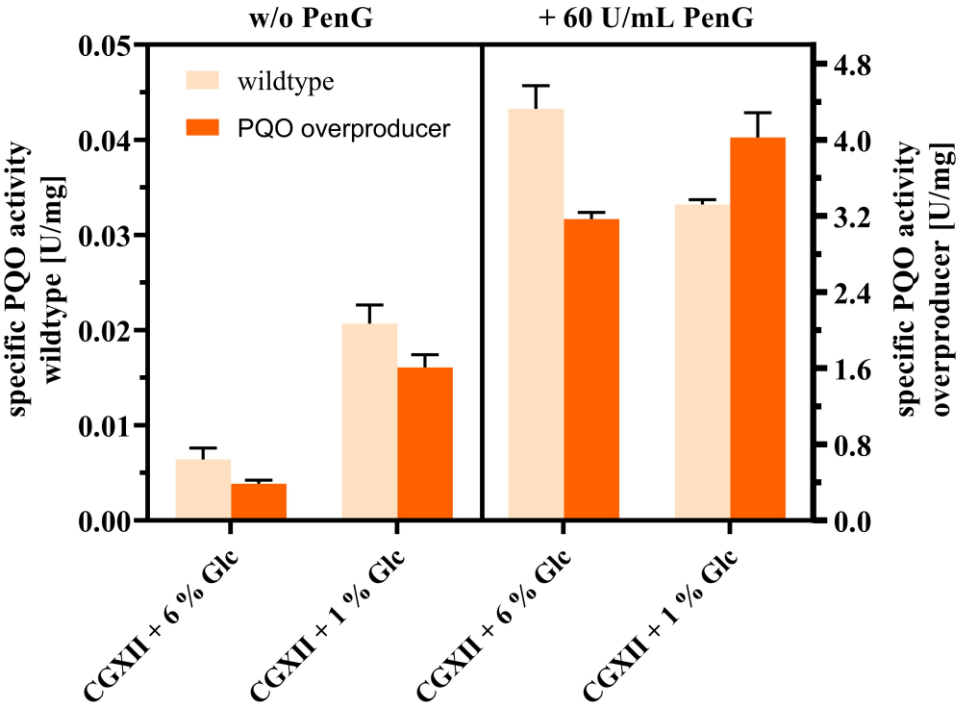


**Fig. 26: Specific PQO activity in cell extracts of *C. glutamicum* and *C. glutamicum* Δ*pqo* (pEKEx2-*pqo*) (PQO overproducer) in glucose minimal medium with or without the addition of Penicillin G (PenG).**

PQO activity in cell extracts of *C. glutamicum* (represented in light orange) and *C. glutamicum* Δ*pqo* (pEKEx2-*pqo*) (represented in dark orange), cultivated in glucose minimal medium with either 6 % or 1 % glucose. 60 U/mL Penicillin G was either omitted (left) or added after 3.6 h of cultivation (right). Cells were harvested after 24 h of cultivation. (N = 3). Glc, glucose.

In the cultures without Penicillin G, both the wildtype strain and the *pqo* overexpressing strain displayed higher overall activities in 1 % glucose minimal medium (0.02 U/mg protein and 1.6 U/mg protein, respectively) than in 6 % glucose minimal medium (0.006 U/mg protein and 0.39 U/mg protein, respectively). When comparing the PQO activities under glutamate producing and non-producing conditions, activities were found to be higher in glutamate producing conditions. For the wildtype strain in 1 % glucose minimal medium, activities were 1.7-fold higher, while for the PQO overproducer, activities were 2.5-fold higher. In 6 % glucose minimal medium, the wildtype strain displayed a 6.7-fold higher activity in glutamate producing conditions, while the PQO overproducer exhibited an 8.1-fold higher activity.

Taken together, PQO activity was found to be higher under glutamate producing conditions compared to non-producing conditions, and this trend was consistent across both glucose concentrations tested. These findings provide valuable insights into the regulatory mechanisms underlying PQO activity and suggest an important role of PQO under biotechnological relevant conditions.

#### 3.4.2.2 Co-culture experiments reveal that PQO is irrelevant in cultivations with 2xTY medium, glucose or acetate minimal medium

Considering the diverse conditions under which different *C. glutamicum* strains were cultivated in this study, resulting in varying PQO activity patterns, and yet, no apparent phenotype was linked to the presence or absence of full-length PQO (except for the overproduction of the PQO-$\Delta_{C17}$ truncated variant, which enabled an *aceE*-deficient strain to use glucose partially for biomass generation as discussed in section 3.4.1), co-culture experiments were conducted to explore whether PQO presence or absence confers any benefits to cells.

To facilitate qualitative monitoring of the abundance of wildtype and a PQO-deficient *C. glutamicum* strain in a co-culture, fluorescent variants for each strain were constructed. For both strains, two variants, one carrying the gene for the constitutive overproduction of the red fluorescent protein mCherry and the other carrying the gene for the green fluorescent protein Mut2, were created. This resulted in the four following strains: *C. glutamicum* (pPBEx2$^{\dagger}$-*mCherry*), *C. glutamicum* (pPBEx2$^{\dagger}$-*mut2*), *C. glutamicum* Δ*pqo* (pPBEx2$^{\dagger}$-*mCherry*) and *C. glutamicum* Δ*pqo* (pPBEx2$^{\dagger}$-*mut2*). First, each of the four strains was cultivated individually to exclude any possible interference of the fluorescent proteins with observed phenotype or PQO activity compared to their respective parental strain. All strains showed the same growth rate and the same maximum $OD_{600}$ as the respective parental strain in cultivations within 2xTY

medium, glucose or acetate minimal medium and the respective fluorescent proteins were functional (data not shown). Additionally, PQO activities were determined in cell extracts of all four strains at mid-exponential and stationary phase (24 h of cultivation). Once again, the *pqo* deletion strain exhibited no detectable activity under all tested conditions. For the two wildtype strains either overproducing mCherry or Mut2 and cultivated in 2xTY medium, glucose or acetate minimal medium, respectively, the activities measured in cell extracts were almost identical to the ones of the 'normal' wildtype strain, as shown in **Tab. 9**. These findings confirmed that both fluorescent proteins do not interfere with the PQO enzyme assay.

**Tab. 9: Specific PQO activity in cell extracts of *C. glutamicum*, *C. glutamicum* (pPBEx2†-*mCherry*) and *C. glutamicum* (pPBEx2†-*mut2*).**

PQO activity in cell extracts of *C. glutamicum*, *C. glutamicum* (pPBEx2†-*mCherry*) and *C. glutamicum* (pPBEx2†-*mut2*), cultivated in either 2xTY medium, glucose or acetate minimal medium, determined at the mid-exponential and stationary phase (24 h of cultivation). (N = 3).

| strain | 2xTY | | CGXII + 1 % glucose | | CGXII + 1 % acetate | |
|---|---|---|---|---|---|---|
| | exp | stat | exp | stat | exp | stat |
| *C. glutamicum* | 0.038 ± 0.006 | 0.078 ± 0.006 | 0.024 ± 0.003 | 0.027 ± 0.002 | 0.012 ± 0.002 | 0.009 ± 0.002 |
| *C. glutamicum* (pPBEx2†-*mCherry*) | 0.040 ± 0.007 | 0.075 ± 0.006 | 0.021 ± 0.003 | 0.024 ± 0.005 | 0.013 ± 0.003 | 0.011 ± 0.002 |
| *C. glutamicum* (pPBEx2†-*mut2*) | 0.037 ± 0.004 | 0.074 ± 0.007 | 0.027 ± 0.004 | 0.026 ± 0.005 | 0.009 ± 0.001 | 0.010 ± 0.002 |

Since the fluorescent strains were not showing deviations in phenotype or PQO activities (**Tab. 9**) compared to the parental wildtype and PQO-deficient strains of *C. glutamicum*, they were suitable for co-culture experiments. For each experiment, two co-cultures in triplicates were created by inoculating a single flask containing either 2xTY medium, 1 % glucose or 1 % acetate minimal medium, with equal amounts of both a fluorescent wildtype strain and a fluorescent PQO-deficient strain. Pre-cultures of the four individual fluorescent strains were grown overnight in 2xTY medium. The first co-culture contained the fluorescent wildtype strain

of *C. glutamicum* overproducing Mut2, and the PQO-deletion strain overproducing mCherry, while the second co-culture was *vice versa*. The initial ratio of 50:50 was monitored using fluorescent measurements (Mut2 signal divided over mCherry signal of each culture, **Fig. 27**) to determine if it remained equal over the course of cultivation between the two different co-cultures, and this was used to examine whether the presence or absence of PQO is detrimental or beneficial for *C. glutamicum*.

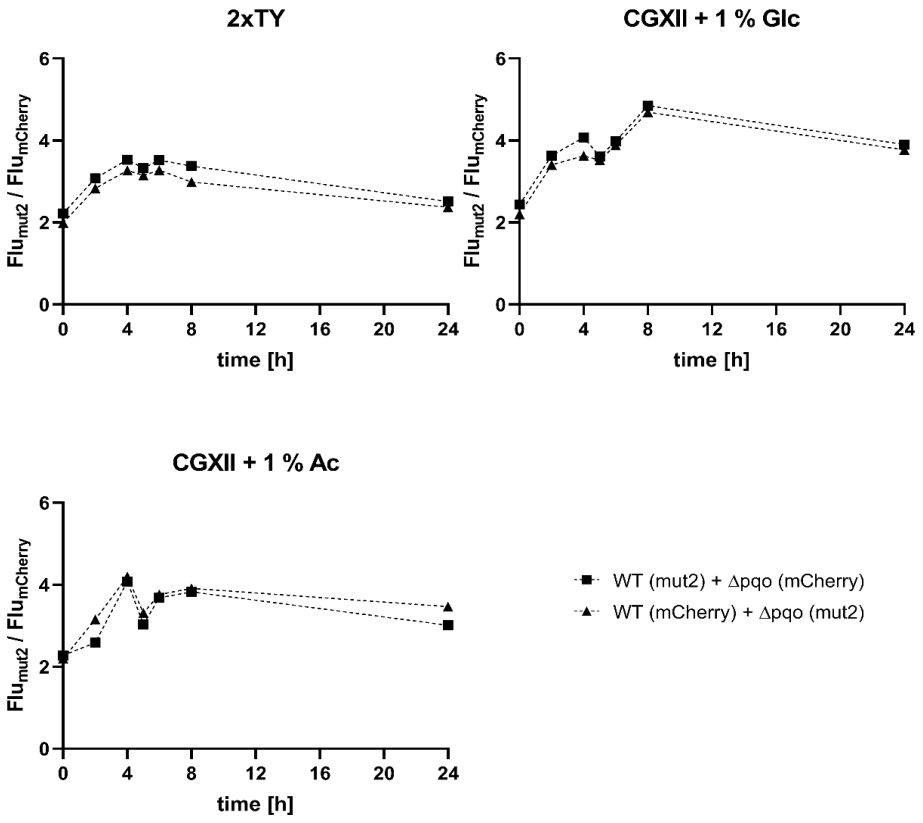


**Fig. 27: Ratio of Mut2 to mCherry fluorescence during co-culture experiments with fluorescent strains of *C. glutamicum* and *C. glutamicum* Δ*pqo*, cultivated in different media.**

A co-culture was started with equal amounts of the fluorescent wildtype strain of *C. glutamicum* overproducing Mut2, and the PQO-deletion strain overproducing mCherry, and *vice versa* for a second co-culture. Each co-culture was cultivated in triplicates. The presented ratios display the mean values of Mut2 fluorescence divided over mCherry fluorescence obtained from three independent co-cultures each, with standard deviations below 10 %. (N=3). Ac, acetate; Glc, glucose.

The two co-cultures exhibited growth characteristics similar to both the individual wildtype strain and PQO-deficient strain of *C. glutamicum* when grown in 2xTY medium, 1 % glucose or 1 % acetate minimal medium, displaying equivalent growth rates and final optical density at 600 nm (data not shown). As depicted in **Fig. 27**, the ratios of detectable Mut2 fluorescence signal over the mCherry signal in both co-cultures were increasing in the beginning of the cultivation in 2xTY medium and then decreased slightly as the co-cultures reached the stationary phase. All ratios were greater than 1, indicating that the Mut2 signal was consistently more intense than the mCherry signal. However, the ratios of the two co-cultures were nearly identical, indicating that the initial ratio of 50:50 between the wildtype and the PQO-deletion strain of *C. glutamicum* remained constant.

A similar trend was observed when both co-cultures were cultivated in 1 % glucose minimal medium, again suggesting the initial ratio of 50:50 between the wildtype and the PQO-deletion strain remained constant. When both co-cultures were cultivated in 1 % acetate minimal medium, the ratios of Mut2 fluorescence signal over the mCherry signal increased at the beginning of the cultivation, then slightly dipped after four hours of cultivation, and plateaued after six hours. Again, the ratios between the two co-cultures were similar, indicating that the ratio of wildtype to PQO-deletion strain of *C. glutamicum* remained constant throughout the cultivation.

To validate whether the presence or absence of PQO in *C. glutamicum* is beneficial or detrimental under the tested conditions, PQO activities were assessed in the co-cultures, as shown in **Fig. 28**. It was hypothesized that if the 50:50 ratio between the wildtype and PQO-deficient strains of *C. glutamicum* remained constant throughout the cultivations, as suggested by the fluorescent measurements mentioned above, then PQO activities should only be half of the activities under conditions when the wildtype strain was cultivated alone.

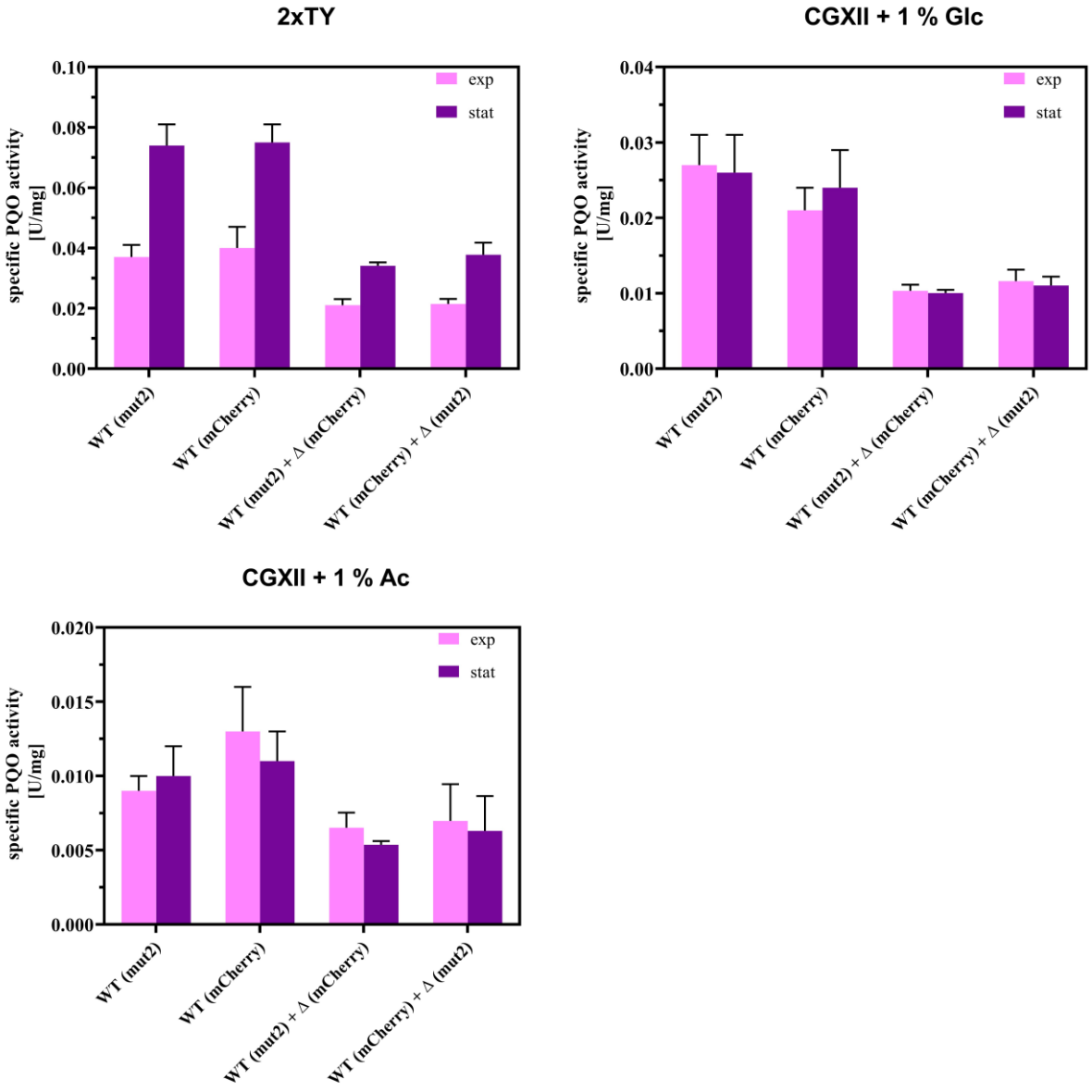


**Fig. 28: Specific PQO activity in cell extracts of fluorescent strains of *C. glutamicum* and co-cultures of fluorescent strains of *C. glutamicum* and *C. glutamicum* Δ*pqo*, cultivated in different media.**

A co-culture was started with equal amounts of the fluorescent wildtype strain of *C. glutamicum* overproducing Mut2, and the PQO-deletion strain overproducing mCherry, and *vice versa* for a second co-culture. The values depicted for both fluorescent wildtype strains are also shown in Tab. 9. All cultures were harvested at both the exponential (**exp,** light violet) and stationary phase (**stat, 24 h,** deep violet). (N=3). Ac, acetate; Glc, glucose.

As depicted in **Fig. 28**, PQO activities of both co-cultures were consistently at a level of 50 % when compared to the cultures containing the fluorescent wildtype variants alone, supporting the hypothesis that PQO is neither beneficial nor detrimental to *C. glutamicum* under the tested conditions. In the experiments conducted in 2xTY medium, the Mut2- or mCherry-fluorescent variant of the wildtype strain exhibited a specific PQO activity of 0.037 and 0.040 U/mg protein at the exponential phase, respectively. The co-cultures showed specific activities of 0.021 U/mg protein in the same condition, corresponding to an average 55 % PQO activity compared to the wildtype strains. At the stationary phase, the Mut2- or mCherry-fluorescent variant of the wildtype strain displayed a specific PQO activity of 0.075 and 0.074 U/mg protein, respectively. The co-culture with the Mut2-variant of the wildtype strain showed a specific activity of 0.034 U/mg protein, while the other co-culture showed 0.038 U/mg protein, resulting in an average twofold lower activity. Similarly, in glucose minimal medium, the Mut2-wildtype strain exhibited a specific PQO activity of 0.027 U/mg protein, and the mCherry-wildtype strain had a specific activity of 0.021 U/mg protein at the exponential phase. In contrast, the co-culture with Mut2-wildtype had a specific activity of 0.010 U/mg protein, while the co-culture with mCherry-wildtype had a specific activity of 0.012 U/mg protein, corresponding again to an average twofold reduction in activity compared to the fluorescent wildtype strains. At the stationary phase, PQO activities for Mut2-wildtype and mCherry-wildtype strains were 0.026 U/mg protein and 0.024 U/mg protein, respectively. Co-cultures with Mut2-wildtype and mCherry-wildtype had specific activities of 0.010 U/mg protein and 0.011 U/mg protein, respectively, resulting in averaged 43 % PQO activity compared to the respective fluorescent wildtype strains.

In acetate minimal medium, the Mut2-wildtype strain exhibited a specific PQO activity of 0.009 U/mg protein at the exponential phase, while the mCherry-wildtype strain showed a specific activity of 0.013 U/mg protein. Both co-cultures exhibited a specific activity of 0.007 U/mg protein, corresponding to an averaged 1.56-fold reduced activity. At the stationary phase, the Mut2-wildtype strain showed a specific PQO activity of 0.010 U/mg protein, while the mCherry-wildtype strain showed a specific activity of 0.011 U/mg protein. The co-culture with Mut2-wildtype and PQO-deficient strain exhibited a specific activity of 0.005 U/mg protein, and the co-culture with mCherry-wildtype and PQO-deficient strain exhibited a specific activity of 0.006 U/mg protein, hence resulting in twofold reduced activity on average.

Additional experiments were conducted using stationary cells from the co-cultures mentioned above, and these cells were passaged repeatedly up to three times into fresh medium (data not shown). The results of these experiments were consistent with the original findings and further

support the hypothesis that the presence or absence of PQO does not confer a significant benefit or disadvantage to *C. glutamicum* when cultivated in 2xTY medium, glucose or acetate minimal medium.

#### 3.4.2.3 Prescence of PQO is likely contributing to cell death under glutamate producing conditions

In section 3.4.2.1, PQO activity was found to be higher in the wildtype strain of *C. glutamicum* under glutamate producing conditions (using Penicillin G) when compared to non-producing conditions. No phenotype associated with this altered activity was observed, when comparing the wildtype with the PQO-deletion strain of *C. glutamicum*.

Hence, it was decided to analyze the behavior of the fluorescent co-cultures (mentioned in section 3.4.2.2) under glutamate producing conditions, using Penicillin G for induction in 1 % glucose minimal medium. The growth of the co-cultures under glutamate producing conditions was impacted by the addition of Penicillin G at 2.5 h of cultivation, resulting in growth stop after 2 h and final $OD_{600}$ values of approximately 2.5 **(Fig. 29a)**. Both co-cultures grew indistinguishable from each other and produced 5 g glutamate /L after 24 h of cultivation (data not shown). **Fig. 29b** shows that the ratios of detectable Mut2 fluorescence signal over mCherry signal in both co-cultures were initially increasing but then decreased after 3.5 h of cultivation. The Mut2 wildtype strain and mCherry PQO-deletion strain co-culture had a strong decreasing ratio until 24 h of cultivation, while the mCherry wildtype strain and Mut2 PQO-deletion strain co-culture ratio slightly increased afterwards. These results suggest that the PQO deletion strain of *C. glutamicum* outperformed the wildtype strain in both co-cultures under glutamate producing conditions.

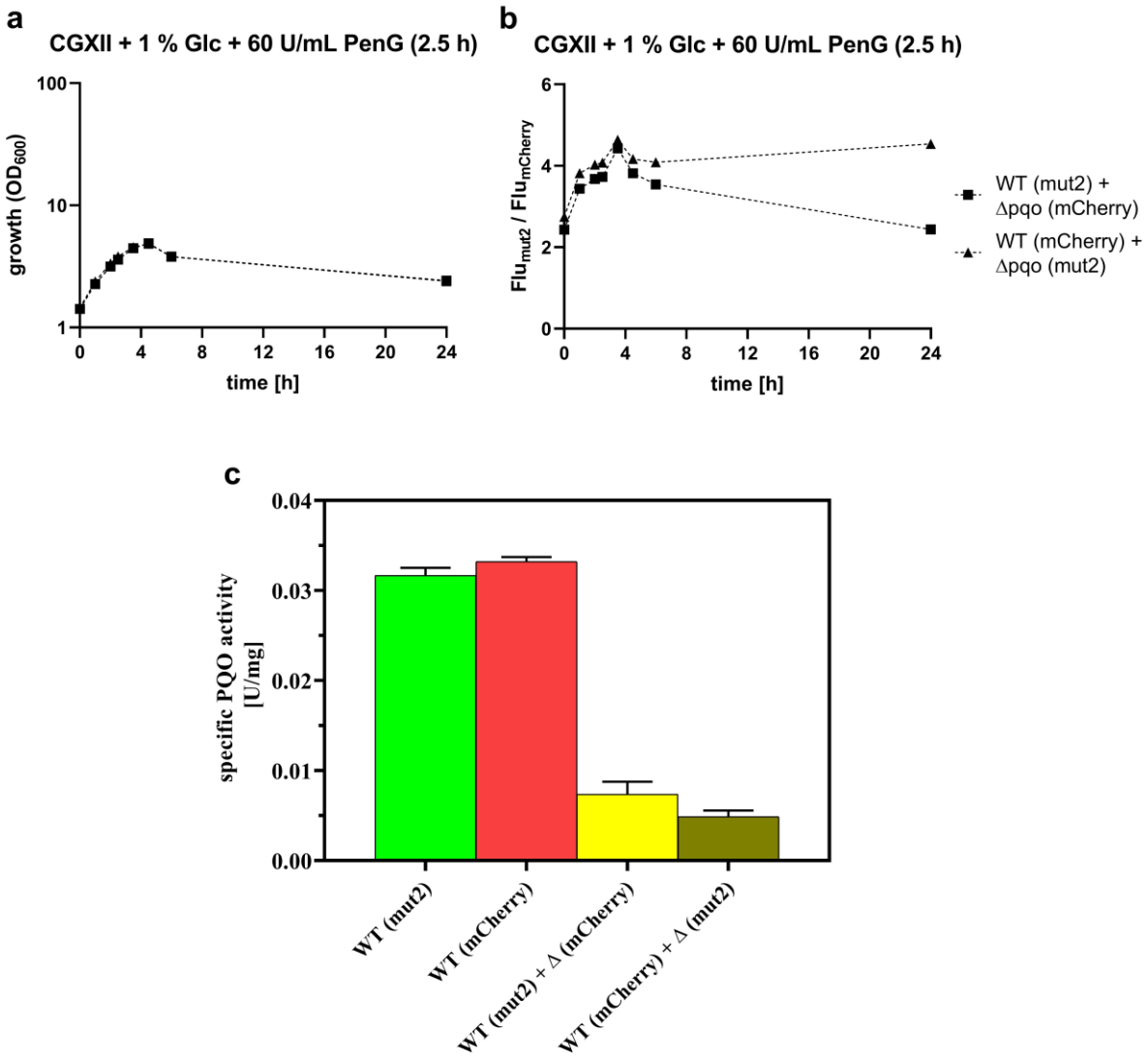


**Fig. 29: Growth, ratio of Mut2 over mCherry fluorescence and specific PQO activity of fluorescent *C. glutamicum* co-cultures in glucose minimal medium with the addition of 60 U Penicillin G (PenG)/mL.**

Fluorescent co-cultures of different *C. glutamicum* strains, cultivated under glutamate producing conditions, using 60 U Penicillin G/mL for induction (after 2.5 h) in 1 % glucose minimal medium. A co-culture was started with equal amounts of the fluorescent wildtype strain of *C. glutamicum* overproducing Mut2 and the PQO-deletion strain overproducing mCherry, and *vice versa* for a second co-culture. (a) Growth curves of the two co-cultures, (b) fluorescent ratio of Mut2 over mCherry signal of the two co-cultures, (c) specific PQO activity in cell extracts of both fluorescent wildtype strains cultivated individually (represented in green and red, respectively) and both co-cultures (represented in yellow and gold, respectively). The presented data displays the mean values obtained from three independent cultures, with standard deviations below 10 %, if no error bars are displayed. Glc, glucose.

According to **Fig. 29c**, the PQO activities of both co-cultures were consistently less than half of those exhibited by the fluorescent wildtype variants when cultivated alone. This pattern suggests that the fluorescent PQO-deletion strains outcompeted the fluorescent wildtype counterparts within co-cultures. Hence, PQO may be detrimental to *C. glutamicum* under the tested conditions. To illustrate, the Mut2- or mCherry-fluorescent variant of the wildtype strain showed a specific PQO activity of 0.033 and 0.031 U/mg protein after 24 h of cultivation, respectively. The co-culture with the Mut2-variant of the wildtype strain showed a specific activity of 0.007 U/mg protein, while the other co-culture showed 0.005 U/mg protein, resulting in an average 5.3-fold lower activity.

To investigate whether the PQO-deletion strain of *C. glutamicum* outperforms the wildtype strain is a progressive trend, a follow-up experiment was conducted. Cells from the co-cultures after 24 h of cultivation were used to inoculate fresh 1 % glucose minimal medium, but no growth was observed. This indicated that the previous cultivation conditions with Penicillin G were lethal to the cells (data not shown).

## 3.4.3 PQO is highly active when *C. glutamicum* is cultivated in acidic conditions

### 3.4.3.1 Absence of urea in CGXII minimal medium leads to acidification of extracellular pH in cultivations with *C. glutamicum*

In a previous study, Follmann *et al*. (2009) investigated pH homeostasis in *C. glutamicum* using transcriptomic and proteomic analyses. The results revealed that *pqo* transcript levels were up to twofold higher when *C. glutamicum* was cultivated under acidic conditions (pH 6.0) in glucose minimal medium, compared to more neutral pH values (pH 7.5). However, enzymatic activity data were not provided to support this observation.

To address this issue, preliminary experiments were conducted by cultivating *C. glutamicum* wildtype, a PQO-deficient and a PQO overproducer strain [*C. glutamicum* Δ*pqo* and *C. glutamicum* Δ*pqo* (pEKEx2-*pqo*), respectively] in 1 % glucose CGXII minimal medium with or without the addition of urea. The “standard” formulation of CGXII minimal medium contains urea, which is cleaved by the urease enzyme in *C. glutamicum* to release ammonia and carbon dioxide (Puskás *et al.*; 2000; Beckers *et al*., 2004). While *C. glutamicum* can utilize urea as a nitrogen source, growth may not be affected when urea is not present in CGXII medium, and instead may serve as a buffering substance (Unthan *et al*., 2014). Hence, by omitting urea from CGXII medium, the pH during the cultivation is more likely to drop to acidic values.

To investigate the long-term effects of PQO activity on *C. glutamicum*, it was also decided to extend the duration of the cultivation of the *C. glutamicum* strains to nine days instead of one or two days. This decision was made based on previous observations of the *S. aureus* homologue of the corynebacterial PQO, which was found to generate acetate in the late stationary phase, leading to cell death in prolonged cultivations with pH values dropping to about pH 5, but only in cultivations with more than 25 mM glucose (Patton *et al*., 2005).

**Fig. 30** shows the growth curves of investigated *C. glutamicum* strains in 1 % glucose minimal medium with or without urea. The wildtype strain reached a maximum $OD_{600}$ of 16 after 7 h cultivation in the standard medium, with a subsequent drop to a value of 10. When urea was omitted, the wildtype strain reached a maximum $OD_{600}$ of 11 after 7 h of cultivation, which remained constant for the remaining cultivation course. Extracellular pH during the cultivations is also shown in the right panel of **Fig. 30**. The pH profile of the wildtype strain was different in both conditions. In the "standard" medium, the pH increased from 7.2 to 9 after 96 h of cultivation, and then decreased to a final value of 8. On the other hand, in cultivations without urea, the pH value dropped from 7.0 to 6.2 after 24 h of cultivation, and remained constant thereafter. The PQO-deficient strain showed a similar behavior compared to the wildtype, since it grew in both cultivation conditions equally. The pH profile is almost similar to the one of the wildtype, except that in the “standard” medium, the pH value dropped after 48 h instead of 96 h. The PQO-overproducer strain showed a maximum $OD_{600}$ of 14 after 24 h of cultivation in standard medium and when urea was omitted, the strain reached a maximum $OD_{600}$ of 9 after 24 h of cultivation. In both cases, the $OD_{600}$ remained constant thereafter. The pH profile of the PQO-overproducer strain was similar to those of the wildtype and PQO-deletion strains of *C. glutamicum*. In the absence of urea, the medium became acidic, while in its presence, the medium was slightly alkaline.

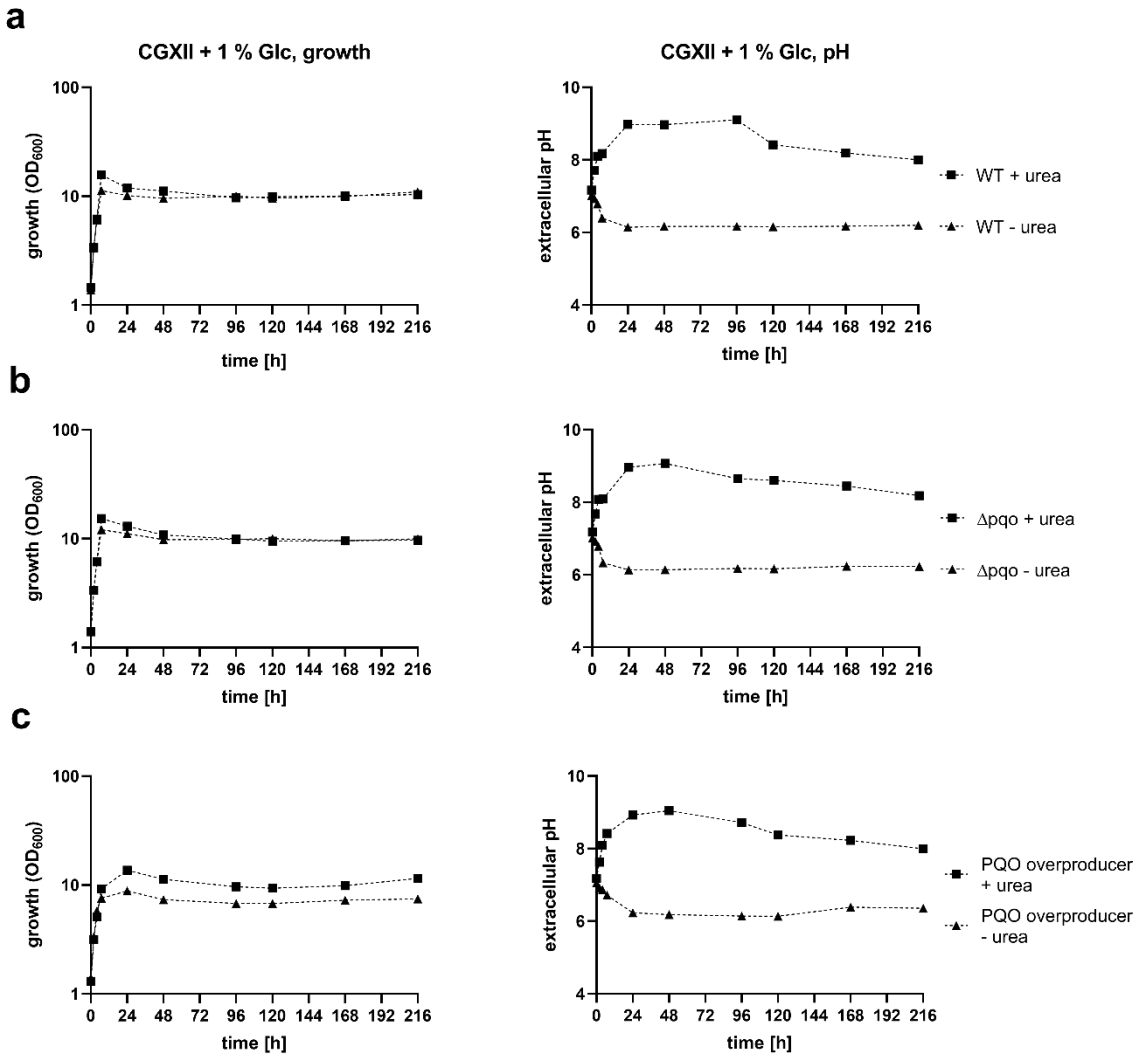


**Fig. 30: Growth and extracellular pH of *C. glutamicum* strains in 1 % glucose minimal medium with or without addition of urea.**

Growth of *C. glutamicum* (a), *C. glutamicum* Δ*pqo* (b) and *C. glutamicum* Δ*pqo* (pEKEx2-*pqo*) (c, PQO overproducer), cultivated in CGXII minimal medium with 1 % glucose and urea (squares) or 1 % glucose without urea (triangles). The presented data displays the mean values obtained from three independent cultures, with standard deviations below 10 %. Glc, glucose.

In order to achieve a greater reduction in extracellular pH during cultivation of *C. glutamicum* strains in glucose minimal medium, cultivations with 4 % glucose as the carbon source rather than with 1 % glucose were conducted. The growth curves of the investigated *C. glutamicum* strains in 4 % glucose minimal medium with or without urea are shown in **Fig. 31**. The lack of urea had a significant impact on the growth of all strains tested, with $OD_{600}$ values being much lower than those reached by strains cultivated in "standard" glucose CGXII minimal medium.

Moreover, the pH dropped to much lower values when strains were cultivated in 4 % glucose minimal medium without urea.

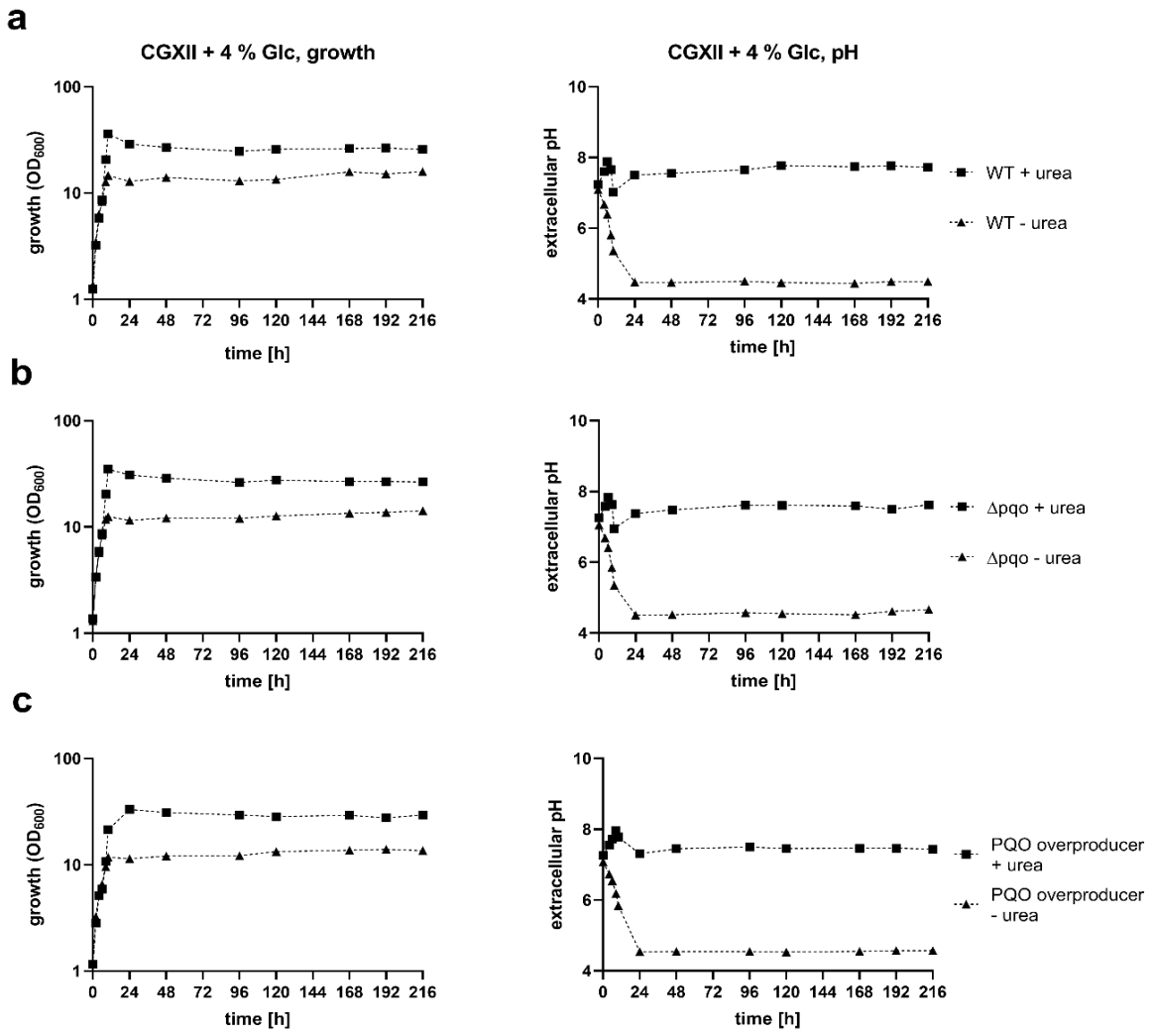


**Fig. 31: Growth and extracellular pH of *C. glutamicum* strains in 4 % glucose minimal medium with or without addition of urea.**

Growth of *C. glutamicum* (a), *C. glutamicum* Δ*pqo* (b) and *C. glutamicum* Δ*pqo* (pEKEx2-*pqo*) (c, PQO overproducer), cultivated in CGXII minimal medium with 4 % glucose with urea (squares) and in the same medium without urea (triangles). The presented data displays the mean values obtained from three independent cultures, with standard deviations below 10 %. Glc, glucose.

For the wildtype strain, a maximum $OD_{600}$ of 36 was reached after 10 h cultivation in the "standard" medium, with a subsequent drop to a value of 26. When urea was omitted, the wildtype strain reached an $OD_{600}$ of 14 after 10 h of cultivation, which increased slightly until the end of the cultivation to approximately 16. The extracellular pH during the cultivations is shown in the right panel of **Fig. 31**. The pH profile of the wildtype strain differed between the two conditions. In the "standard" medium, the pH increased from 7.2 to 8 after 6 h of cultivation, then decreased to 7.0 after 10 h, and increased again to a final value of 7.7. On the other hand, in cultivations where urea was omitted, the pH value dropped from 7.0 to 4.5 after 24 h of cultivation, and remained constant thereafter. The PQO-deficient strain showed a similar behavior compared to the wildtype strain, as it grew equally well in both cultivation conditions. The pH profile was almost identical to that of the wildtype strain. The PQO-overproducer strain reached a maximum $OD_{600}$ of 33 after 24 h of cultivation in the "standard" medium, and the $OD_{600}$ slightly decreased to 30 afterwards. When urea was omitted, the strain reached an $OD_{600}$ of 12 after 24 h of cultivation, which increased slightly to a value of 14 at the end of the cultivation. The pH profile of the PQO-overproducer strain was slightly different from that of the wildtype and PQO-deletion strains of *C. glutamicum*. In the presence of urea, the extracellular pH increased to 8 after 8.5 h of cultivation, then dropped to 7.3 after 24 h, and remained almost constant. In the absence of urea, the extracellular pH profile was identical to that of the wildtype and PQO-deletion strains of *C. glutamicum*.

Taken together, the absence of urea in CGXII glucose minimal medium led to an acidification of the extracellular pH during cultivations with *C. glutamicum* strains. This effect was significantly enhanced if higher concentrations of glucose were used. However, between the three examined *C. glutamicum* strains, no substantial difference in growth behavior was observed.

Whether the prolonged cultivation at acidic pH showed an effect on PQO activity patterns was analyzed by measuring the activity in cell extracts from the cultures grown either in glucose minimal medium with or without urea. The results are depicted in **Fig. 32**.

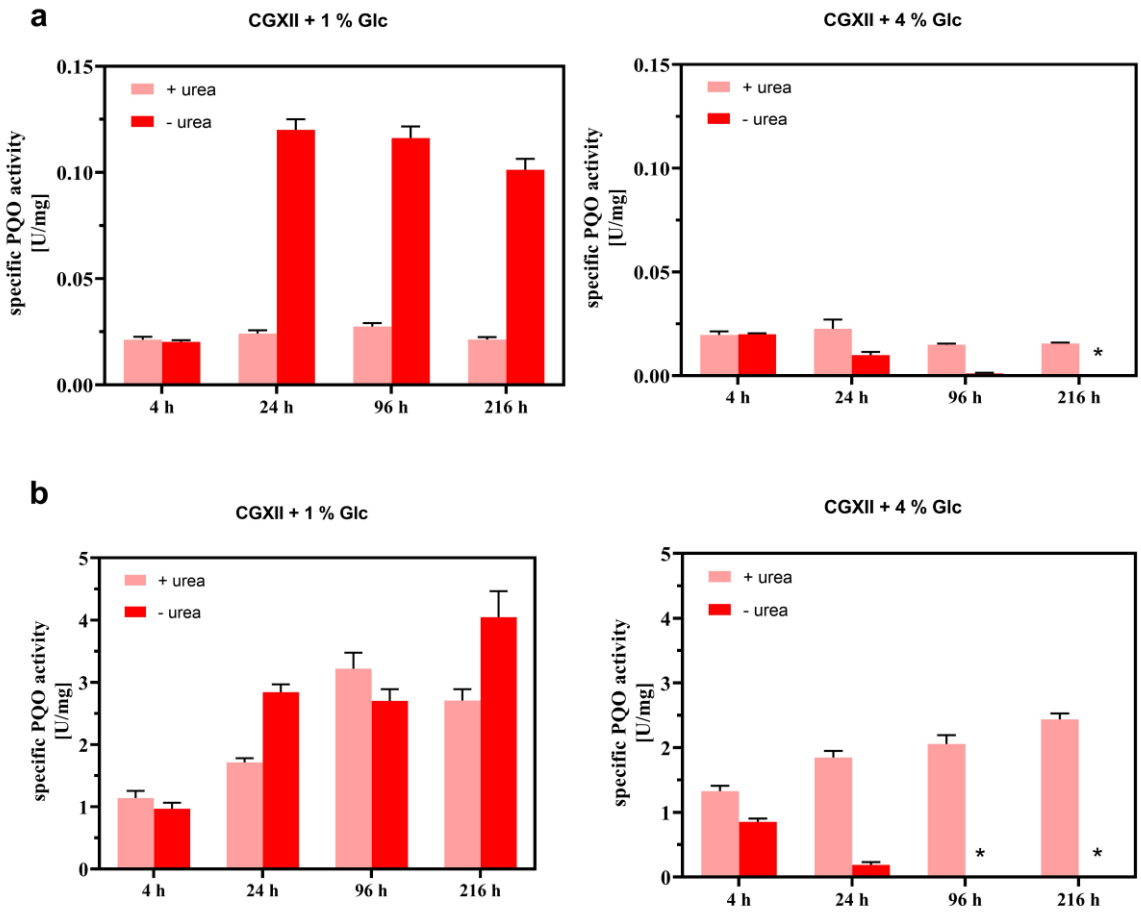


**Fig. 32: Specific PQO activity in cell extracts of *C. glutamicum* wildtype (a) and PQO overproducer (b) cultivated in 1 % or 4 % glucose minimal medium with or without addition of urea.**

Specific PQO activity in cell extracts of *C. glutamicum* (a), and *C. glutamicum* Δ*pqo* (pEKEx2-*pqo*) (b), cultivated in CGXII minimal medium with 1 % glucose (left) or 4 % glucose (right), urea either being present (light red bars) or omitted (red bars). Asterisks denote that no activity was detectable. (N = 3). Glc, glucose.

The *pqo* deletion strain did not show any detectable activity under all conditions tested (data not shown). For the wildtype strain cultivated in 1 % glucose minimal medium with urea present, the activities ranged between 0.022 to 0.027 U/mg protein after 4 h, 24 h, 96 h, and 216 h of cultivation. The omission of urea from the cultivation had a significant effect on PQO activity. After 4 h of cultivation, the wildtype strain showed almost identical activity compared to the PQO activity detected in the same strain when cultivated with urea (0.020 and 0.021 U/mg protein, respectively). As the extracellular pH decreased to 6.2 after 24 h of

cultivation, the activity of the wildtype strain cultivated without urea was fivefold higher (0.12 and 0.024 U/mg, respectively). This trend was consistent for the other two data sets after 96 h and 216 h of cultivation, respectively.

However, the trend of increased PQO activity observed in the wildtype strain cultivated without urea in 1 % glucose minimal medium was not observed in 4 % glucose minimal medium. In the presence of urea, PQO activity in the cell extracts was 0.02 U/mg protein after 4 h of cultivation and 0.022 U/mg protein after 24 h, followed by a slight decrease to 0.015 U/mg until the end of cultivation. When urea was absent, the PQO activity after 4 h of cultivation was identical to the activity observed in the presence of urea. However, coinciding with the drop in extracellular pH to 4.5 after 24 h of cultivation, PQO activity in the wildtype strain decreased to 0.01 U/mg protein. After 96 h of cultivation, PQO activity was nearly undetectable and after 216 h, no activity was detected. These results suggest that PQO activity is affected by the extracellular pH, and (prolonged) cultivation at acidic pH can lead to a significant increase (pH = 6.2) or decrease (pH = 4.5) in PQO activity.

The PQO-overproducer strain exhibited an increase in PQO activity until 96 h of cultivation in 1 % glucose minimal medium with urea present, reaching a maximum activity of 3.22 U/mg protein. After 216 h, PQO activity lowered to 2.71 U/mg protein. The omission of urea had a moderate effect on PQO activity, with a slightly lower activity observed after 4 h of cultivation compared to cultivation with urea (1.14 and 0.97 U/mg protein, respectively). At 24 h, the PQO overproducer strain exhibited a 1.7-fold higher activity when grown in the absence of urea compared to with urea, coinciding with a decrease in extracellular pH to 6.2. After 96 h of cultivation, the activity was lower when cultivated without urea (3.22 and 2.71 U/mg protein, respectively). After 216 h of cultivation, activity was 1.5-fold higher for the PQO overproducer strain cultivated in absence of urea compared to in presence of urea (2.71 and 4.05 U/mg protein, respectively).

In 4 % glucose minimal medium with urea, the PQO-overproducer strain showed a gradual increase in specific PQO activity with time, from 1.33 U/mg protein after 4 h of cultivation to 2.44 U/mg protein after 216 h of cultivation. However, when urea was absent from the medium, the strain exhibited a significantly lower PQO activity after 24 h of cultivation when compared to the activity observed in the strain cultivated with urea (0.19 and 1.84 U/mg protein, respectively), coinciding with a drop in extracellular pH to 4.5. The PQO activity was nearly or even not detectable after 96 and 216 h of cultivation, similar to the wildtype strain.

Taken together, it can be concluded that PQO activity is strongly affected by the presence or absence of urea in the cultivation medium, as well as by the glucose concentration and pH of the medium. PQO activity in the wildtype strain was upregulated up to fivefold in moderate acidic conditions (pH = 6.2) when urea was omitted from the medium, whereas the PQO-overproducer strain showed only a moderate increase in PQO activity under these conditions. This may indicate that *pqo* transcript levels are upregulated at these conditions.

#### 3.4.3.2 Dependency of constant extracellular pH on PQO activity in *C. glutamicum*

To investigate whether the upregulation of PQO activity in *C. glutamicum* wildtype strain observed in section 3.4.3.1 is solely due to the lowered extracellular pH, a series of batch fermentations were carried out at different constant pH values without the use of a buffering system (both MOPS and urea being omitted), as the titration system of the DASGIP® fermentation plant allowed for constant pH cultivations. A majority of these experiments (including an additional series of batch fermentations performed at pH values of 7.0, 8.0, 8.5, and 9.0) were conducted as part of Münßinger's master thesis (Münßinger, 2022), which was done under my supervision.

As shown in **Fig. 33**, the growth rates of individual *C. glutamicum* cultures varied depending on the chosen extracellular pH. At pH 5.0, the strain displayed a growth rate of 0.06 $h^{-1}$, which increased with higher extracellular pH values until the span of pH 7.0 to 8.5. In this range, the growth rates were highest with values ranging between 0.34 to 0.37 $h^{-1}$. At a constant pH of 9.0, the growth rate decreased to 0.3 $h^{-1}$.

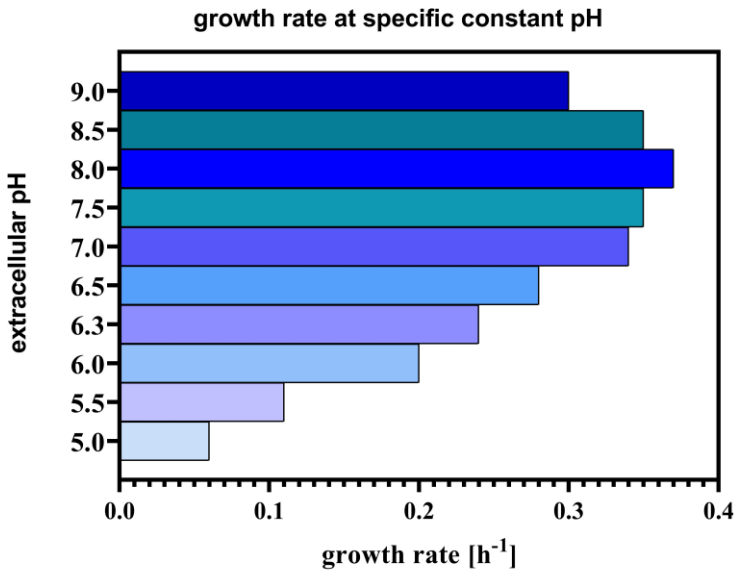


**Fig. 33: Growth rates of *C. glutamicum* in individual batch fermentations at different extracellular pH, kept constant during cultivation in 1 % glucose minimal medium without MOPS and urea.**

The growth rates were determined during exponential growth phase of the respective *C. glutamicum* culture. All experiments were performed as batch fermentations in the DASGIP® fermentation plant, pH was kept constant with the titration system using 2 M sulfuric acid and 2 M potassium hydroxide as acid and base, respectively.

Specific PQO activity of the respective cultures were determined from cell extracts after 4 h, 8 h, 24 h and partly for 48 h of cultivation and the values are depicted in **Fig. 34**.

After 4 h of cultivation, slightly different PQO activities were observed in *C. glutamicum* wildtype cultures grown in the absence of urea and MOPS at different constant extracellular pH values. The specific PQO activities of cultures grown at pH 5.0, 5.5, and 6.0 were slightly higher than those at pH values between pH 6.3 and 9.0. After 8 hours of cultivation, PQO activities in cell extracts of cultures grown at pH 6.0, 6.3, and 6.5 were up to 1.9-fold higher than those after 4 hours of cultivation. For cultures grown at pH 8.5 and 9.0, PQO activities after 8 hours of cultivation were lower (0.022 to 0.015 U/mg protein and 0.026 to 0.014 U/mg protein, respectively). In the remaining cultures, specific PQO activity remained almost constant.

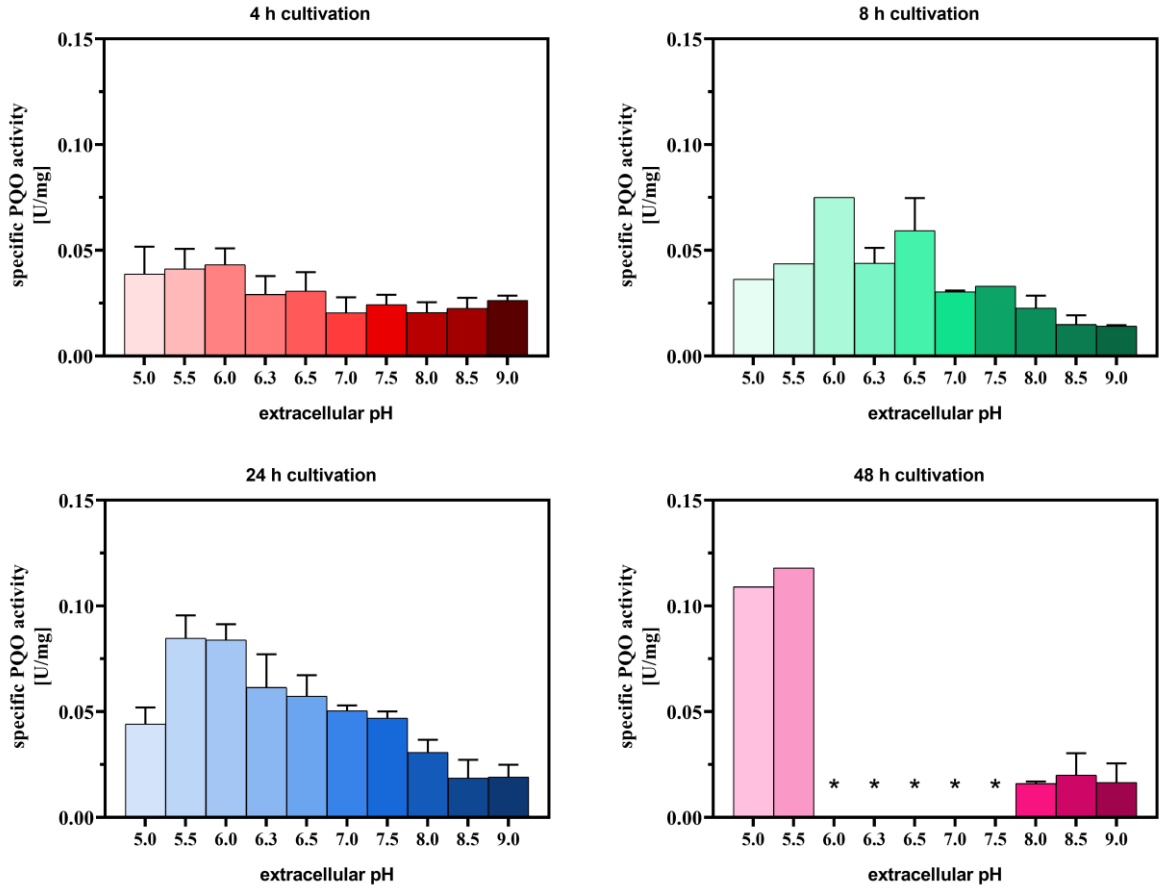


**Fig. 34: Specific PQO activity in cell extracts of *C. glutamicum* wildtype, cultivated in 1 % CGXII glucose minimal medium without MOPS and urea at constant extracellular pH in the DASGIP® fermentation plant.**

Specific PQO activity in cell extracts of *C. glutamicum,* cultivated in CGXII minimal medium with 1 % glucose within the DASGIP® fermentation plant, at constant extracellular pH, after 4 h (red), 8 h (green), 24 h (blue) and 48 h (magenta) of cultivation. If error bars are shown, the experiment was performed at least twice. Asterisks denote that activity was not determined at the indicated condition.

The specific PQO activity in cell extracts of *C. glutamicum* cultures after 24 h of cultivation showed a clear correlation with the chosen extracellular pH, apart from the cultivation at pH 5.0. The data indicated that the lower the pH during cultivation, the higher the specific activity. The specific activity decreased gradually with increasing pH, from 0.085 U/mg protein at pH 5.5 to 0.019 U/mg protein at both pH 8.5 and pH 9.0.

To verify whether this trend persisted beyond 24 h, PQO activity was determined in cultures of *C. glutamicum* grown for 48 h under two "opposing" conditions: pH 5.0 and 5.5 for acidic, and

pH 8.0, 8.5, and 9.0 for alkaline conditions. The wildtype strain showed a specific PQO activity of 0.11 U/mg protein at pH 5.0 and 0.12 U/mg protein at pH 5.5. In alkaline conditions, i.e. pH 8.0, 8.5, and 9.0, the activities were 5.5-7.5-fold lower compared to those of the wildtype strain cultivated under acidic conditions (0.016, 0.020 and 0.016 U/mg protein, respectively).

The results presented here provide again strong evidence of a clear correlation between the extracellular pH during cultivation and the specific PQO activity in *C. glutamicum*. Lower pH values were consistently associated with higher detectable PQO activity levels, supporting the idea of a direct relationship between these two factors.

### 3.4.4 Low growth rates during cultivations with *C. glutamicum* are associated with high PQO activity

Investigation of specific PQO activity in cell extracts of both wildtype and the PQO overproducing strain of *C. glutamicum* revealed that the specific activity during stationary phase is generally higher than during exponential growth, leading to the question of whether the growth rate of the organism affects PQO activity. Also, as depicted in section 3.4.3.1 and 3.4.3.2, it was shown that PQO activity at acidic pH is significantly higher than under neutral or alkaline conditions. However, cultivations at acidic pH were also associated with lowered growth rates, as *C. glutamicum* preferentially grows in slightly alkaline conditions (Follmann *et al*., 2009).

To examine whether the growth rate displayed by *C. glutamicum* during its cultivation affects PQO activity, a systematic investigation was carried out by conducting continuous fermentation processes at different dilution rates, and thus at different growth rates, ranging from 0.05 $h^{-1}$ to 0.4 $h^{-1}$. These experiments were conducted as part of Münßinger's master thesis (Münßinger, 2022), which was done under my supervision. The cultures were grown in CGXII minimal medium supplemented with 1 % glucose using the DASGIP® fermentation plant. Samples for PQO activity determinations were taken at the beginning of each continuous fermentation and after the fifth total volume exchange for each dilution rate, marking the end of the fermentation process.

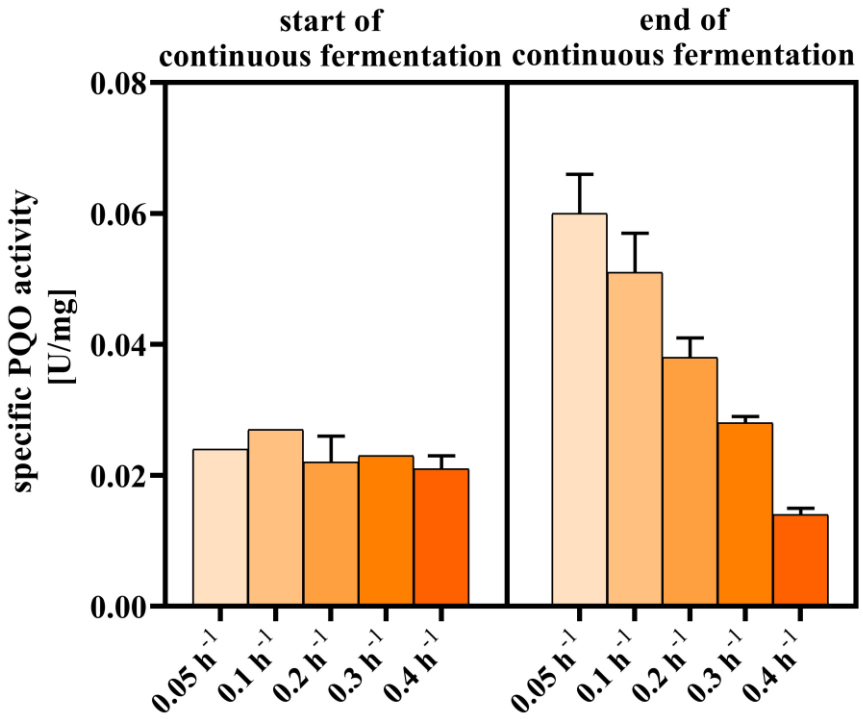


**Fig. 35: Specific PQO activity in cell extracts of *C. glutamicum* wildtype, cultivated in 1 % CGXII glucose minimal medium without MOPS and urea at constant growth rates in the DASGIP® fermentation plant.**

The figure shows the PQO activity in cell extracts from *C. glutamicum* at the start (without volume exchange) and at the end of continuous fermentation processes (fifth volume exchange) with dilution rates corresponding to the growth rates of the organism indicated below the bar charts. All fermentations were conducted with 700 mL culture in 1.5 L DASGIP® parallel bioreactors at 30 °C, pH 7, and a constant dissolved oxygen level of 30 % in CGXII minimal medium supplemented with 1 % glucose and 30 µg protocatechuic acid /mL in the feed solution during the continuous process. If error bars are shown, the experiment was performed in triplicates.

At the beginning of each continuous fermentation, the specific PQO activities of *C. glutamicum* were comparable, ranging from 0.021 U/mg to 0.027 U/mg protein (**Fig. 35**). At the end of each process, the activities ranged from 0.060 U/mg protein at the lowest dilution/growth rate of 0.05 $h^{-1}$ to a specific activity of 0.014 U/mg protein at the highest dilution/growth rate of 0.4 $h^{-1}$. These findings suggest that the corynebacterial PQO may be particularly relevant under conditions of low growth rates in *C. glutamicum*, shedding light on its potential physiological significance.

# 4 Discussion

The overall aim of this study was not only to elucidate the characteristics and regulatory features of PQO but also to unravel its structural properties, thereby contributing to a comprehensive understanding of the role of PQO in controlling the carbon flux at the pyruvate node in *C. glutamicum.*

## 4.1 High *in vitro* PQO activity may be negatively correlated with *in vivo* TCA cycle activity

This study systematically analyzed PQO-specific activities in cells grown in media containing glucose or acetate, harvested at different growth phases of batch cultures in shake flasks (see section 3.1). The absence of growth phenotype differences among wildtype, PQO-deficient, and PQO overproducing strains under a variety of conditions highlights the non-essential role of this enzyme in these contexts. Additionally, the dependency of growth rate on PQO activity was examined in glucose-limited continuous fermentation. Variations in PQO activity patterns between the wildtype and PQO overproducer strains indicated a relationship among growth phase, carbon source, growth rate, and enzyme activity. Specifically, PQO activity in batch cultures of the wildtype strain was growth phase-dependent only when cultivated in complex media, with or without additional carbon sources. Activity levels at the stationary phase were up to fourfold higher than those in the exponential phase. Introducing either 1 % glucose or 1 % acetate to complex medium resulted in gradually lower specific PQO activities. When cultivated in acetate minimal medium, the wildtype strain exhibited approximately half the activity compared to cells grown in glucose minimal medium. The overall lowest activity levels were detected in cells grown in acetate minimal medium. In the context of continuous fermentation, PQO activities in the wildtype strain varied with specific activities ranging from 0.060 U/mg protein at the lowest dilution/growth rate of 0.05 $h^{-1}$ to 0.014 U/mg protein at the highest dilution/growth rate of 0.4 $h^{-1}$.

The variations in *C. glutamicum* PQO activity observed under various cultivation conditions may indicate a regulatory relationship between PQO and certain enzymes or metabolic processes in the TCA cycle. The TCA cycle plays a crucial role in central carbon metabolism, serving both catabolic and anabolic functions. Catabolically, it converts acetyl-CoA, derived from different carbon sources, to $CO_2$, a process that generates essential reducing equivalents (NADH and menaquinol) for respiratory energy production and ATP synthesis (reviewed in

Bott, 2007; Bott and Niebisch, 2003). Anabolically, the TCA cycle provides key intermediates like 2-oxoglutarate and oxaloacetate, vital for synthesizing glutamate and aspartate amino acid families, respectively, along with producing NADPH and succinyl-CoA. Additionally, certain TCA cycle enzymes participate in other pathways, such as the glyoxylate shunt (reviewed in Bott, 2007).

Wendisch *et al*. (2000) analyzed metabolic fluxes in the central carbon metabolism of *C. glutamicum* during growth in minimal medium supplemented with glucose, acetate, or a combination of both. Their findings indicated that during acetate cultivation, acetate is activated to acetyl-CoA by the enzymes ACK and PTA and primarily channeled into the TCA cycle, as 76 % of the acetyl-CoA was converted to isocitrate via citrate synthase and aconitase. In this scenario, both the TCA cycle and the glyoxylate shunt, involving key enzymes like isocitrate lyase and malate synthase, were markedly active. The glyoxylate shunt functions as an anaplerotic route, with significant PEP/pyruvate formation from oxaloacetate and malate observed. Conversely, glucose cultivation resulted in diminished TCA cycle activity and the absence of the glyoxylate shunt, with anaplerosis predominantly occurring through PEP or pyruvate carboxylation (Wendisch *et al*., 2000). Cultivation with a glucose-acetate mixture exhibited intermediate TCA cycle activity and limited glyoxylate shunt involvement, mainly for anaplerotic purposes. Here, acetyl-CoA was primarily generated through acetate activation via ACK and PTA, with little contribution of the PDHC (Wendisch *et al*., 2000).

It is crucial to note that *in vitro* enzyme activities may not precisely align with *in vivo* activities or fluxes. Slight variations in citrate synthase activity in *C. glutamicum*, a key enzyme for substrate entry into the TCA cycle, were observed by Eikmanns *et al*. (1994), indicating at best minimal enzyme regulation based on the carbon source in the growth medium. However, specific aconitase activity varied with the carbon source used, it was fourfold higher in cells grown in acetate-minimal medium compared to those grown in glucose-minimal medium (Krug *et al*., 2005). Emer *et al*. (2009) reported that in cells grown in a mixture of acetate and glucose, specific aconitase activity was 2.8-fold higher than in cells grown solely on glucose. The activity of isocitrate dehydrogenase, responsible for converting isocitrate to 2-oxoglutarate, appeared independent of the growth substrate and phase, suggesting constitutive formation (Eikmanns *et al*., 1995). Succinate dehydrogenase activity, catalyzing formation of succinate to fumarate, was 1.8-fold higher in cells grown in acetate- compared to those grown in glucose minimal medium (Molenaar *et al*., 2000). The same study found that the activity of malate:quinone oxidoreductase, which catalyzes the conversion of malate to oxaloacetate (see introduction, **Fig. 1**), was 3.4 times higher in cells grown in acetate- than in glucose-minimal

medium. A similar regulation pattern was seen for cytoplasmic malate dehydrogenase (Molenaar *et al*., 2000). These *in vitro* findings suggest that TCA cycle activity is enhanced in cells cultivated with acetate as opposed to those grown in glucose-minimal medium.

Current data on metabolic fluxes in *C. glutamicum* cultivated in complex medium are limited. It can be hypothesized that *in vivo* TCA cycle activity is potentially reduced when *C. glutamicum* is cultivated in complex media, considering the availability of biomass precursors e.g. for amino acid synthesis. In a study by Goldbeck *et al*. (2021), where pediocin PA-1 production was established in *C. glutamicum*, amino acid content was assessed during the early stationary phase in different strains. The utilization of $^{13}$C-labeled glucose in 2xTY medium demonstrated its role in the *de novo* synthesis of TCA cycle-derived amino acids (e.g. L-glutamate, L-aspartate) and glycolytic amino acids like glycine. This implies that the addition of an external carbon source to complex medium enhances TCA cycle activity *in vivo*, compared to cultivations in complex medium alone.

Taken these observations together, the *in vitro* PQO assays indicate an inverse relationship between PQO activity and the *in vivo* TCA cycle activity. Higher PQO activity correlates with reduced or absent TCA cycle activity that varies according to the specific cultivation medium and carbon source utilized. Thus, it can be hypothesized that at lower growth rates, TCA cycle activity is reduced in comparison to higher growth rates. This hypothesis is supported by the observed inverse correlation between PQO activity and growth rate, which is further elaborated in section 4.4.

## 4.2 PQO may be regulated via acetylation and succinylation through non-enzymatic means

The observation that specific PQO activity may be negatively correlated with TCA cycle activity prompts further investigation into the regulatory mechanisms of PQO in *C. glutamicum*. Notably, the PQO activity pattern in the PQO overproducer strain provides insights (see section 3.1). Despite overall PQO activities being up to 30 times higher in absolute terms, when compared to the wildtype strain, the carbon source- and cultivation medium-dependent activity remained qualitatively similar. For instance, as with the wildtype, maximum activity of the PQO-overexpressing strain was observed in extracts of 2xTY medium-grown cells at the stationary phase and about 14-fold lower activities in extracts of acetate minimal medium-grown cells at both growth phases. Given that in the PQO-overproducer strain *pqo* gene expression is driven exclusively by the artificial $P_{tac}$ promoter, this activity pattern strongly

suggests that PTM may play a more critical role than transcriptional regulation in determining PQO activity under the conditions tested.

To investigate this hypothesis, PQO was isolated and purified from stationary phase cells of the PQO overproducer strain cultivated in 2xTY medium and in acetate minimal medium (see section 3.2). Kinetic analyses of these PQO variants revealed similar $K_m$ values, yet the $k_{cat}$ values varied markedly, with PQO from 2xTY medium-grown cells displaying approximately sixfold higher specific activity compared to that from acetate minimal medium-grown cells. These results lend support to the premise that PQO activity in *C. glutamicum* is modulated by the cultivation conditions via PTM. Mass spectrometry analysis of both PQO variants identified cultivation-dependent PTMs, particularly highlighting certain lysine residues prone to succinylation and acetylation. Notably, these lysine residues were more frequently acylated in cells grown in CGXII minimal medium than in those grown in 2xTY medium.

PTMs play a crucial role in diversifying the functions of proteins that are encoded by a single gene. In *C. glutamicum*, both common PTMs (such as phosphorylation and acetylation/succinylation) and less frequent modifications (including pupylation and mycoloylation) have been documented (Bendt *et al*., 2003; Mizuno *et al*., 2016; Küberl *et al*., 2014; Huc *et al*., 2010). Regarding acetylation and succinylation, the study by Mizuno *et al*. (2016) described the changes in the acylome of *C. glutamicum* under glutamate production conditions. They reported an increase in acetylated proteins over cultivation time in minimal medium containing 6 % glucose, while a decrease was noted when glutamate production was induced with Tween40. Conversely, the level of succinylated proteins remained constant under non-producing conditions but increased during glutamate production. Specifically focusing on PQO, they identified acetylation at lysine residues K19 and K304, and only under glutamate-producing conditions, also succinylation at K213. However, the study did not provide detailed quantification of these post-translational modifications on PQO The impact of acetylation/succinylation on proteins was evidenced for proteins involved in the central carbon metabolism of *C. glutamicum*. For instance, PEP carboxylase (PEPCx) was found acetylated at K653, and analysis of mutations introduced at this site led to the conclusion that acetylation decreased enzyme activity and subsequent reduction in glutamate production (Nagano-Shoji *et al*., 2017). Similarly, OdhI, an inhibitor of ODHC, was found to be succinylated at K133, affecting negatively its binding affinity to ODHC, though phosphorylation remains the predominant modulator of this interaction (Komine-Abe *et al*., 2017). Additionally, acetylation at K391 on the E2 subunit of PDHC/ODHC was shown to decrease its binding efficiency with E1p (AceE) and E3 (LPD) (Komine-Abe *et al*., 2021).

These observations led to an investigation into the regulatory mechanisms of lysine acetylation and succinylation in PQO within *C. glutamicum*. In some bacteria, lysine-protein acetylation is known to occur through two primary mechanisms. The first involves enzymatic acetylation, where lysine acetyltransferases (KATs) use acetyl-CoA as an acetyl-group donor (reviewed in Christensen *et al*., 2019; Hentchel and Escalante-Semerena, 2015). However, in *C. glutamicum*, the presence of KATs has not yet been reported. The second mechanism is non-enzymatic acetylation, using either acetyl-CoA or acetyl phosphate as the acetylating agent. This mechanism is widespread in various bacteria, including *E. coli*, as evidenced by studies indicating that the PTA-ACK-pathway significantly contributes to global acetylation (Kuhn *et al*., 2014; Weinert *et al*., 2013a). Specifically, *E. coli* strains deficient in the *ack* gene exhibited increased acetyl phosphate levels, correlating with enhanced acetylation, whereas strains lacking both *pta* and *ack* genes showed markedly lower acetyl phosphate levels and reduced protein acetylation (Kuhn *et al*., 2014; Weinert *et al*., 2013a). Contrastingly, in *C. glutamicum*, deletion of only the *pta* gene affected overall protein acetylation, leading to a decrease in acetylation levels and thus differing from the pattern observed in *E. coli* (Mizuno *et al*., 2016).

Regarding protein succinylation in *E. coli*, it was observed that this modification often coincides with acetylation at identical sites (Weinert *et al*., 2013b). Succinylation levels were found to be significantly influenced by growth conditions and mutations impacting succinyl-CoA metabolism within the TCA cycle. Consequently, it was inferred that succinylation is predominantly affected by intracellular succinyl-CoA concentrations and likely occurs through non-enzymatic means (Weinert *et al*., 2013b). This hypothesis is further supported by the observation that succinylation in *E. coli* predominantly affects abundant proteins, suggesting a low-level, non-enzymatic occurrence (Weinert *et al*., 2013b). This is corroborated by studies demonstrating the high reactivity of succinyl-CoA, which was shown to modify bovine serum albumin more effectively than acetyl-CoA *in vitro* (Wagner *et al*., 2017).

This leads to the possibility that *C. glutamicum* may also undergo non-enzymatic succinylation of lysine residues at proteins, a phenomenon not yet explored in existing literature. It can be assumed that increased activity in the TCA cycle might elevate intracellular succinyl-CoA levels, consequently making some proteins susceptible to succinylation, especially those with surface-exposed lysine residues. Given the observed inverse relationship between PQO activity patterns in the wildtype and the PQO overproducer on the one hand and the *in vivo* TCA cycle activity on the other, a hypothesis emerges. It suggests that the diminished activity of PQO, especially noted in cells grown in acetate medium, could be a consequence of succinylation at

lysine residues. This hypothesis aligns with the understanding that higher TCA cycle activity could lead to an increase in succinylated proteins, potentially influencing PQO activity.

Whether acetylation or succinylation of a protein affects its function/activity can be investigated by three means (reviewed in Christensen *et al*., 2019). The first method involves isolating the protein from cells grown under conditions contributing to acetylation or succinylation, and then comparing it to the same protein obtained from cells under conditions that induce these modifications less frequently. A limitation of this approach is that the protein might be modified at several residues, hiding the specific impact of a single modification. The second technique is the *in vitro* modification of proteins using agents like acetyl-CoA, acetyl phosphate, or succinyl-CoA. While this method can provide valuable insights, it may result in a heterogeneous population of modified proteins, complicating the analysis. The third approach, demonstrated by the research of Komine-Abe *et al.* (2017), involves the creation of genetic mimics. For instance, to understand the effect of succinylation at a particular lysine residue, that residue can be replaced with another amino acid. For example, glutamate might be used to mimic the charge of succinyl-lysine, or alanine for a neutral effect. However, this method only mimics the modification (by net charge) and may not accurately reflect the natural modified state.

In this study, particular attention was given to two lysine residues within PQO, K93 and K325. As shown in the mass spectrometry analysis of PQO purified from cells cultivated under different conditions, these residues are particularly prone to acetylation and succinylation, respectively, especially in the PQO overproducer strain when cultivated in acetate minimal medium (abundancy > 40 %). Variants of PQO enzyme were created and overproduced in the *C. glutamicum* Δ*pqo*-background, where lysine was replaced by either alanine (K to A) or glutamate (K to E). These mutant strains, cultivated in 2xTY, glucose, and acetate minimal media, showed significant differences in PQO activity. For K325, the lysine-to-glutamate substitution aimed to mimic a succinylated lysine, from the perspective of net charge, and was expected to decrease activity across all conditions. This expectation held true for most conditions, except in cells grown in acetate minimal medium during the exponential phase and in glucose minimal medium at the stationary phase. Conversely, the lysine-to-alanine substitution at K325, intended to prevent succinylation and thus increase activity, particularly in acetate minimal medium, showed similar activities to the lysine-to-glutamate variant. These results suggest that structural aspects of PQO are more influential than previously thought and should not be neglected. K325, when unmodified, is close to K202 and N199, with a separation of about 7.0 Å (see section 3.3). Succinylation at K325 alters the electronic charge dynamics with these residues from repulsion to attraction due to the introduction of a negative charge.

Additionally, the inclusion of a succinyl group decreases the inter-residue distance, potentially altering the structure of PQO, particularly within the FAD-binding domain. However, substituting lysine with glutamate or alanine did not reduce the inter-residue spacing to K202 and N199, potentially making an interaction less likely.

Regarding K93, which undergoes acetylation, the lysine-to-glutamate mutation flips the charge of the unmodified lysine, while lysine-to-alanine maintains the net charge of an acetylated lysine. Determining whether acetylation enhances or decreases PQO activity is challenging. In the assays, both variants generally exhibited activity equal to or lower than the wildtype enzyme, with an exception observed in cells cultivated in acetate minimal medium and harvested in the exponential phase. Again, structural aspects need to be considered. K93 is located within the pyrimidine-binding domain and is positioned approximately 10 Å away from the adenine ring of the bound FAD cofactor in its unmodified state. This distance decreases when K93 is acetylated, potentially leading to an electrostatic interaction with the positively charged adenine moiety of FAD. Thus, mutations at this residue that impede post-translational modifications could affect the stability of the bound cofactor. Although replacing the lysine with glutamate introduces a negative charge, a PyMol analysis indicated that this change does not shorten the distance to the FAD cofactor. This suggests a potentially reduced likelihood of interaction between them.

A crucial consideration in this context is the limitation of focusing solely on individual amino acids to understand the overall impact of PTMs on PQO. During this work, other lysine residues such as K121 (identified in the structure, see below) or K500 (detected through mass spectroscopy analysis) were also found to be modified. This highlights the need for a broader approach that accounts for the cumulative effects of PTMs across multiple residues. Additionally, the three-dimensional structure of PQO itself plays a significant role. Therefore, understanding activity, stability and cofactor binding of PQO, requires a combined view that covers both the collective influence of PTMs and the structural dynamics of the protein.

An important aspect to consider in the context of PTM in *C. glutamicum*, specifically regarding acetylation or succinylation of PQO, is their apparent irreversibility (Christensen *et al*., 2019). Such modifications, if they alter the activity or structure, might also affect PQO's potential interactions with other proteins, potentially leading to undesired phenotypic outcomes. This raises the question of how *C. glutamicum* manages to reverse these modifications, especially given their potential impact on the adaptability of the organism to changing environmental conditions.

One aspect to consider is the 'dilution' of modified proteins through the synthesis of new, unmodified proteins. However, this mechanism might not be sufficient in certain scenarios. For instance, in conditions where the organism faces a limitation in a specific nutrient, like nitrogen, while having an excess of other nutrients such as carbon, protein biosynthesis could halt. In such scenarios, a possible role for PQO might be to divert the available carbon flux from the TCA cycle instead to the end-product acetate and providing reduced quinols to the respiratory chain. Modified PQO might not effectively fulfill this function.

The reversibility of acetylation is made possible by lysine deacetylases (KDACs) in some bacteria. These can be classified in two families, one of which are sirtuins, requiring $NAD^+$ as a co-substrate (reviewed in Christensen *et al*., 2019). Interestingly, the only known sirtuin-type deacetylase in *E. coli*, CobB, exhibits both deacetylase and desuccinylase activities (Colak *et al*., 2013). *C. glutamicum* has two sirtuin-type KDAC homologues, *cg0108* and *cg0745* (Mizuno *et al*., 2016). Despite deletion of these genes not significantly affected the overall abundance of acetylated or succinylated proteins in *C. glutamicum* (Mizuno *et al*., 2016), the gene product of *cg0745* has been shown to deacetylate PEPCx (Nagano-Shoji *et al*., 2017). In principle, it is possible that either one or both KDAC homologues in *C. glutamicum* deacetylate or desuccinylate modified PQO.

## 4.3 PQO is very similar to PoxB from *E. coli*, but differs significantly at its C-terminus important for membrane binding and activation mechanism

The structural analysis of PQO from *C. glutamicum*, presented in section 3.3, was intended, among others, to explore the regulation of PQO activity through acylation. In fact, PTMs were identified on lysine residues K121 and K325 in the high-resolution structure of the full-length PQO, isolated from cells grown in acetate minimal medium. The limited detection of PTMs may be attributed to the necessity for exceptionally high resolution in structural analysis and the potential loss of PTMs during protein crystallization and X-ray diffraction analysis (M. Bellinzoni, personal communication). The specific nature of the modification on K121 remained ambiguous, and interestingly, this residue was not identified as modified in the mass spectrometry analysis. To further investigate K121 as a modification/acylation target, variants of PQO were created in a *C. glutamicum* Δ*pqo*-background with lysine at position 121 substituted by alanine (K to A), glutamate (K to E), or arginine (K to R). Structural analysis revealed that K121 is positioned within the tetrameric assembly of PQO, so that two K121 residues are in relatively close neighborhood. Alterations at this site, particularly those

preventing PTM, might influence the stability and assembly of the PQO tetramer. The K121R mutation, which preserves the charge of an unmodified lysine and maintains a similar side chain length, exhibited a neutral or positive effect on enzyme activity compared to the wildtype enzyme. In contrast, the K121A and K121E mutations typically resulted in similar or decreased activities. This outcome implies a possible negative regulatory function of PTM at K121, as the K to R mutation, conserving charge, either maintained or enhanced enzyme activity. Conversely, the charge-altering mutations (K to A/E) negatively influenced enzyme activity, although these changes also obstruct PTM. However, these mutations mimic the charge of acetylated lysine (net charge = 0) or succinylated lysine (net charge = -1). Furthermore, spatial factors and interactions within the structure of PQO should be considered, given that the side chains of alanine and glutamate are shorter than that of an unmodified lysine residue.

In this work, the three-dimensional structure of PQO from *C. glutamicum* was solved. The successful determination of this structure can be attributed to three key factors:

Firstly, the effectiveness of the Triton X-114 extraction method in purifying PQO directly from *C. glutamicum* was pivotal. This method ensured both high purity and adequate concentration of the samples, which was corroborated by SDS-PAGE analysis. Furthermore, the samples were found to be suitable for both crystallization trials and mass spectrometry analysis. Secondly, the availability of high-throughput screening facilities for crystallization in 96-well plates using the 'sitting drop' method, in the laboratory of our collaborator M. Bellinzoni, significantly facilitated the process. By exploiting the knowledge from previous crystallization conditions of the homologous enzyme PoxB from *E. coli* (Neumann *et al*., 2008), crystals of PQO suitable for X-ray diffraction analysis were rapidly obtained (M. Bellinzoni, personal communication). Lastly, the initial structure of PQO was solved by molecular replacement, using the coordinates of the *E. coli* homologue PoxB (Neumann *et al*., 2008; M. Bellinzoni, personal communication). The structure was resolved in a ternary complex with the cofactors TPP (in complex with $Mg^{2+}$-cation) and FAD, equal to both *E. coli* PoxB and the soluble pyruvate oxidase (POX) from *L. plantarum* (Muller and Schulz, 1993). Despite POX in *L. plantarum* mediating a different reaction - the oxidative decarboxylation of pyruvate in the presence of phosphate and oxygen to produce acetyl phosphate, carbon dioxide, and hydrogen peroxide (Sedewitz *et al*., 1984) - its structural similarity to *E. coli* PoxB was important. Notably, the structure of *L. plantarum* POX (PDB: 1POW) had previously served as a model for solving the structure of PoxB (Neumann *et al*., 2008).

Regarding the resolution of the PQO structure, it was refined to a final value of 1.26 Å, based on diffraction sets obtained from PQO purified from *C. glutamicum* cells grown in acetate minimal medium. This resolution surpasses that of POX from *L. plantarum* (2.1 Å) and PoxB from *E. coli* (2.9 Å). Higher resolution structures enable more detailed observation of intermolecular interactions and PTMs at specific residues, thereby helping to understand structural and functional aspects of the protein (Acharya and Lloyd, 2005; M. Bellinzoni, personal communication).

Structural analysis revealed that the corynebacterial PQO closely resembles the PoxB of *E. coli*, with both being tetrameric flavoproteins sharing similar positions for cofactors (FAD and TPP) and analogous amino acids constituting their active sites (see section 3.3.1). However, the C-terminal domain of PQO differs significantly, featuring an amphipathic α-helix in contrast to the antiparallel β-sheet found in PoxB, leading to a different conformation that does not obstruct the active site like in PoxB. The orientation of the amphipathic α-helix in PQO also contrasts with the direction of homologous amino acids in PoxB.

The distinctiveness of the C-terminal domain in PQO is also evident in its predicted structure as determined by AlphaFold2. This artificial intelligence-driven algorithm is widely used to predict three-dimensional structures of proteins, with high accuracy (Jumper *et al.*, 2021). The predicted PQO structure, accessible via UniProt (accession number: Q8NMG5; **Fig. 36**), generally exhibits a high level of confidence. Nonetheless, two specific areas are identified with lower confidence: one spanning residues S343-H356 within a large α-helix starting at residue R328, and most of the C-terminal region, covering residues L535-P579. There was no information available regarding the oligomeric state of PQO or potential cofactor binding sites.

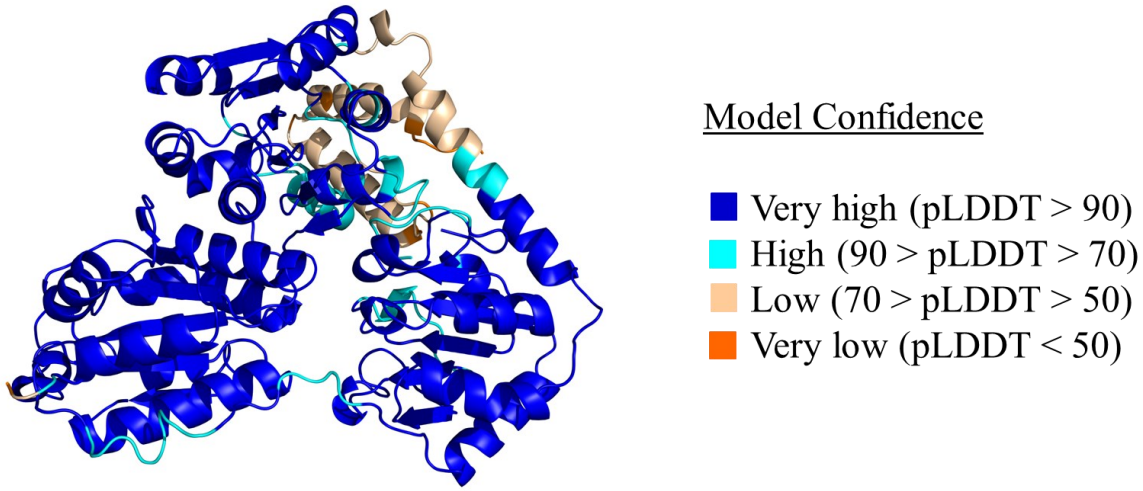


**Fig. 36: Cartoon overview of PQO from *C. glutamicum*, as predicted by AlphaFold2.**

Schematic overview of the predicted structure of *C. glutamicum* PQO, featuring confidence levels based on the predicted Local Distance Difference Test (pLDDT). The figure presents the tertiary structure of *C. glutamicum* PQO as predicted by AlphaFold2 (UniProt accession number: Q8NMG5). The color-coding corresponds to the confidence level for each residue, indicated by pLDDT scores ranging from 0 (very low confidence) to 100 (very high confidence). These scores provide an assessment of the reliability of the model on a residue-by-residue basis. Low to very low confidence regions include S343-H356 and L535-P579 at the C-terminal end of the protein.

A structural alignment using PyMol compared the predicted PQO structure from AlphaFold2 with that obtained through experimental data in this study. This comparison was aimed at evaluating the predictive accuracy of AlphaFold2. The two structures share a striking similarity overall (**Fig. 37a**, RMSD = 0.46 Å). However, deviations were observed in the previously mentioned low-confidence regions. In the first of both regions (S343-H356), a minor discrepancy exists between the predicted and actual structures. Beyond this point, at residue P358, the structures align closely. Significant differences emerge again at the C-terminus, starting with residue L535 (**Fig. 37b**).

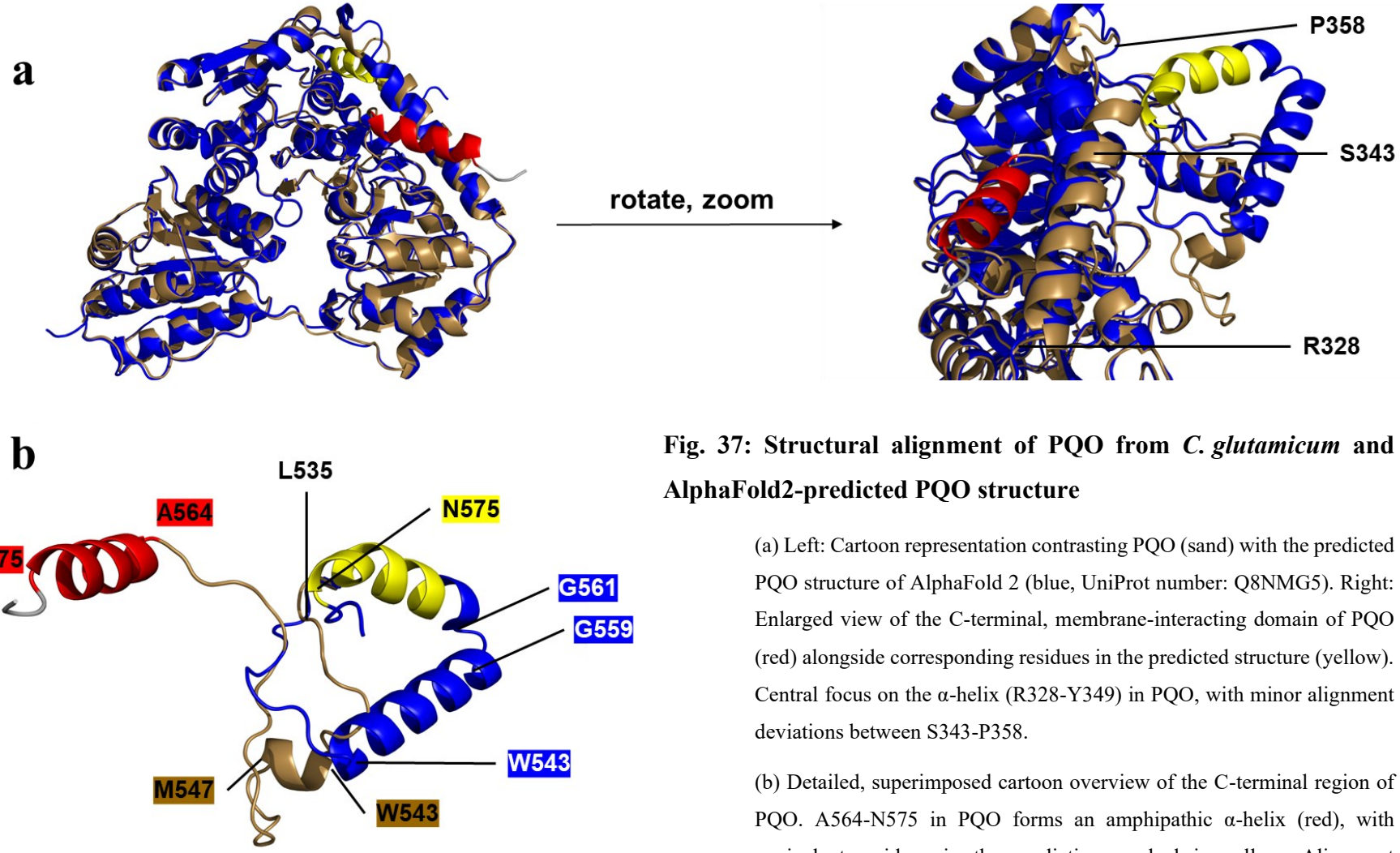


**Fig. 37: Structural alignment of PQO from *C. glutamicum* and AlphaFold2-predicted PQO structure**

(a) Left: Cartoon representation contrasting PQO (sand) with the predicted PQO structure of AlphaFold 2 (blue, UniProt number: Q8NMG5). Right: Enlarged view of the C-terminal, membrane-interacting domain of PQO (red) alongside corresponding residues in the predicted structure (yellow). Central focus on the α-helix (R328-Y349) in PQO, with minor alignment deviations between S343-P358.

(b) Detailed, superimposed cartoon overview of the C-terminal region of PQO. A564-N575 in PQO forms an amphipathic α-helix (red), with equivalent residues in the prediction marked in yellow. Alignment divergences begin at L535. The experimentally determined structure shows a W543-M547 helical segment, whereas in the AlphaFold2 prediction, this helix is oriented oppositely, extending to G559.

In the experimentally determined structure, a 26-residue segment (A534-F558) forms an extended conformation, creating a cap over the FAD-binding domain of the enzyme. Within this segment, a brief α-helix spans from W543 to M547. The glycine-rich sequence GGGVG (residues 559-563) runs beneath the elongated R328-Y349 α-helix, positioning an amphipathic α-helix (residues A564-N575) above it. Conversely, in the AlphaFold-predicted structure, a short disordered region is followed by an α-helix covering residues W543-G559, which shows an opposite direction compared to the brief helical segment in the experimentally determined structure. This segment leads to a loop formed by G560, and subsequently, the final α-helix (residues G561-N575). Due to the positioning of the short disordered region and the presence of the longer α-helix (W543-G559) – which is absent in the experimentally derived structure – the final α-helix (G561-N575) in the predicted structure is located oppositely, albeit pointing similarly, to its counterpart in the experimental structure.

While the predicted structure of PQO, as per AlphaFold2, aligns significantly with the experimentally obtained structure, this comparison also reveals certain critical limitations inherent in the algorithm. One of the notable limitations of AlphaFold2 is its inability to incorporate cofactors in the predictive model. This exclusion is significant, considering the pivotal role cofactors play in understanding the functional dynamics of proteins. Furthermore, AlphaFold2 does not provide insights into the oligomeric state of proteins. This omission is crucial, as the oligomeric state is a key factor in understanding the functionality of proteins. Hence, the algorithm may face challenges in accurately predicting the active site of a protein. Also noticeable in this comparison is the fact that caution needs to be taken to predicted regions of low or very low confidence. These regions are often intrinsically disordered regions, making it difficult to infer protein function *in vivo* from the AlphaFold2 structure (summarized in Ruff and Pappu, 2021).

Despite these limitations, AlphaFold2 demonstrates significant strengths. The high degree of alignment between its predictions and the actual structure of PQO validates its accuracy in certain aspects. The implications of the capabilities of AlphaFold2 extend to rational drug design (reviewed in Nussinov *et al*., 2022) and crystallography. For crystallographers, an AlphaFold2 model could serve as a search model, particularly in the absence of experimental structures or homologues. Also, the ability of the algorithm to identify low-confidence regions, correlating with intrinsically disordered regions, is crucial for accurate interpretation. Specifically, for PQO, the misprediction of the crucial C-terminus in PQO, which is important for lipid/detergent binding and the activation mechanism of the protein (discussed in detail below), underscores the necessity for further experimental verification.

The distinct C-terminal structure of PQO from *C. glutamicum*, particularly the unique folding and positioning of its α-helix, raises questions about its functional implications, given its non-obstructive nature to the active site. To confirm whether this structure was a result of the Triton X-114 extraction process, a $His_6$-tagged PQO variant underwent purification from an *E. coli* strain and subsequent analysis through X-ray crystallography. The structure was indistinguishable from the native PQO, thus confirming that the unique α-helical structure of PQO at its C-terminus is an inherent characteristic, unaffected by the extraction method. The drastic difference at the C-terminus between PQO and PoxB is unexpected, given that enzymatic data suggest a catalytic mechanism for PQO similar to that of PoxB.

Hence, further work was done to decipher the functional importance of the α-helix at the C-terminus of the PQO enzyme. For this purpose, a truncated PQO variant (PQO-$\Delta_{C17}$), missing the carboxy-terminal 17 amino acids, was created, and overproduced in *C. glutamicum* Δ*pqo*-background, revealing that these amino acids are crucial for lipid/detergent interaction and enzyme activation. Two key observations supported this conclusion: first, the purification of PQO using Triton X-114 resulted in substantially lower protein recovery for the truncated variant compared to the full-length PQO. Second, in cell extracts, the truncated PQO showed higher specific activity than the full-length PQO when the respective overproducer strains were grown in 2xTY medium, an activity that did not depend on the DDM detergent, unlike the full-length PQO. However, purified full-length PQO exhibited higher specific activity compared to the truncated variant, indicating potential stability issues for the truncated PQO outside the *C. glutamicum* cell environment. Structural analysis of the truncated PQO revealed that diffracting crystals were only obtained in the presence of 2 mM TPP and 5 mM $MgCl_2$, suggesting decreased enzyme stability without the thiamine cofactor. The resolved structure showed the standard PQO tetramer configuration bound with FAD and TPP. However, there was no electron density for the rest of the C-terminal domain, suggesting enhanced flexibility in this area. Apart from this, the structure closely resembled that of the full-length protein, with no notable conformational differences.

The structural analysis of PQO, and the biochemical data obtained in this study raise the question: does PQO perform a different role *in vivo* compared to its *E. coli* homologue? While the biochemical studies suggest strong similarities between PQO and PoxB, notable structural differences at the C-terminus prompt speculation about differences in the interactions of PQO and PoxB with membranes or with other proteins *in vivo*. One theory is that PQO might play a role in the transfer of reducing equivalents through quinols from the cytosol to the membrane-associated respiratory chain in a mechanism analogous to that observed for PoxB (Koland *et*

*al*., 1984). Specifically in *C. glutamicum*, it can be hypothesized that PQO facilitates electron transfer to the cytochrome $bc_1$-$aa_3$ supercomplex, a component critical for aerobic growth in this organism (Bott and Niebisch, 2003). Additionally, PQO may engage in interactions with proteins possessing hydrophobic domains. To thoroughly investigate these possibilities, it is advised to conduct in-depth protein-lipid interaction studies, such as Surface Plasmon Resonance, which can provide insights into the specific interactions of PQO with cellular membranes. These studies may reveal critical aspects of the functional mechanisms of PQO and its potential unique roles in the cell, thus contributing to the understanding of its enigmatic biological significance. Utilizing fluorescent fusion constructs may also help to determine whether PQO functions as a peripheral membrane protein *in vivo*, as previously suggested (Schreiner and Eikmanns, 2005). Also, co-immunoprecipitation trials cold be performed to elucidate possible interactions of other proteins in *C. glutamicum* with PQO. Additionally, creating and analyzing fusion proteins by swapping the C-termini of corynebacterial PQO and PoxB from *E. coli* may provide insights into the functional roles of these regions in both organisms.

## 4.4 PQO and its potential role in redirecting carbon flux away from the TCA cycle

While glycolysis and oxidative decarboxylation of pyruvate by the PDHC are common and well studied in many bacteria (reviewed in Sauer and Eikmanns, 2005), the nature and the role of the alternative pyruvate oxidation pathway catalyzed by PQO in *C. glutamicum* is still less clear. While biochemically and structurally well-characterized during this work, the physiological role in *C. glutamicum* is yet to be determined. This paragraph explores the efforts made to decipher this role (see section 3.4).

In *C. glutamicum*, PQO, in conjunction with ACK and PTA, theoretically offers a bypass for the PDHC reaction. However, practical efforts to effectively utilize this alternative route have so far been unsuccessful. A *pqo*-deficient mutant displayed no significant phenotype under diverse conditions. Interestingly, overexpression of *pqo* only partially improved growth deficits in an *aceE*-deficient (and consequently PDHC-deficient) strain in 2xTY complex medium, suggesting a potential for PQO to compensate for PDHC deficiency (Schreiner *et al*., 2006). However, this PDHC-deficient strain could not grow solely on glucose minimal medium, requiring acetate supplementation, even in a strain with *pqo* overexpression. Further research within this and past studies indicate that acetate produced by PQO is not converted to acetyl-CoA via the ACK-PTA pathway. Therefore, PDHC remains the primary enzyme for generating

acetyl-CoA in *C. glutamicum* during growth on substrates entering central carbon metabolism pathways other than through acetyl-CoA (Schreiner *et al*., 2005). During growth on acetate, this substrate is activated to acetyl-CoA through the ACK and PTA pathway (Reinscheid *et al*., 1999), thereby making PDHC activity non-essential.

The low substrate affinity of PQO for pyruvate and its dependency on the presence of lipids/detergents for optimal activity, suggest that pyruvate decarboxylation by PQO is not favored by *C. glutamicum* under the tested conditions thus far. This finding aligns with the notion that converting pyruvate to acetyl-CoA via PQO, ACK, and PTA is less energetically efficient than via PDHC, given the ATP requirement for acetate activation (Schreiner *et al*., 2006).

As shown in chapter 3.3.2, a C-terminal truncated PQO variant (PQO-$\Delta_{C17}$) overcomes two limitations of *in vivo* PQO activity as a PDHC substitute: it does not require membrane proximity for maximal activity, typically induced in the full-length variant by high pyruvate concentrations. This is supported by the observation that the recovery of PQO-$\Delta_{C17}$ using the Triton X-114 extraction method was significantly lower compared to the full-length variant, suggesting a reduced association with lipids/detergents. Also *in vitro* assays show that the specific activity of the truncated variant is not reliant on the presence of the detergent DDM, contrary to the full-length PQO which requires DDM for maximal activity. Kinetic analysis indicates that this truncated variant exhibits slightly higher affinity for pyruvate than the full-length protein, as evidenced by a lower $K_m$ value. This novel variant essentially redefines the role of PQO. In minimal medium containing both glucose and acetate, overproduction of the PQO-$\Delta_{C17}$ variant enabled an *aceE*-deficient strain to utilize glucose for biomass production, although only partially. This is evidenced by a maximum optical density that is lower than the wildtype but higher than the *aceE*-deficient parental strain. Analysis of activity patterns in the *aceE*-deficient strain overproducing the PQO-$\Delta_{C17}$ variant revealed a notable trend: during the exponential growth phase, the specific activities were generally higher, while they were lower in the stationary phase. This contrasts with the strain overexpressing the full-length PQO variant under comparable conditions, which exhibited higher activities in the stationary phase. A reasonable explanation for these observations could be linked to the previously mentioned hypothesis that PTMs, particularly succinylation, possibly inhibit PQO activity. Given that succinylation typically occurs non-enzymatically in the presence of high succinyl-CoA levels, likely associated with high TCA cycle activity, it is reasonable to infer that overproducing PQO-$\Delta_{C17}$ in an *aceE*-deficient strain alters the overall carbon flux. This alteration might reduce the extent of succinylation, particularly during the exponential growth phase of the organism.

Consequently, purifying both the full-length and truncated variants of PQO and conducting mass spectrometry analysis could potentially show a lower abundancy of succinylated lysine residues in the truncated variant compared to the full-length variant.

Integrating the findings from previous studies with the current data indicates that *in vivo* relevance of PQO under the so far tested conditions is minimal for several reasons: Firstly, PQO activation requires relatively high intracellular pyruvate concentrations (> 30 mM), but typical levels in *C. glutamicum* range from 0.5 to 0.8 mM (Petersen *et al*., 2001), favoring pyruvate binding by PDHC ($K_m$ = 1.7 mM; Schreiner *et al*., 2005). Secondly, high TCA cycle activity obviously correlates with abundant PQO modification through PTM, likely reducing its activity. Thirdly, PQO achieves maximal activity only when in proximity to membranes. These factors collectively act as barriers, preventing *C. glutamicum* from utilizing the less efficient PQO-ACK-PTA pathway for pyruvate decarboxylation to acetyl-CoA, and instead favoring the direct PDHC pathway.

These findings lead to the intriguing possibility that PQO may play a more significant role under conditions of pyruvate accumulation or when PDHC is inactive *in vivo*. Research exploring pH homeostasis in *C. glutamicum* through transcriptome and proteome analyses under varying constant extracellular pH levels found an up to elevenfold increase in pyruvate levels at acidic pH (6.0) compared to neutral pH (7.5). Additionally, *pqo* transcript levels were up to twofold higher in acidic conditions (Follmann *et al*., 2009). The present work here provides enzymatic activity data supporting this observation. In shake flask experiments designed to simulate acidification (by omitting urea from glucose minimal medium) led to extracellular pH acidification in wildtype, PQO-deletion, and PQO overproducer strains of *C. glutamicum*. The acidification was more pronounced with higher glucose concentrations, dropping the pH to as low as 4.5. Enzymatic data aligned partially with findings of Follmann *et al*. (2009), showing an up to a fivefold increase in PQO activity in the wildtype strain under moderately acidic conditions without urea, whereas the PQO-overproducer strain exhibited only a modest increase.

Intriguingly, when the extracellular pH was reduced to 4.5 (cultivation in medium containing high concentrations of glucose in absence of urea), PQO activity was almost completely absent in both strains, a finding that deviates from the correlation mentioned above. This unexpected result might be attributed to the capacity of *C. glutamicum* to regulate its internal pH. While the bacterium typically maintains an internal pH of around 7.5 under external pH levels ranging

from 6 to 9, the internal pH drops to about 6 when faced with an external pH of 4.5 (Follmann *et al*., 2009). This shift in internal pH could significantly influence gene transcription and protein biosynthesis processes.

Follmann *et al*. (2009) also observed oxidative stress and impaired reactive oxygen species (ROS)-defense at acidic extracellular pH, along with an activated iron starvation response, leading to TCA cycle downregulation. Consistent with observations in this work, low TCA cycle activity correlates with high *in vitro* PQO activity, further supporting this hypothesis. In such scenarios, PQO appears to redirect carbon flux away from the TCA cycle towards acetate production, thus avoiding intracellular pyruvate accumulation. Though this may impede biomass generation, the resulting reduced quinols could contribute to energy maintenance via the respiratory chain. However, no significant differences in growth behavior were observed among the wildtype, PQO-deletion, and PQO overproducer strains of *C. glutamicum*. This suggests that under the conditions tested, the role of PQO in energy maintenance is not manifested phenotypically, possibly due to the ability of the organism to reroute carbon flux through alternative pathways. Another potential reason for the lack of phenotypic variation among the strains could be that any contribution of PQO to energy maintenance might be more evident in scenarios of competitive survival or when exposed to new nutrients, rather than in standard growth conditions.

To determine if the observed increase in PQO activity in cultivations omitting urea in glucose minimal medium in the *C. glutamicum* wildtype strain is attributed to the reduced extracellular pH, a series of batch fermentations were conducted at various constant pH levels using the DASGIP® fermentation plant. The outcome was consistent, demonstrating that lower extracellular pH values were consistently linked with higher PQO activity, independent of the presence or absence of urea. This consistency supports the idea of a direct correlation between extracellular pH levels during cultivation of *C. glutamicum* and PQO activity. In addition to the PQO activity observations, growth rates of *C. glutamicum* cultures varied with extracellular pH. At pH 5.0, the growth rate was 0.06 $h^{-1}$, increasing with higher pH values, peaking at 0.34 to 0.37 $h^{-1}$ between pH 7.0 and 8.5. However, at pH 9.0, the growth rate declined to 0.3 $h^{-1}$.

The observed growth rates of *C. glutamicum* at different constant extracellular pH values, which correlated inversely with the detectable PQO activity, lead to a discussion in the context of related research. Notably, Abdel-Hamid *et al*. (2001) point out the importance of *E. coli* PoxB, especially in the absence of PDHC. They found that during continuous fermentation under glucose-limited, aerobic conditions, the native promoter of PoxB maintained steady-

states exclusively at lower dilution rates. This preference for lower growth rates indicates a strategic adaptation, where *E. coli* utilizes a less direct route for converting pyruvate to acetyl-CoA via acetate. Hence in this work, dependency of the growth rate on PQO activity was systematically analyzed in glucose-limited continuous fermentation. At the end of each process, the activities ranged from 0.060 U/mg protein at the lowest dilution/growth rate of 0.05 $h^{-1}$ to a specific activity of 0.014 U/mg protein at the highest dilution/growth rate of 0.4 $h^{-1}$.

A potential reason for the observed trend might be that in bacteria experiencing lower growth rates, particularly under nutrient-limited conditions, a substantial increase in the proportion of energy allocated to protein synthesis is observed (Stouthamer *et al*., 1990). This strategic redirection of resources primarily supports the synthesis of essential proteins involved in vital functions such as nutrient uptake and stress response, rather than promoting rapid cell division (Stouthamer *et al*., 1990). In many bacteria, the PDHC is a large tripartite complex of multiple copies of the individual subunits E1p, E2p and E3, with a central core composed by a varying number of E2p subunits (Bruch *et al*., 2021). While the exact number of E2p subunits and the symmetry of the core differ across species, they generally range between 24 to 60 E2p subunits, contributing to PDHC's status as an exceptionally large protein complex (Bruch *et al*., 2021). Both the E1 and E3 subunit generally bind to this E2 core through the peripheral subunit binding domain of the E2 component (Milne *et al*., 2002; Milne *et al*., 2006). Hence, cells may need to choose between synthesizing the simpler PQO enzyme and the associated net ATP cost required to activate acetate produced by PQO to acetyl-CoA via the ACK-PTA pathway, or the synthesis of the large PDHC.

This consideration is specifically challenged in *C. glutamicum* however, as the E2p core is pared down to its fundamentally active trimeric configuration, positioning it as an anomaly (Bruch *et al*., 2021). Also, *C. glutamicum* is known for an unique PDHC/2-oxoglutarate dehydrogenase complex (ODHC) supercomplex (Niebisch *et al*., 2006; Kinugawa *et al*., 2020; Sundermeyer *et al*., 2023). The primary role of ODHC in the TCA cycle is the oxidative decarboxylation of 2-oxoglutarate, thereby forming succinyl-CoA and catalyzing the reduction of $NAD^+$ to NADH. Commonly, the structure of ODHC encompasses three subunits: 2-oxoglutarate decarboxylase (E1o), dihydrolipoyl transsuccinylase (E2o), and E3, with the last one also forming a part of PDHC. A distinguishing feature of *C. glutamicum* and several related actinobacteria is their lack of a separate E2o subunit. They possess rather a fusion where the E1o subunit contains the succinyl transferase domain of E2o. Remarkably, the merged E1oE2o protein, despite having the succinyl transferase domain, lacks the lipoyl-binding domains characteristic of the standard E2o subunits. As a result, to transfer the succinyl group to CoA

using the lipoic acid residues, an essential interaction between the corynebacterial E1oE2o (OdhA) and E2p (AceF) is necessary (Hoffelder *et al*., 2010). Additionally, a novel study has revealed that all four subunits of this unique supercomplex (OdhA, AceE, AceF, and LPD) co-localize at the cell poles (Sundermeyer *et al*., 2023). Given these unique aspects of *C. glutamicum*, the observed higher PQO activities at low growth rates could be indicative of a different metabolic background compared to organisms like *E. coli*. To further explore whether PQO, in conjunction with ACK and PTA, can bypass the PDHC reaction at low growth rates, future studies could employ a PDHC-deficient *C. glutamicum* strain in continuous fermentation under glucose-limited conditions at low dilution rates and test whether the strain can maintain steady states.

Supporting the enzymatic data obtained in this study, a comprehensive study on metabolic and transcriptomic responses of *C. glutamicum* to varying growth rates in glucose-limited continuous fermentations indicate an inverse relationship between *pqo* transcript levels and growth rates (Graf *et al*., 2020). Precisely, when comparing growth rates of 0.2 $h^{-1}$ and 0.4 $h^{-1}$, the *pqo* transcript levels were observed to be approximately twofold lower at the higher growth rate of 0.4 $h^{-1}$ (Graf *et al*., 2020). Interestingly, it is likely that TCA cycle activity is again negatively correlated to PQO activity, as the gene coding for citrate synthase showed reduced transcript levels with reduced growth rates, along with the genes coding for ACK and PTA (Graf *et al*., 2020). In contrast, genes involved in malate, PEP and succinate production (*aceB*, *mdh*, *pck*, *sucC*, and *sucD*) were upregulated at lower growth rates (Graf *et al*., 2020). The upregulation of genes coding for succinyl-CoA synthetase (*sucC* and *sucD*) at low growth rates aligns with the hypothesis that succinyl-CoA levels influence post-translational modifications at lysine residues of PQO, thereby affecting PQO activity. Thus, it is plausible that PQO activity under lower growth rates is regulated not only at the gene level but also, to an undetermined extent, at the protein level through PTMs. However, during the cultivation of *C. glutamicum* strains under different media and carbon sources, PQO activity regulation seems primarily driven by PTMs, as discussed in section 4.1.

Future research should focus on quantifying intracellular pyruvate levels in *C. glutamicum* in relation to growth rates, a parameter not assessed in the study by Graf *et al*. (2020). The current data imply that intracellular pyruvate concentrations increase at lower growth rates, which in turn enhances *pqo* transcript levels. This relationship is expected to result in elevated PQO enzyme activity, as observed *in vitro*, for the organism to cope better with intracellular pyruvate accumulation.

Previous studies have established the biotechnological significance of PQO. Specifically, *pqo* deletion has been demonstrated to positively influence the production of lysine, 2-ketoisovalerate, and isobutanol in *C. glutamicum* (Blombach *et al*., 2008; Krause *et al*., 2010; Blombach *et al*., 2011). A plausible explanation for this observation may be that, in the absence of *pqo*, pyruvate accumulation leads instead to an increased carbon flux towards these biosynthetic pathways, which rely on substantial intracellular pyruvate pools. This hypothesis is supported by observations under lysine production conditions, where carbon flux to the TCA cycle via PDHC is reduced (Wittmann and Heinzle, 2002), suggesting a critical role for PQO under these specific metabolic conditions. Also, the absence of *pqo* might enhance anaplerotic flux through pyruvate carboxylase (PCx, see introduction **Fig. 1**) under high pyruvate conditions by reducing competition for pyruvate. In past studies, PCx activity was shown to be a critical factor in lysine biosynthesis (Peters-Wendisch *et al*., 2001).

*C. glutamicum* is well known for its potential to produce glutamate (reviewed in Wendisch, 2020). Consequently, this study focused on analyzing PQO activity in wildtype, PQO-deletion, and PQO-overproducer strains under conditions inducing glutamate production via Penicillin G addition. Notably, PQO activity was higher under glutamate-producing conditions in both wildtype and PQO-overproducing strains. This result suggests that PQO regulation is likely at the protein level rather than on transcriptional level, as the *pqo* gene in the PQO-overproducing strain is exclusively under the control of the artificial $P_{tac}$ promoter. Despite unchanged TCA cycle flux via the PDHC in glutamate-producing *C. glutamicum* cells compared to exponential growing cells (Marx *et al*., 1997), it is noteworthy that glutamate production correlates with reduced ODHC activity, thereby diminishing succinyl-CoA production and redirecting flux towards glutamate synthesis (Shimizu *et al*., 2003). This shift could potentially lead to decreased succinylation of PQO at surface-exposed lysine residues. Mizuno *et al*. (2016) identified succinylation at lysine residue K213 in PQO during glutamate production, although its abundance was not quantified. Further investigation by K. Zauner (bachelor thesis under my supervision), where mutations at K213 were introduced, indicated that this residue does not significantly influence PQO activity or growth phenotype in the respective mutant PQO overproducer strains under all conditions tested. Consequently, the role of this specific residue in regulating PQO activity appears minimal. Despite increased PQO activities under glutamate production conditions, no distinct growth phenotypes or significant variations in glutamate excretion were observed among the three strains studied.

This study evaluated diverse *C. glutamicum* strains under varying cultivation conditions, which resulted in distinct PQO activity patterns. Interestingly, no direct correlation between the

presence or absence of full-length PQO and growth phenotype was observed. Also, the results of co-culture experiments with fluorescently labelled strains demonstrated that neither the presence nor the absence of PQO conferred a significant competitive advantage or disadvantage under these conditions. However, a different pattern emerged under glutamate production conditions. Here, the PQO-deletion strain exhibited a growth advantage over the wildtype strain after addition of Penicillin G and 24 h of this co-cultivation. This was substantiated through both fluorescence intensity measurements and enzyme assays. The total PQO activity in this co-culture was less than 50 % of that of the corresponding fluorescently labeled wildtype strains when cultivated alone. This suggests that PQO presence might be detrimental in this specific context. This disadvantage was observable only in competitive scenarios. A possible explanation for this phenomenon is that under glutamate-producing conditions, the inability of PQO to be regulated through succinylation at lysine residues might result in an undesired diversion of carbon flux towards acetate production. This diversion potentially limits the availability of pyruvate for anaplerotic reactions, which are crucial under these metabolic conditions.

The experimental data presented in this study collectively indicate that PQO, together with ACK and PTA, does not function as a substitute for the PDHC reaction under all conditions tested. This conclusion aligns with observations in *E. coli.* In *E. coli*, systematic analysis revealed high expression levels of *pta* and *ack* during the exponential phase, which decrease upon transitioning to the stationary phase (Dittrich *et al*., 2005). In contrast, the expression of *poxB* is lower in the exponential phase and increases during the transition to the stationary phase (Dittrich *et al*., 2005). This expression pattern in *E. coli* implies a strategic choice to avoid redirecting acetate, produced by PoxB, into the TCA cycle as acetyl-CoA. The role of PoxB has been postulated to act as a metabolic 'safety valve', converting excess pyruvate to acetate, rather than to acetyl-CoA through PDHC. This process helps in preserving the intracellular pools of CoA or $NAD^+$ for other metabolic activities (Abdel-Hamid *et al*., 2001; De Mey *et al*., 2007), a mechanism that becomes particularly crucial in conditions where there are enzymatic bottlenecks in the TCA cycle or constraints in the respiratory pathway necessary for re-oxidizing NADH (Vemuri *et al*., 2006). Such regulatory mechanisms are hypothesized to be vital for maintaining metabolic homeostasis, particularly under stress conditions or in the presence of metabolic imbalances.

To sum up, the primary role of PQO at the PEP-pyruvate-oxaloacetate node in *C. glutamicum* appears to be the diversion of carbon flux away from the TCA cycle under certain conditions. This is particularly evident when there is an accumulation of pyruvate, likely due to redox imbalances or limited CoA-pools. To validate this hypothesis, a series of targeted experiments is proposed. The first approach involves redox balance studies, focusing on assessing the impact of PQO activity on the cellular redox state, particularly under conditions that lead to pyruvate accumulation. This includes measuring the intracellular NADH/$NAD^+$ and NADPH/$NADP^+$ ratios in strains with varying levels of *pqo* expression, to understand how PQO influences the overall redox balance of the cell. The second strategy involves the quantification of intracellular CoA-pools in *C. glutamicum* under different growth conditions. Comparing strains with altered PQO activity will elucidate if there is indeed a correlation between PQO activity and changes in CoA-pool sizes. Thirdly, comprehensive metabolic flux analysis should be performed. Specifically, this analysis should quantify carbon flux through the TCA cycle in strains with modified *pqo* expression. Lastly, to confirm whether PQO diverts carbon flux towards acetate production in dependence of TCA cycle activity, acetate production should be systematically quantified. This will involve measuring acetate in strains with altered PQO and/or TCA cycle activity.

All in all, this study establishes a critical foundation for understanding the role of PQO in modulating carbon flux at the PEP-pyruvate-oxaloacetate node in *C. glutamicum*. The revelation of its regulation via PTMs, specifically acetylation and succinylation of lysine residues, provides new insights into the metabolic flexibility of this organism. Notably, the inverse relationship between PQO and TCA cycle activities, given the latter's importance in producing amino acids and other biotechnologically relevant compounds, highlights the pivotal role of PQO. The comprehensive kinetic and structural analyses of PQO and its variants lay a robust groundwork for future bioengineering efforts aimed at optimizing metabolic pathways to enhance the efficiency of the aforementioned compound production. With the structure of PQO resolved in high resolution, critical residues involved in the activity of PQO, including those in the active site or targeted by PTMs, are now identified, offering a starting point for generating mutant PQO variants through rational design. Such precision in modulating PQO activity allows for finely tuned adjustments in carbon flux at the PEP-pyruvate-oxaloacetate node. Furthermore, this research advances our understanding of the enigmatic physiological role of PQO, providing substantial evidence for its function in redirecting carbon flux away from the TCA cycle. This sets a solid foundation for future experiments in this topic.

# References

**Abdel-Hamid AM, Attwood MM, Guest JR** (2001) Pyruvate oxidase contributes to the aerobic growth efficiency of *Escherichia coli*. Microbiology **147**:1483–1498.

**Abe S, Takayama K-I, Kinoshita S** (1967) Taxonomical Studies on Glutamic Acid-Producing Bacteria. The Journal of General and Applied Microbiology **13**:279–301.

**Acharya KR, Lloyd MD** (2005) The advantages and limitations of protein crystal structures. Trends in Pharmacological Sciences **26**:10–14.

**Bakkes PJ, Ramp P, Bida A, Dohmen-Olma D, Bott M, Freudl R** (2020) Improved pEKEx2-derived expression vectors for tightly controlled production of recombinant proteins in *Corynebacterium glutamicum*. Plasmid **112**:102540.

**Becker J, Rohles CM, Wittmann C** (2018) Metabolically engineered *Corynebacterium glutamicum* for bio-based production of chemicals, fuels, materials, and healthcare products. Metabolic Engineering **50**:122–141.

**Beckers G, Bendt AK, Krämer R, Burkovski A** (2004) Molecular Identification of the Urea Uptake System and Transcriptional Analysis of Urea Transporter- and Urease-Encoding Genes in *Corynebacterium glutamicum*. J Bacteriol **186**:7645–7652.

**Bendt AK, Burkovski A, Schaffer S, Bott M, Farwick M, Hermann T** (2003) Towards a phosphoproteome map of *Corynebacterium glutamicum*. Proteomics **3**:1637–1646.

**Blombach B, Riester T, Wieschalka S, Ziert C, Youn J-W, Wendisch VF, Eikmanns BJ** (2011) *Corynebacterium glutamicum* Tailored for Efficient Isobutanol Production. Applied and Environmental Microbiology **77**:3300–3310.

**Blombach B, Schreiner ME, Bartek T, Oldiges M, Eikmanns BJ** (2008) *Corynebacterium glutamicum* tailored for high-yield L-valine production. Appl Microbiol Biotechnol **79**:471–479.

**Blombach B, Seibold GM** (2010) Carbohydrate metabolism in *Corynebacterium glutamicum* and applications for the metabolic engineering of L-lysine production strains. Appl Microbiol Biotechnol **86**:1313–1322.

**Bott M** (2007) Offering surprises: TCA cycle regulation in *Corynebacterium glutamicum*. Trends in Microbiology **15**:417–425.

**Bott M, Niebisch A** (2003) The respiratory chain of *Corynebacterium glutamicum*. J Biotechnol **104**:129–153.

**Bruch EM, Vilela P, Yang L, Boyko A, Lexa-Sapart N, Raynal B, Alzari PM, Bellinzoni M** (2021) Actinobacteria challenge the paradigm: A unique protein architecture for a well-known, central metabolic complex. PNAS **118**:e2112107118.

**Chang YY, Cronan JE** (1984) An *Escherichia coli* mutant deficient in pyruvate oxidase activity due to altered phospholipid activation of the enzyme. PNAS **81**:4348–4352.

**Chang YY, J E Cronan J** (1983) Genetic and biochemical analyses of *Escherichia coli* strains having a mutation in the structural gene (*poxB*) for pyruvate oxidase. Journal of Bacteriology 756-762.

**Christensen DG, Xie X, Basisty N, Byrnes J, McSweeney S, Schilling B, Wolfe AJ** (2019) Post-translational Protein Acetylation: An Elegant Mechanism for Bacteria to Dynamically Regulate Metabolic Functions. Frontiers in Microbiology **10**.

**Clamp M, Cuff J, Searle SM, Barton GJ** (2004) The Jalview Java alignment editor. Bioinformatics **20**:426–427.

**Colak G, Xie Z, Zhu AY, Dai L, Lu Z, Zhang Y, Wan X, Chen Y, Cha YH, Lin H, Zhao Y, Tan M** (2013) Identification of Lysine Succinylation Substrates and the Succinylation Regulatory Enzyme CobB in *Escherichia coli*. Molecular & Cellular Proteomics **12**:3509–3520.

**Cunningham CC, Hager LP** (1971) Crystalline Pyruvate Oxidase from *Escherichia coli*: III. PHOSPHOLIPID AS AN ALLOSTERIC EFFECTOR FOR THE ENZYME. Journal of Biological Chemistry **246**:1583–1589.

**Cunningham CC, Hager LP** (1975) Reactivation of the lipid-depleted pyruvate oxidase system from *Escherichia coli* with cell envelope neutral lipids. Journal of Biological Chemistry **250**:7139–7146.

**De Mey M, De Maeseneire S, Soetaert W, Vandamme E** (2007) Minimizing acetate formation in *E. coli* fermentations. Journal of Industrial Microbiology and Biotechnology **34**:689–700.

**Dittrich CR, Bennett GN, San K-Y** (2005) Characterization of the Acetate-Producing Pathways in *Escherichia coli*. Biotechnology Progress **21**:1062–1067.

**Eikmanns BJ** (2005) Central metabolism: tricarboxylic acid cycle and anaplerotic reactions. In: Eggeling L, Bott M (eds) Handbook of *Corynebacterium glutamicum*. CRC, Boca Raton, FL, 241–276.

**Eikmanns BJ, Follettie MT, Griot MU, Sinskey AJ** (1989) The phosphoenolpyruvate carboxylase gene of *Corynebacterium glutamicum*: Molecular cloning, nucleotide sequence, and expression. Molec Gen Genet **218**:330–339.

**Eikmanns BJ, Metzger M, Reinscheid D, Kircher M, Sahm H** (1991) Amplification of three threonine biosynthesis genes in *Corynebacterium glutamicum* and its influence on carbon flux in different strains. Appl Microbiol Biotechnol **34**:617–622.

**Eikmanns BJ, Rittmann D, Sahm H** (1995) Cloning, sequence analysis, expression, and inactivation of the *Corynebacterium glutamicum icd* gene encoding isocitrate dehydrogenase and biochemical characterization of the enzyme. J Bacteriol **177**:774–782

**Eikmanns BJ, Thum-Schmitz N, Eggeling L, Ludtke K-U, Sahm H** (1994) Nucleotide sequence, expression and transcriptional analysis of the *Corynebacterium glutamicum gltA* gene encoding citrate synthase. Microbiology **140**:1817–1828.

**Emer D, Krug A, Eikmanns BJ, Bott M** (2009) Complex expression control of the *Corynebacterium glutamicum* aconitase gene: Identification of RamA as a third transcriptional regulator besides AcnR and RipA. Journal of Biotechnology **140**:92–98.

**Follmann M, Ochrombel I, Krämer R, Trötschel C, Poetsch A, Rückert C, Hüser A, Persicke M, Seiferling D, Kalinowski J, Marin K** (2009) Functional genomics of pH homeostasis in *Corynebacterium glutamicum* revealed novel links between pH response, oxidative stress, iron homeostasis and methionine synthesis. BMC Genomics **10**:621.

**Gibson DG, Young L, Chuang R-Y, Venter JC, Hutchison CA, Smith HO** (2009) Enzymatic assembly of DNA molecules up to several hundred kilobases. Nat Methods **6**:343–345.

**Goldbeck O, Desef DN, Ovchinnikov KV, Perez-Garcia F, Christmann J, Sinner P, Crauwels P, Weixler D, Cao P, Becker J, Kohlstedt M, Kager J, Eikmanns BJ, Seibold GM, Herwig C, Wittmann C, Bar NS, Diep DB, Riedel CU** (2021) Establishing recombinant production of pediocin PA-1 in *Corynebacterium glutamicum*. Metab Eng **68**:34–45.

**Gourdon P, Baucher M-F, Lindley ND, Guyonvarch A** (2000) Cloning of the Malic Enzyme Gene from *Corynebacterium glutamicum* and Role of the Enzyme in Lactate Metabolism. Appl Environ Microbiol **66**:2981–2987.

**Grabau C, Cronan JE** (1984) Molecular cloning of the gene (*poxB*) encoding the pyruvate oxidase of *Escherichia coli*, a lipid-activated enzyme. J Bacteriol **160**:1088–1092.

**Graf M, Haas T, Teleki A, Feith A, Cerff M, Wiechert W, Nöh K, Busche T, Kalinowski J, Takors R** (2020) Revisiting the Growth Modulon of *Corynebacterium glutamicum* Under Glucose Limited Chemostat Conditions. Frontiers in Bioengineering and Biotechnology **8**:584614.

**Gu T, Galera-Gómez PA** (1995) Clouding of Triton X-114: The effect of added electrolytes on the cloud point of Triton X-114 in the presence of ionic surfactants. Colloids and Surfaces A: Physicochemical and Engineering Aspects **104**:307–312.

**Hager LP** (1957) Trypsin activation of a ferricyanide-linked pyruvic acid oxidation. J Biol Chem **229**:251–263.

**Hanahan D** (1983) Studies on transformation of *Escherichia coli* with plasmids. J Mol Biol **166**:557–580.

**Hentchel KL, Escalante-Semerena JC** (2015) Acylation of Biomolecules in Prokaryotes: a Widespread Strategy for the Control of Biological Function and Metabolic Stress. Microbiology and Molecular Biology Reviews **79**:321–346.

**Hoffelder M, Raasch K, van Ooyen J, Eggeling L** (2010) The E2 Domain of OdhA of *Corynebacterium glutamicum* Has Succinyltransferase Activity Dependent on Lipoyl Residues of the Acetyltransferase AceF. J Bacteriol **192**:5203–5211.

**Hoischen C, Krämer R** (1990) Membrane alteration is necessary but not sufficient for effective glutamate secretion in *Corynebacterium glutamicum*. J Bacteriol **172**:3409–3416.

**Huc E, Meniche X, Benz R, Bayan N, Ghazi A, Tropis M, Daffé M** (2010) O-Mycoloylated Proteins from *Corynebacterium*: An Unprecedent Post-Translational Modification In Bacteria. Journal of Biological Chemistry **285**:21908–21912.

**Inoue H, Nojima H, Okayama H** (1990) High efficiency transformation of *Escherichia coli* with plasmids. Gene **96**:23–28.

**Jumper J, Evans R, Pritzel A, Green T, Figurnov M, Ronneberger O, Tunyasuvunakool K, Bates R, Žídek A, Potapenko A, Bridgland A, Meyer C, Kohl SAA, Ballard AJ, Cowie A, Romera-Paredes B, Nikolov S, Jain R, Adler J, Back T, Petersen S, Reiman D, Clancy E, Zielinski M, Steinegger M, Pacholska M, Berghammer T, Bodenstein S, Silver D, Vinyals O, Senior AW, Kavukcuoglu K, Kohli P, Hassabis D** (2021) Highly accurate protein structure prediction with AlphaFold. Nature **596**:583–589.

**Kalinowski J, Bathe B, Bartels D, Bischoff N, Bott M, Burkovski A, Dusch N, Eggeling L, Eikmanns BJ, Gaigalat L, Goesmann A, Hartmann M, Huthmacher K, Krämer R, Linke B, McHardy AC, Meyer F, Möckel B, Pfefferle W, Pühler A, Rey DA, Rückert C, Rupp O, Sahm H, Wendisch VF, Wiegräbe I, Tauch A** (2003) The complete *Corynebacterium glutamicum* ATCC 13032 genome sequence and its impact on the production of L-aspartate-derived amino acids and vitamins. J Biotechnol **104**:5–25.

**Kinugawa H, Kondo N, Komine-Abe A, Tomita T, Nishiyama M, Kosono S** (2020) *In vitro* reconstitution and characterization of pyruvate dehydrogenase and 2-oxoglutarate dehydrogenase hybrid complex from *Corynebacterium glutamicum*. MicrobiologyOpen **9**:e1113.

**Klaffl S, Eikmanns BJ** (2010) Genetic and Functional Analysis of the Soluble Oxaloacetate Decarboxylase from *Corynebacterium glutamicum*. Journal of Bacteriology **192**:2604–2612.

**Kogure T, Inui M** (2018) Recent advances in metabolic engineering of *Corynebacterium glutamicum* for bioproduction of value-added aromatic chemicals and natural products. Appl Microbiol Biotechnol **102**:8685–8705.

**Koland JG, Miller MJ, Gennis RB** (1984) Reconstitution of the membrane-bound, ubiquinone-dependent pyruvate oxidase respiratory chain of *Escherichia coli* with the cytochrome d terminal oxidase. Biochemistry **23**:445–453.

**Komine-Abe A, Kondo N, Kubo S, Kawasaki H, Nishiyama M, Kosono S** (2021) Characterization of lysine acetylation in the peripheral subunit-binding domain of the E2 subunit of the pyruvate dehydrogenase-2-oxoglutarate dehydrogenase hybrid complex from *Corynebacterium glutamicum*. Bioscience, Biotechnology, and Biochemistry **85**:874–881.

**Komine-Abe A, Nagano-Shoji M, Kubo S, Kawasaki H, Yoshida M, Nishiyama M, Kosono S** (2017) Effect of lysine succinylation on the regulation of 2-oxoglutarate dehydrogenase inhibitor, OdhI, involved in glutamate production in *Corynebacterium glutamicum*. Bioscience, Biotechnology, and Biochemistry **81**:2130–2138.

**Krause FS, Blombach B, Eikmanns BJ** (2010) Metabolic engineering of *Corynebacterium glutamicum* for 2-ketoisovalerate production. Appl Environ Microbiol **76**:8053–8061.

**Krug A, Wendisch VF, Bott M** (2005) Identification of AcnR, a TetR-type Repressor of the Aconitase Gene *acn* in *Corynebacterium glutamicum*. Journal of Biological Chemistry **280**:585–595.

**Küberl A, Fränzel B, Eggeling L, Polen T, Wolters DA, Bott M** (2014) Pupylated proteins in *Corynebacterium glutamicum* revealed by MudPIT analysis. Proteomics **14**:1531–1542.

**Kuhn ML, Zemaitaitis B, Hu LI, Sahu A, Sorensen D, Minasov G, Lima BP, Scholle M, Mrksich M, Anderson WF, Gibson BW, Schilling B, Wolfe AJ** (2014) Structural, Kinetic and Proteomic Characterization of Acetyl Phosphate-Dependent Bacterial Protein Acetylation. PLOS ONE **9**:e94816.

**Laemmli UK** (1970) Cleavage of structural proteins during the assembly of the head of bacteriophage T4. Nature **227**:680–685.

**Li M, Yao S, Shimizu K** (2007) Effect of *poxB* gene knockout on metabolism in *Escherichia coli* based on growth characteristics and enzyme activities. World J Microbiol Biotechnol **23**:573–580.

**Liebl W, Bayerl A, Schein B, Stillner U, Schleifer KH** (1989) High efficiency electroporation of intact *Corynebacterium glutamicum* cells. FEMS Microbiology Letters **65**:299–303.

**Marx A, Striegel K, de Graaf AA, Sahm H, Eggeling L** (1997) Response of the central metabolism of *Corynebacterium glutamicum* to different flux burdens. Biotechnol Bioeng **56**:168–180.

**Mather MW, Gennis RB** (1985) Spectroscopic studies of pyruvate oxidase flavoprotein from *Escherichia coli* trapped in the lipid-activated form by cross-linking. J Biol Chem **260**:10395–10397.

**Milne JLS, Shi D, Rosenthal PB, Sunshine JS, Domingo GJ, Wu X, Brooks BR, Perham RN, Henderson R, Subramaniam S** (2002) Molecular architecture and mechanism of an icosahedral pyruvate dehydrogenase complex: a multifunctional catalytic machine. The EMBO Journal **21**:5587–5598.

**Milne JLS, Wu X, Borgnia MJ, Lengyel JS, Brooks BR, Shi D, Perham RN, Subramaniam S** (2006) Molecular Structure of a 9-MDa Icosahedral Pyruvate Dehydrogenase Subcomplex Containing the E2 and E3 Enzymes Using Cryoelectron Microscopy. Journal of Biological Chemistry **281**:4364–4370.

**Mizuno Y, Nagano-Shoji M, Kubo S, Kawamura Y, Yoshida A, Kawasaki H, Nishiyama M, Yoshida M, Kosono S** (2016) Altered acetylation and succinylation profiles in *Corynebacterium glutamicum* in response to conditions inducing glutamate overproduction. MicrobiologyOpen **5**:152–173.

**Molenaar D, van der Rest ME, Drysch A, Yücel R** (2000) Functions of the membrane-associated and cytoplasmic malate dehydrogenases in the citric acid cycle of *Corynebacterium glutamicum*. J Bacteriol **182**:6884–6891.

**Molenaar D, van der Rest ME, Petrović S** (1998) Biochemical and genetic characterization of the membrane-associated malate dehydrogenase (acceptor) from *Corynebacterium glutamicum*. Eur J Biochem **254**:395–403.

**Münßinger S** (2022) Master thesis with the topic: Regulation of the Pyruvate: Quinone Oxidoreductase in *Corynebacterium glutamicum* depending on the Growth Rate. University of Ulm.

**Muller YA, Schulz GE** (1993) Structure of the thiamine- and flavin-dependent enzyme pyruvate oxidase. Science **259**:965–967.

**Mullis K, Faloona F, Scharf S, Saiki R, Horn G, Erlich H** (1986) Specific enzymatic amplification of DNA *in vitro*: the polymerase chain reaction. Cold Spring Harb Symp Quant Biol **51 Pt 1**:263–273.

**Nagano-Shoji M, Hamamoto Y, Mizuno Y, Yamada A, Kikuchi M, Shirouzu M, Umehara T, Yoshida M, Nishiyama M, Kosono S** (2017) Characterization of lysine acetylation of a phosphoenolpyruvate carboxylase involved in glutamate overproduction in *Corynebacterium glutamicum*. Molecular Microbiology **104**:677–689.

**Neumann P, Weidner A, Pech A, Stubbs MT, Tittmann K** (2008) Structural basis for membrane binding and catalytic activation of the peripheral membrane enzyme pyruvate oxidase from *Escherichia coli*. PNAS **105**:17390–17395.

**Niebisch A, Kabus A, Schultz C, Weil B, Bott M** (2006) Corynebacterial Protein Kinase G Controls 2-Oxoglutarate Dehydrogenase Activity via the Phosphorylation Status of the OdhI Protein. Journal of Biological Chemistry **281**:12300–12307.

**Nussinov R, Zhang M, Liu Y, Jang H** (2022) AlphaFold, Artificial Intelligence (AI), and Allostery. J Phys Chem B **126**:6372–6383.

**Patton TG, Rice KC, Foster MK, Bayles KW** (2005) The *Staphylococcus aureus cidC* gene encodes a pyruvate oxidase that affects acetate metabolism and cell death in stationary phase. Molecular Microbiology **56**:1664–1674.

**Petersen S, Mack C, de Graaf AA, Riedel C, Eikmanns BJ, Sahm H** (2001) Metabolic consequences of altered phosphoenolpyruvate carboxykinase activity in *Corynebacterium glutamicum* reveal anaplerotic regulation mechanisms *in vivo*. Metab Eng **3**:344–361.

**Peters-Wendisch P, Schiel B, Wendisch VF, Katsoulidis E, Mockel B, Sahm H, Eikmanns BJ** (2001) Pyruvate carboxylase is a major bottleneck for glutamate and lysine production by *Corynebacterium glutamicum*. Journal of Molecular Microbiology and Biotechnology **3(2)**:295-300.

**Peters-Wendisch PG, Wendisch VF, Paul S, Eikmanns BJ, Sahm H** (1997) Pyruvate carboxylase as an anaplerotic enzyme in *Corynebacterium glutamicum*. Microbiology **143**:1095–1103.

**Puskás LG, Inui M, Yukawa H** (2000) Structure of the urease operon of *Corynebacterium glutamicum*. DNA Seq **11**:383–394, 467.

**Recny MA, Grabau C, Cronan JE, Hager LP** (1985) Characterization of the alpha-peptide released upon protease activation of pyruvate oxidase. Journal of Biological Chemistry **260**:14287–14291.

**Recny MA, Hager LP** (1983) Isolation and characterization of the protease-activated form of pyruvate oxidase. Evidence for a conformational change in the environment of the flavin prosthetic group. Journal of Biological Chemistry **258**:5189–5195.

**Reinscheid DJ, Schnicke S, Rittmann D, Zahnow U, Sahm H, Eikmanns BJ** (1999) Cloning, sequence analysis, expression and inactivation of the *Corynebacterium glutamicum pta-ack* operon encoding phosphotransacetylase and acetate kinase. Microbiology **145 (Pt 2)**:503–513.

**Riedel C, Rittmann D, Dangel P, Möckel B, Petersen S, Sahm H, Eikmanns BJ** (2001) Characterization of the phosphoenolpyruvate carboxykinase gene from *Corynebacterium glutamicum* and significance of the enzyme for growth and amino acid production. J Mol Microbiol Biotechnol **3**:573–583.

**Ruff KM, Pappu RV** (2021) AlphaFold and Implications for Intrinsically Disordered Proteins. Journal of Molecular Biology **433**:167208.

**Russell P, Hager LP, Gennis RB** (1977) Characterization of the proteolytic activation of pyruvate oxidase. Control by specific ligands and by the flavin oxidation-reduction state. Journal of Biological Chemistry **252**:7877–7882.

**Sambrook J, Fritsch EF, Maniatis T** (1989) Molecular cloning: a laboratory manual, 2nd ed. Cold Spring Harbor Laboratory Press, Cold Spring Harbor, N.Y.

**Sambrook J, Russell DW** (2001) Molecular cloning: a laboratory manual, 3rd ed. Cold Spring Harbor Laboratory Press, Cold Spring Harbor, N.Y.

**Sauer U, Eikmanns BJ** (2005) The PEP—pyruvate—oxaloacetate node as the switch point for carbon flux distribution in bacteria. FEMS Microbiology Reviews **29**:765–794.

**Schreiner ME** (2004) Dissertation with the topic: Physiologische und biochemische Untersuchungen zu den Pyruvat-decarboxylierenden Enzymen in *Corynebacterium glutamicum.* University of Ulm.

**Schreiner ME, Eikmanns BJ** (2005) Pyruvate:Quinone Oxidoreductase from *Corynebacterium glutamicum*: Purification and Biochemical Characterization. J Bacteriol **187**:862–871.

**Schreiner ME, Fiur D, Holátko J, Pátek M, Eikmanns BJ** (2005) E1 Enzyme of the Pyruvate Dehydrogenase Complex in *Corynebacterium glutamicum*: Molecular Analysis of the Gene and Phylogenetic Aspects. Journal of Bacteriology **187**:6005–6018.

**Schreiner ME, Riedel C, Holátko J, Pátek M, Eikmanns BJ** (2006) Pyruvate:Quinone Oxidoreductase in *Corynebacterium glutamicum*: Molecular Analysis of the *pqo* Gene, Significance of the Enzyme, and Phylogenetic Aspects. J Bacteriol **188**:1341–1350.

**Schwinde JW, Hertz PF, Sahm H, Eikmanns BJ, Guyonvarch A** (2001) Lipoamide dehydrogenase from *Corynebacterium glutamicum*: molecular and physiological analysis of the *lpd* gene and characterization of the enzyme. Microbiology **147**:2223–2231.

**Sedewitz B, Schleifer KH, Götz F** (1984) Purification and biochemical characterization of pyruvate oxidase from *Lactobacillus plantarum*. Journal of Bacteriology **160**:273–278.

**Shimizu H, Tanaka H, Nakato A, Nagahisa K, Kimura E, Shioya S** (2003) Effects of the changes in enzyme activities on metabolic flux redistribution around the 2-oxoglutarate branch in glutamate production by *Corynebacterium glutamicum*. Bioprocess Biosyst Eng **25**:291–298.

**Sousa FM, Fernandes B, Pereira MM** (2023) The protein family of pyruvate:quinone oxidoreductases: Amino acid sequence conservation and taxonomic distribution. Biochimica et Biophysica Acta (BBA) - Bioenergetics **1864**:148958.

**Stouthamer AE, Bulthius BA, van Verseveld HW** (1990) Energetics of growth at low growth rates and its relevance for the maintenance concept. In: RK Poole, MJ Bazin, CW Keevil (eds). Microbial growth dynamics. Special Publications of the Society for General Microbiology, **28**. Oxford: IRL Press. p 85–193.

**Sundermeyer L, Folkerts J-G, Lückel B, Mack C, Baumgart M, Bott M** (2023) Cellular localization of the hybrid pyruvate/2-oxoglutarate dehydrogenase complex in the actinobacterium *Corynebacterium glutamicum*. Microbiol Spectrum **11(5)**:e02668-23.

**Thompson JD, Higgins DG, Gibson TJ** (1994) CLUSTAL W: improving the sensitivity of progressive multiple sequence alignment through sequence weighting, position-specific gap penalties and weight matrix choice. Nucleic Acids Res **22**:4673–4680.

**Towbin H, Staehelin T, Gordon J** (1979) Electrophoretic transfer of proteins from polyacrylamide gels to nitrocellulose sheets: procedure and some applications. PNAS **76**:4350–4354.

**Unthan S, Grünberger A, van Ooyen J, Gätgens J, Heinrich J, Paczia N, Wiechert W, Kohlheyer D, Noack S** (2014) Beyond growth rate 0.6: What drives *Corynebacterium glutamicum* to higher growth rates in defined medium. Biotechnol Bioeng **111**:359–371.

**Vemuri GN, Altman E, Sangurdekar DP, Khodursky AB, Eiteman MA** (2006) Overflow Metabolism in *Escherichia coli* during Steady-State Growth: Transcriptional Regulation and Effect of the Redox Ratio. Applied and Environmental Microbiology **72**:3653–3661.

**Ventura M, Canchaya C, Tauch A, Chandra G, Fitzgerald GF, Chater KF, van Sinderen D** (2007) Genomics of Actinobacteria: tracing the evolutionary history of an ancient phylum. Microbiol Mol Biol Rev **71**:495–548.

**Wagner GR, Bhatt DP, O'Connell TM, Thompson JW, Dubois LG, Backos DS, Yang H, Mitchell GA, Ilkayeva OR, Stevens RD, Grimsrud PA, Hirschey MD** (2017) A Class of Reactive Acyl-CoA Species Reveals the Non-enzymatic Origins of Protein Acylation. Cell Metab **25**:823-837.

**Walsh CT** (1989) Enzymes in the D-alanine branch of bacterial cell wall peptidoglycan assembly. Journal of Biological Chemistry **264**:2393–2396.

**Weidner A, Neumann P, Pech A, Stubbs MT, Tittmann K** (2009) New insights into the membrane-binding and activation mechanism of pyruvate oxidase from *Escherichia coli*. Journal of Molecular Catalysis B: Enzymatic **61**:88–92.

**Weinert BT, Iesmantavicius V, Wagner SA, Schölz C, Gummesson B, Beli P, Nyström T, Choudhary C** (2013a) Acetyl-Phosphate Is a Critical Determinant of Lysine Acetylation in *E. coli.* Molecular Cell **51**:265–272.

**Weinert BT, Schölz C, Wagner SA, Iesmantavicius V, Su D, Daniel JA, Choudhary C** (2013b) Lysine Succinylation Is a Frequently Occurring Modification in Prokaryotes and Eukaryotes and Extensively Overlaps with Acetylation. Cell Reports **4**:842–851.

**Wendisch VF** (2020) Metabolic engineering advances and prospects for amino acid production. Metabolic Engineering **58**:17–34.

**Wendisch VF, de Graaf AA, Sahm H, Eikmanns BJ** (2000) Quantitative Determination of Metabolic Fluxes during Coutilization of Two Carbon Sources: Comparative Analyses with *Corynebacterium glutamicum* during Growth on Acetate and/or Glucose. Journal of Bacteriology **182**:3088–3096.

**Wille G, Ritter M, Weiss MS, König S, Mäntele W, Hübner G** (2005) The Role of Val-265 for Flavin Adenine Dinucleotide (FAD) Binding in Pyruvate Oxidase: FTIR, Kinetic, and Crystallographic Studies on the Enzyme Variant V265A. Biochemistry **44**:5086–5094.

**Wittmann C, Heinzle E** (2002) Genealogy Profiling through Strain Improvement by Using Metabolic Network Analysis: Metabolic Flux Genealogy of Several Generations of Lysine-Producing *Corynebacteria*. Appl Environ Microbiol **68**:5843–5859.

**Wolf S, Becker J, Tsuge Y, Kawaguchi H, Kondo A, Marienhagen J, Bott M, Wendisch VF, Wittmann C** (2021) Advances in metabolic engineering of *Corynebacterium glutamicum* to produce high-value active ingredients for food, feed, human health, and well-being. Essays in Biochemistry **65**:197–212.

**Zhang T-F, Hager LP** (1987) A single-step large-scale purification of pyruvate oxidase. Archives of Biochemistry and Biophysics **257**:485–487.

**Zhang X, Bayles KW, Luca S** (2017) *Staphylococcus aureus* CidC Is a Pyruvate:Menaquinone Oxidoreductase. Biochemistry **56**:4819–4829.

# List of acronyms

| | |
|---|---|
| μ | growth rate |
| Ac | acetate |
| ACK | acetate kinase |
| ATCC | American Type Culture Collection |
| ATP | adenosine triphosphate |
| BHI | Brain-Heart-Infusion |
| BHIS | BHI with sorbitol |
| BLAST | Basic Local Alignment Search Tool |
| bp | base pair |
| BSA | bovine serum albumin |
| CoA | coenzyme A |
| d | layer thickness of a cuvette |
| DCPIP | 2,6-dichloroindophenol |
| DDM | n-dodecyl-β-D-maltoside |
| DMSO | dimethyl sulfoxide |
| DNA | desoxyribonucleic acid |
| DTT | dithiothreitol |
| E | extinction |
| e.g. | example given |
| E1o | 2-oxoglutarate dehydrogenase |
| E1p | pyruvate decarboxylase |
| E2o | dihydrolipoamide succinyltransferase |
| E2p | dihydrolipoamide acetyltransferase |
| E3 | see LPD |
| EDTA | ethylenediaminetetraacetic acid |
| *et al.* | *et alli* (‘and others’) |
| exp | exponential phase |
| FAD | flavine adenosine dinucleotide |
| Fig. | figure |
| Flu | fluorescence |
| g | gram or gravity of earth (9.81 $m/s^2$) |
| GC content | guanine-cytosine content |
| Glc | glucose |

| | |
|---|---|
| GRAS | generally recognized as safe |
| h | hours |
| HEPES | 1-piperazineethanesulfonic acid |
| i.e. | *id est* (‘that is’) |
| IPTG | isopropyl-β-D-thiogalactopyranoside |
| KAT | lysine acetyltransferase |
| $k_{cat}$ | catalytic rate constant, turnover number |
| kDa | kilodalton |
| KDAC | lysine deacetylase |
| $K_m$ | Michaelis constant |
| L, mL, µL | liter, milliliter, microliter |
| LPD | lipoamide dehydrogenase |
| M, mM, µM | molar (mol/L), millimolar (mmol/L), micromolar (µmol/L) |
| MDH | malate dehydrogenase |
| ME | malic enzyme |
| MES | 2-(n-morpholino)ethanesulfonic acid |
| mol | unit of amount of substance, $6.022\times10^{23}$ elementary entities |
| MOPS | 3-(n-morpholino)propanesulfonic acid |
| MQO | malate:quinone oxidoreductase |
| $NAD(P)^+$ | nicotinamide adenine dinucleotide (phosphate), oxidized |
| NAD(P)H | nicotinamide adenine dinucleotide (phosphate), reduced |
| nm | nanometer |
| OD | optical density |
| ODHC | 2-oxoglutarate dehydrogenase complex |
| ODx | oxaloacetate decarboxylase |
| PCR | polymerase chain reaction |
| PDHC | pyruvate dehydrogenase complex |
| PEP | phosphoenolpyruvate |
| PEPCk | phosphoenolpyruvate carboxykinase |
| PEPCx | phosphoenolpyruvate carboxylase |
| PK | pyruvate kinase |
| POX | (soluble) pyruvate oxidase |
| PoxB | pyruvate:quinone oxidoreductase from *Escherichia coli* |
| $PoxB_{\Delta23}$ | pyruvate:quinone oxidoreductase from *Escherichia coli*, lacking the last 23 carboxy-terminal amino acid residues |
| PP | pyrophosphate, diphosphate |

| | |
|---|---|
| PQO | pyruvate:quinone oxidoreductase from *Corynebacterium glutamicum* |
| PQO-$\Delta_{C17}$ | pyruvate:quinone oxidoreductase from *Corynebacterium glutamicum*, lacking the last 17 carboxy-terminal amino acid residues |
| PTA | phosphotransacetylase |
| PTM | post-translational modification |
| PVDF | polyvinylidene fluoride |
| PYC | pyruvate carboxylase |
| RMSD | root-mean-square deviation |
| RNA | ribonucleic acid |
| rpm | rounds per minute |
| SDS | sodium dodecyl sulfate |
| SDS-PAGE | sodium dodecyl sulfate polyacrylamide gelectrophoresis |
| SOB | super optimal broth |
| stat | stationary phase |
| t | time |
| Tab. | table |
| TAE | tris-acetate-EDTA |
| TB | tris-borate |
| TBST | tris buffered saline with Tween20 |
| TCA | tricarboxylic acid |
| TES | trace element solution |
| TEV | tobacco etch virus |
| TG | tris-glycerol |
| TPP | thiamine diphosphate |
| Tris | tris(hydroxymethyl)aminomethane |
| TY | tryptone yeast |
| U | enzyme unit |
| UV | ultraviolet |
| V | volume |
| $V_{max}$ | velocity of an enzymatic reaction at saturating substrate concentration |
| w/o | without |
| WT | wildtype |
| Δ | (chromosomal) deletion of gene(s) |
| ε | molar extinction coefficient |

# Poster presentations and publication

### Poster presentations

Da Silva Lameira C, Bellinzoni M, Yang L, Bruch EM, Haberbosch D, Eikmanns BJ. Regulation and Structural Characterization of the Pyruvate:Quinone Oxidoreductase (PQO) from *Corynebacterium glutamicum.* 22 February 2022, VAAM annual conference (Online)

Da Silva Lameira C, Münßinger S, Eikmanns BJ. Unraveling the Physiological Relevance of Pyruvate:Quinone Oxidoreductase (PQO) from *Corynebacterium glutamicum*: Activity Highlighted under acidic pH and low Growth Rates. 10-13 September 2023, VAAM annual conference, Göttingen

### Publication

Da Silva Lameira C, Münßinger S, Yang L, Bellinzoni M, Eikmanns BJ. Pyruvate:Quinone Oxidoreductase of *Corynebacterium glutamicum*: Kinetic, Structural and Physiological Aspects (2024). Manuscript in preparation

# Declaration

Hiermit erkläre ich, dass ich die vorliegende Arbeit selbständig verfasst und keine anderen als die von mir angegebenen Quellen und Hilfsmittel benutzt habe. Zitate wurden als solche vollständig kenntlich gemacht.

_____ _____

Ort, Datum Unterschrift

# DANKSAGUNG

Die Danksagung wurde aus Gründen des Datenschutzes entfernt.

# LEBENSLAUF

Der Lebenslauf wurde aus Gründen des Datenschutzes entfernt.